UC Santa Cruz

UC Santa Cruz Electronic Theses and Dissertations

Title

Engineering photosynthetic bacteria as factories for the sustainable manufacturing of vitamins and medications

Permalink

Author

Hicks, McKenna

Publication Date

2019

Peer reviewed|Thesis/dissertation

UNIVERSITY OF CALIFORNIA

SANTA CRUZ

ENGINEERING PHOTOSYNTHETIC BACTERIA AS FACTORIES FOR THE SUSTAINABLE MANUFACTURING OF VITAMINS AND MEDICATIONS

A thesis submitted in partial satisfaction
of the requirements for the degree of

MASTER OF SCIENCE

in

MICROBIOLOGY AND ENVIRONMENTAL TOXICOLOGY

by

McKenna Hicks

June 2019

The Thesis of McKenna Hicks
is approved:

———————————————————

Professor David Bernick, Chair

———————————————————

Professor Karen Ottemann

———————————————————

Professor Chad Saltikov

———————————————————

Lori Kletzer
Vice Provost and Dean of Graduate Studies

Table of Contents

List of Figures

List of Tables

Abstract

Engineering photosynthetic bacteria as factories for the sustainable manufacturing
of vitamins and medications

by

McKenna Hicks

Much of the world struggles with inadequate access to essential medicines and proper nutrition due to high pharmaceutical prices and unreliable distribution. Moreover, the industrial chemical synthesis of such products has a detrimental environmental impact due to the sheer volume of hazardous byproducts generated in the manufacturing process and the exorbitant energy overhead. My solution is to decentralize the production of these critical resources by engineering cyanobacteria to produce essential medicines and supplements sustainably, photosynthetically, and on-site at local healthcare facilities. Biosynthesis of products in cyanobacteria is eco-friendly because they use sunlight as their energy, water as an electron donor, and air as their carbon source. I have undertaken two separate engineering endeavors in *Synechococcus elongatus* PCC 7942 to produce acetaminophen and human-usable vitamin B12. The genes for acetaminophen, *4ABH* and *nhoA*, were transformed into PCC 7942, which was then analyzed via HPLC and a colorimetric assay, and confirmed as acetaminophen-producing. Vitamin B12 assembly was tested in PCC 7942, which was confirmed to remodel its native, inactive pseudo-B12 into human-active vitamin B12. The aim of this B12 work is to show that, since the addition of the genes *ssuE* and *bluB* enable vitamin B12 assembly in PCC 7942, they may also enable its production in the closely-related, edible, and robust cyanobacterium, *Arthrospira platensis*, which contains nearly all essential vitamins, but lacks human-usable vitamin B12. The addition of vitamin B12 to the metabolic spectrum of this organism would improve its nutritional profile and create an easy-to-cultivate multivitamin. To facilitate the first steps of this work, I developed a novel axenicity protocol for *A. platensis*, and sequenced the genome of strain UTEX 2340 using the Oxford Nanopore MinION. This sequencing identified a novel cyanophage present within the *A. platensis* genome. This work paves the way for solar-powered chemical synthesis and furthers research into *A. platensis* and its biotechnological applications.

Acknowledgments

I would like to first acknowledge my PI, committee chair, and dear friend, Dr. David Bernick, for his endless support, guidance, and training the past couple of years. From experiment troubleshooting, to making sure I ate and got enough sleep – I would not be where I am today without him. I would also like extend my deepest gratitude towards the rest of my committee, Dr. Karen Ottemann and Dr. Chad Saltikov, for their valuable advice and teaching. This work would not have been possible without the UCSC Microbiology and Environmental Toxicology department, which allowed me to conduct this research. I gratefully acknowledge the UCSC Biomolecular Engineering department for allowing me to use the teaching lab space for the first year of my research.

I would like to thank the UCSC iGEM 2017 team, Bugs Without Borders, with whom I began this research journey. I would specifically like to acknowledge my mentor and friend, Logan Mulroney, who was my iGEM mentor the summer before I began my graduate research until today. I would also like to thank the current and past members of the SynBio Lab group who have helped me with my lab work, specifically Thuy-Khanh Tran Dao, Sophia Sneddon, and Melody Azimi.

I would like to thank my previous PI, Dr. Christopher Vollmers, for first introducing and training me to research, and secondly for his help with my MinION library preparation. I very much appreciate the support from the Akeson Lab, who helped with my MinION sequencing runs and allowed me to occasionally use their lab space. I thank the Millhauser Lab, and their PhD student Graham Roseman, for letting me use their lyophilizer. I acknowledge my friend, Colin Hortman, for teaching me how to operate the HPLC. Special thanks to my boyfriend, Henry Hinton, for setting up the HPLC, helping me with some figures, doing copious amounts of proofreading, and listening to me vent my frustrations to him.

I thank my family for their support throughout my graduate career, especially my grandparents. I also owe a huge thanks to my cats, Poo and Zoey, for their emotional support during these stressful couple of years.

1 Harnessing a sustainable future using *Arthrospira*: a review of current technologies and future prospects

1.1 Introduction

Arthrospira is a genus of cyanobacteria (blue-green algae), which are thought to be Earth's first oxygen producers [1]. *Arthrospira* are microscopic, photosynthetic, filamentous prokaryotes that form multicellular cylindrical trichomes [2]. The cells forming the trichomes align in a pattern that varies from tightly coiled to linear and this spiral structure contributes to the name "*Arthrospira*". Figure 1 shows helical and linear trichomes of *Arthrospira*.
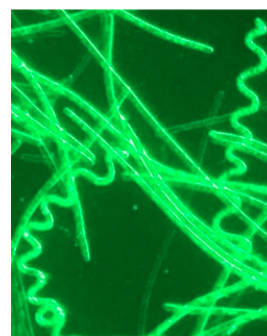
Arthrospira are commonly referred to as *Spirulina*, which is more traditional than taxonomic. Previously, species forming helical trichomes were classified into a

Figure 1: Coiled and uncoiled *Arthrospira* trichomes.

single genus, *Spirulina*, but recent biochemical, morphological, and physiological studies showed two clearly different genera and that the edible *Arthrospira* species have little in common with *Spirulina* species [2]. Furthermore, *16S rRNA* and *rpoC1* gene sequencing showed that *Arthrospira* strains formed a tight cluster that was distinct from *Spirulina* [3]. Consequently, the confusing nomenclature of *Arthrospira* was born. Commercially, the term *Spirulina* refers to the Food and Drug Administration (FDA) approved *Arthrospira*; the most commonly consumed strains are *A. platensis* and *A. maxima* [4]. Historically, *Arthrospira* species such as *A. platensis* and *A. maxima* were grouped into the genus *Spirulina* and thus had the names *S. platensis* and *S. maxima*, but the recent separation of the two genera changed the name of these species to their current *A. platensis* and *A. maxima*.

Arthrospira have been consumed by humans for centuries, dating back to ancient civilizations like the Aztecs [5]. *Arthrospira* are consumed around the world for the nutritional benefits and are considered one of the most nutrient dense organism in the world [6].

Arthrospira grow under simple conditions, requiring only sunlight, water, CO_2, nitrogen, and salts for survival [7]. *Arthrospira* thrive in alkaline (pH 9-11) and high-salt environments, making it difficult for many contaminating species to survive [7]. Their simple cultivation and resistance to contamination makes *Arthrospira* an attractive organism for many biotechnological and agricultural applications.

In a laboratory setting, *Arthrospira* are commonly grown in one of many standard media recipes [8, 9], though approximately 80% of the cost of cyanobacteria cultivation are due to consumption of these medium nutrients and water [10]. Because the ingredients for these optimized mediums can be expensive, several studies have successfully shown *Arthrospira* growth using cheaper non-conventional ingredients, including human urine [11], commercially available fertilizers and salts [12], seawater [13], and various kinds of agricultural, domestic, and industrial effluents (see Section 1.2). The culturing success using these alternative ingredients demonstrates that *Arthrospira* can be cheap and easily cultivated in geographic locations spanning from rural to urban.

Arthrospira have many sustainable biotechnological applications, including effluent (wastewater) treatment, biofuels, nutritional supplementation, and abundant medicinal properties. While fixing CO_2, *Arthrospira* are able to clean up pollutants from wastewater and the biomass can in turn be used as a feedstock for biofuels. The dense nutrient composition and simple cultivation of *Arthrospira* render it a promising remedy for micronutrient deficiencies, which affect more than two billion people around the world according to the Centers for Disease Control and Prevention (CDC) [14]. Lastly, *Arthropira* have been shown to remedy multiple metabolic dysfunctions, have anti-inflammatory, antioxidant, anti-angiogenic, anti-cancer, and anti-viral properties, and have both radio- and neuroprotective benefits.

The above applications had been demonstrated with wild-type *Arthrospira* and its extracts. With the growing industry of genetic engineering, the aforementioned applications of *Arthrospira* can be considerably improved and its biotechnological applications can be expanded. Previously, a stable genetic transformation system for *Arthrospira* was widely sought after but nonexistent. Recently, though, a stable

transformation of *Arthrospira* was achieved, a feat that the scientific community has long been awaiting [15].

This review discusses the biotechnological applications of *Arthrospira*, future prospects of these applications, and their overall role in harnessing a sustainable future.

1.2 Phycoremediation

Phycoremediation is a form of bioremediation in which algae is used to treat wastes [16]. *Arthrospira*'s simple cultivation allows them to thrive in a wide range of growth media, including wastewater. Some wastewater pollutants, such as nitrogen or phosphorus, foster *Arthrospira* growth, which simultaneously clears these pollutants from the water. Using wastewater to cultivate *Arthrospira* provides a sustainable cycle for water treatment; the *Arthrospira* can clean the water for recycling or release into the environment, and the resulting *Arthrospira* biomass can be used for biofuel production – all while fixing CO_2.

The high cost associated with harvesting cyanobacterial mass from these systems previously hindered the development of this technology [17]. This cost projection has recently decreased with the advent of flocculation and flotation harvesting, which takes advantage of the low-density of cyanobacteria and their ability to float [17, 18]. *Arthrospira* have gas vesicles that enable natural flotation. Researchers found that *A. platensis* float to the water surface during logrithmic growth and that this flotation is exacerbated with the addition of NaCl [17]. Various coagulants and/or surfactants, such as Al^{+3} and cetyl trimethylammonium bromide (CTAB), can be used to coagulate and enhance the migration of cyanobacterial mass to the surface of the water, enabling easy collection [18].

1.2.1 Domestic wastewater and pollution

Arthrospira have shown promise as a sustainable treatment of domestic wastewater. A 2018 study examined the ability of *A. platensis* to clean the Yamuna River water, which is considered India's most polluted river (Figure 2)[19]. This study

found that *A. platensis* cultivated in the Yamuna water using a sunlight wavelength removed nitrate (99.76%), lead (99.22%), nickel (100%), cadmium (90.80%,), and copper (68.57%) [19]. *A. platensis* cells cultivated in the Yamuna water also showed a 16.45% increase in lipids, which are of interest for biofuel production (see Section 1.3). *A. platensis* can also effectively treat saline wastewater, which is applicable to future use because the growing shortage of freshwater makes the use of seawater a viable replacement for toilet water. *A. platensis* grown in synthetic saline wastewater mixed with fresh washing wastewater showed a growth of 0.76g/L with removal of 79.96% of total nitrogen (TN), 93.35% of total phosphorus (TP), and 90.02% of chemical oxygen demand (COD) [20]. In addition to saline wastewater, *A. platensis* cultivated in synthetic municipal wastewater showed a biomass content of 262.50mg/L with 81.51% removal of nitrogen and 80.52% removal of phosphorus with nutrients recovery efficiency of TN and TP of 92.58% and 94.13%, respectively [10].

Figure 2: The Yamuna River in India is one of the most polluted rivers in the world. *Arthrospira* is a sustainable method that can clean the river water. *Image source: India Today 2016.*

1.2.2   Industrial wastewater and heavy metals

In addition to domestic wastewater treatment, *Arthrospira* have been studied for phycoremediation of industrial wastewater due to their ability to withstand and remove heavy metals, even in complex mixes [21, 22]. This was exhibited when, in just one hour, the metal ion uptake by *A. platensis* from complex industrial

effluent removed chromium (37%), zinc (50%), aluminum (60%), strontium (68%), iron (94%), and barium (100%) [22]. Moreover, *A. platensis* cultured in 50% tannery effluent showed removed chromium (71.92%), cadmium (81.54%), and lead (73.04%) [21], which are among the worlds most frequent toxic heavy metals according to the ATSDR's Substance Priority List. Arsenic is first on the ATSDR list, which *A. platensis* accumulates from contaminated water [23]. Another study observing *A. platensis* absorption of industrial effluents removed 100% of chromium and 94% of nickel from a chromium-containing effluent [24]. Additionally, *A. platensis* is suitable as a possible industrial effluent treatment with silver [25] and zinc [26]. *Arthrospira* are undoubtedly well suited to removing heavy metals from wastewater, and using *Arthrospira* to treat heavy metal contamination is considered more economically feasible and sustainable than the standard use of chemical precipitation and ion exchange [21].

1.2.3   Agricultural wastewater

Beyond industrial wastes, *Arthrospira* have been investigated for their ability to clean up a plethora of agricultural wastes. The growth of *A. platensis* in wastewater taken from a shrimp farm in Thailand was investigated, and results showed a decrease in COD, nitrogen, zinc, lead, and copper after cultivating *A. platensis* in the wastewater for 30 days [27]. These findings show that shrimp wastewater can be used to cultivate *A. platensis* and simultaneously improve water quality. In another study, *A. platensis* was used to treat fish farming wastewater and caused a 94.8% decrease in the concentration of ammonia, nitrite, nitrate, and phosphate, rendering the *A. platensis*-treated wastewater safe for re-use or release into the environment [28].

Two studies on anaerobically digested wastewater from pig farms concluded the wastewater as a suitable medium for *A. platensis* [29, 30]. The 2017 study reported a high biomass yield with 99% removal of ammonium from the anaerobically digested piggery wastewater (DPW) [29]. The 2010 study cultured *A. platensis* in enriched 20% DPW and reported a high biomass yield and high removal rates for bicarbonate

(380mg/L/d), nitrogen (34 mg/L/d), and phosphorus (4 mg/L/d) [30]. This 2010 study also concluded that the DPW medium was approximately 4.4 times cheaper than the standard *Arthrospira* modified Zarrouk's medium [30].

Arthrospira cultivated during phycoremediation can be used for biofuel production. A 2018 study evaluated *A. platensis*'s biofuel potential when cultivated in dairy farm wastewater, finding that the wastewater supports *A. platensis* growth and fosters a lipid composition that yields suitable biodiesel [31]. Furthermore, the *A. platensis* reduced the COD, phosphate, nitrate, and nitrite concentrations by 98.4% to 100% in just 4 days. This study highlights that *Arthrospira* water treatment can provide a sustainable cultivation of crops for both food and biofuel.

1.2.4 Concluding remarks: phycoremediation

Water is Earth's most precious resource, and billions of people from around the world face severe fresh water scarcity [32]. Water must be conserved and recycled whenever possible, but unfortunately not all current infrastructures incorporate cleaning and recycling of wastewater, leading to polluted waterways and wasted resources. *Arthrospira* have the ability to clean domestic, industrial, and agricultural wastewater using only sunlight and the wastewater as fuel. The water can then be recycled or safely released into the environment, and the *Arthrospira* biomass resulting from the phycoremediation can be used as a source for biofuels.

1.3 Biofuel

Biofuel, fuel derived from biomass, is emerging as an eco-friendly and renewable alternative to fossil fuels. Currently, fossil fuels provide over 70% of the worlds energy [33]. Fossil fuel is a finite resource that will eventually be depleted, thus renewable resources must be developed to eventually replace fossil fuels. Biofuel is the only renewable resource able to replace conventional transportation fuel without any major changes to vehicle machinery [34].

Fortunately, *Arthrospira* is capable of providing multiple types of biofuel. It produces hydrogen via autofermentation and the cell mass of *Arthrospira* can be

anaerobically digested to produce methane, both of which are forms of gaseous bio-fuel. The lipids or carbohydrates in *Arthrospira* are used as a feedstock that can be converted to bioenergy; lipids convert to biodiesel and carbohydrates convert to ethanol [35]. *Arthrospira*'s extreme growth conditions of high pH and high salt protect it from contamination, which allows for a more controlled growth environment and higher productivity. Furthermore, its simple cultivation in sunlight and water, or effluent, combined with its ability to fix CO_2 makes it a safe and sustainable vessel for biofuel production.

1.3.1 Biodiesel

The lipids in *Arthrospira* can be used as a feedstock for biodiesel production. Biodiesel is produced by oil extraction and transesterification; oil extraction is performed with a solvent and transesterification reacts glycerides with an alcohol in a catalyzed reaction to produce biodiesel. One study used *A. platensis* to perform the steps of biodiesel production in a single-stage, producing a biodiesel yield of 79.5% using hexane as a solvent and methanol as an alcohol in an acid-catalyzed reaction [36]. This biodiesel was found to have similar fuel properties when compared to conventional biodiesel and diesel, rendering it a feasible alternative to these conventional fuels. A second study used methanol as a solvent in an acid-catalyzed reaction and achieved an 84.7% yield of biodiesel from *A. platensis* [37]. The quality of this biodiesel was found to be compliant with the European standard for biodiesel, EN 14214. These two studies highlight the feasibility of using *Arthrospira* as a feedstock to achieve high-quality biodiesel.

1.3.2 Hydrogen and methane

In addition to biodiesel, *Arthrospira* can be used to produce hydrogen and methane gas. Hydrogen production via autofermentation has been reported in *A. platensis* [38] and *A. maxima* [39]. *Arthrospira* contain the *hox* genes (*hoxHYEFU*) that encode NiFe hydrogenase, which is a hydrogen-metabolizing enzyme that gives *Arthrospira* the ability to make hydrogen [39]. There are some limitations to this technology,

such as a low solar-to-hydrogen energy conversion efficiency and slow conversion rates under autofermentation conditions [39]. Researchers at Princeton University have investigated these issues by studying the process of H_2 evolution in *A. maxima* [39]. These researchers have found that the key variables for increasing hydrogen production are increased anaerobic ATP production, prior glycogen accumulation, and intracellular reduction potential. The hydrogenase-mediated H_2 uptake reaction was found to be the limiting factor to H_2 yield. Under optimized conditions, the study reported a maximum H_2 production of 36 ml/g dry weight and 18% H_2 in the headspace. This work presents crucial information to the evolution of *Arthrospira* as a H_2 producer.

One study used three stages of fermentation to produce both hydrogen and methane gas using *A. platensis* as a feedstock [40]. *A. platensis* was cultured under nitrogen starvation with CO_2 bubbling and NaCl to increase the carbohydrate content (53.4% of cell mass); carbohydrates are used for fermentative hydrogen production. The cells were then pre-treated with dilute acid and steam heating to give a maximum reducing sugar yield. The pre-treated cells underwent three stages of fermentation i)dark hydrogen ii) photo hydrogen and iii) dark methane. The first two stages produced a hydrogen yield of 429 mL/gVs (milliliter/ gram volatile solids) and the last stage boosted the overall energy yield to 10.51 kJ/gVs. This study highlights *Arthrospira*'s potential to produce hythane, which is a fuel that contains a mixture of hydrogen and methane.

1.3.3 Ethanol

In addition to hydrogen fermentation, carbohydrates are used for ethanol fermentation. *Arthrospira* are typically 15-20% carbohydrate and have high glycogen content (up to 70%), which makes them a potential fermentation feedstock for the production of ethanol [41, 42]. The conventional production of ethanol from plant or algae mass requires multiple pretreatment and enzymatic hydrolysis steps [43], which hinders the development of ethanol as a conventional energy source. A study from Aikawa and colleagues addressed this issue by investigating direct ethanol production

from *A. platensis* biomass using yeast fermentation [43]. They used lysozyme and a recombinant amylase-expressing yeast to eliminate the need for the pretreatment and hydrolysis steps. The fermentation resulted in an ethanol titer of 6.5 g/L and a total ethanol yield relative to glycogen consumption of 86%, which was thought to be the highest yield of bioethanol from an oxygenic photosynthetic organism at the time. They optimized this process by adding $CaCl_2$ to the reaction, which delaminated the polysaccharide layer on the surface of *A. platensis* [44]. This delamination increased the ethanol titer to 48 g/L, which is 93% of the theoretical yield.

Increasing the carbohydrate content of *Arthrospira* could render it as a more useful feedstock for ethanol production [41]. The growth conditions of *Arthrospira* can be manipulated to increase carbohydrate production, but they must be manipulated in a way that still supports total biomass production. For example, phosphorus limitation in the media has been shown to increase the carbohydrate content of the *Arthrospira* biomass, reaching up to 65% dry weight [45, 46]. Because phosphorus is an essential element for ATP, starvation leads to a decreased synthesis of energy-consuming proteins and an increase of carbohydrates and/or lipids [46]. Phosphorus can be decreased an order of magnitude without sacrificing biomass, therefore its limitation promotes carbohydrate production in a way that does not reduce overall yield [45]. Furthermore, under phosphorus limitation *Arthrospira* flocculate and settle, which is useful for biomass harvesting. In addition to phosphorus stress, *Arthrospira* show increased carbohydrate production in nitrogen-stressed conditions. In *A. platensis*, nitrogen limitation was shown to increase carbohydrate content to 74% as well as cause the cells to flocculate and settle [47]. It is hypothesized that nutrient-stressed *Arthrospira* settle because carbohydrates accumulate as glycogen, which has a high specific density (1.40-1.62 g/mL), and in turn causes the density of the cells to increase and therefore sink [47].

1.3.4   Genetic engineering

The studies discussed use environmental stresses to alter the cellular composition of *Arthrospira*. In biofuel research, it is common to edit the genomes of cells

to achieve such changes. One such study altered *Arthrospira*'s genetics using the mutagenesis tool, Atmospheric and room temperature plasma (ARTP), to develop a library of mutants with high carbohydrate content and growth rate [41]. This study generated stable mutants, with one mutant showing a 78% increase in carbohydrates and another mutant showing a 10.5%increase in growth rate.

Like other cyanobacteria, genetically engineering *Arthrospira* for target metabolic processes, such as growth rate or energy component synthesis, would increase its potential in the biofuel industry [48]. A stable system of genetic manipulation in *Arthrospira* was not established until recently, so the field of *Arthrospira* biofuel is expected to grow (see section Section 1.6). Aikawa and colleagues recognized this potential and developed a genome-scale metabolic model of *A. platensis* NIES-39, in which they developed metabolic engineering strategies to increase ethanol and glycogen production [42]. Another genome scale metabolic model had previously been published for *A. platensis*, but it was focused on growth metabolism rather than metabolic engineering strategies [49].

1.3.5 Concluding remarks: biofuels

As fossil fuels begin to deplete, the need for renewable energy sources increases. Biofuels are one of the most promising renewable energy sources because they can be implemented in current machinery without major alterations. *Arthrospira* show promise as one of the keystone species for biofuel production. *Arthrospira*'s ability to grow in wastewater opens the possibility of producing biofuel from waste, which would produce renewable energy and clean water simultaneously. Furthermore, *Arthrospira*'s ability to fix CO_2 makes it an attractive feedstock for fuel production because it would have a negative carbon footprint. It has shown promise as a feedstock for biodiesel, hydrogen and methane gas, and ethanol. All of these results have been achieved by either no treatment or environmental treatment to the *Arthrospira*. With the growing popularity of metabolic engineering, these biofuel processes have the potential to be further optimized through the genetic engineering of *Arthrospira*.

1.4 Nutrition

Arthrospira consumption by humans dates back to the Aztecs, who ate blue-green cakes of "Techuitlatl" [5]. *Arthrospira* have been consumed for centuries because they require simple cultivation and are the most nutrient dense and complete food source in the world [6]. Additionally, these organisms thrive in high alkaline and salt environments, allowing them to evade contamination by other species. These characteristics make *Arthrospira* a promising organism to remedy the micronutrient deficiency aspects of malnutrition. Malnutrition has three sub-categories: hunger and undernourishment, obesity or overnourishment, and micronutrient deficiencies [50]. Essential micronutrients, such as iron, zinc, calcium, iodine, vitamin A, B-vitamins, and vitamin C, are essential for physical and mental development [50]. The WHO estimates that over 2 billion people suffer from micronutrient deficiency, which remains one of the leading causes of global disease burden, especially in low socio-demographically developed regions [51]. The Food and Agriculture Organization of the United Nations (FAO) has issued multiple reports supporting the use of *Arthrospira* to combat malnutrition and has even funded projects in Chad and Angola for developing *Arthrospira* agriculture [52]. The FAO has also urged international organizations to develop small-scale production of *Arthrospira* aimed at providing nutritional supplements for rural and urban communities, diversification of crops in resource-constrained areas, a solution to wastewater treatment, and a high-protein high-vitamin crop for emergency situations [52].

The complete nutrient profile of *Arthrospira* can be found in Table 1, Table 2, Table 3, Table 4, and Table 5; the data is presented as ranges because nutrients vary between sources due to strain and culture conditions. Because all strains are consumed, the data reported stems from the entire *Arthrospira* genus. The current recommended dose of *Arthrospira* per day is 2-8.5g [52]. The general composition of *Arthrospira* is shown in Table 1. In standard growth conditions, *Arthrospira* are composed of 60% protein, 20% carbohydrates, 10% lipids, and the remaining 10% ash and moisture. This nutrient composition can be altered with different growth conditions, such as varying nutrient concentrations, which can produce up to 74%

carbohydrate, 72.5% protein, and 24% lipid [47, 53].

Table 1: The general composition of *Arthrospira*, collected from multiple sources across the entire *Arthrospira* genus. Sources for standard conditions: [52, 54–58]. Sources for altered conditions: [47, 53].

Component	% composition: standard	% composition: alternative
carbohydrates	15.09 - 22.6 %	2.0 - 74.0 %
lipids	7.09 - 13.3 %	5.45 - 23.7 %
proteins	44.9 - 70.0 %	16.5 - 72.5 %
ash	6.70 - 30.9 %	no change
moisture	3.00 - 7.40 %	no change

1.4.1 Amino acids

The amino acid (AA) composition of *Arthrospira* when grown in standard conditions is shown in Table 2. *Arthrospira* has a balanced composition of AAs, providing all 9 essential AAs and 9 non-essential AAs [52, 55, 58–61]. It is worthy to note that one study reported a histidine concentration of up to 10.41 g/ 100g in altered growth media [59].

Table 2: The amino acid composition of *Arthrospira*, collected from multiple sources across the entire *Arthrospira* genus. Amounts are reported in g/100g protein, which is equivalent to g/16g N. Sources: [52, 55, 58–61].

amino acid	composition (g/100g)
Alanine (Ala) (A)	4.7 - 10.81
Arginine (Arg) (R)	4.8 - 10.2
Aspartic acid (Asp) (D)	5.2 - 11.8
Cystine (Cys) (C)	0.3 - 0.9
Glutamic acid (Glu) (E)	7.04 - 17.4
Glycine (Gly) (G)	3.9 - 6.8
Histidine (His) (H)	0.6 - 2.81
Isoleucine (Ile) (I)	3.9 - 7.1
Leucine (Leu) (L)	5.5 - 10.6
Lysine (Lys) (K)	2.4 - 6.2
Methionine (Met) (M)	1.2 -2.75
Phenylalanine (Phe) (F)	1.3 - 5.4
Proline (Pro) (P)	2.1 - 4.6
Serine (Ser) (S)	2.3 - 5.4
Threonine (Thr) (T)	2.9 - 6.6
Tryptophan (Trp) (W)	0.3 - 1.98
Tyrosine (Tyr) (Y)	2.6 - 8.6
Valine (Val) (V)	4.02 - 8.7

1.4.2 Fatty acids

The fatty acid (FA) composition of *Arthrospira* is shown in Table 3 [55, 56, 58, 61, 62]. *Arthrospira* are a rich source of FAs, especially polyunsaturated FAs (PUFA), such as linoleic, γ-linoleic, and α-linoleic acid (LA & GLA & ALA), and monounsaturated FAs (MUFA), such as palmitoleic acid and oleic acid. LA and ALA cannot be synthesized by humans and must be obtained through diet.

Table 3: The fatty acid composition of *Arthrospira* collected from multiple sources across the entire *Arthrospira* genus. Amounts reported in % total fatty acid. Lipid numbers are notated as C:D, where C indicates the number of carbon atoms in the FA and D is the number of double bonds in the FA. Sources: [52, 55, 56, 58, 61, 62].

Common name	lipid number (C:D)	% total lipid	FA type
lauric acid	C12:0	0 - 0.4	SFA
myristic acid	C14:0	0.0 - 0.8	SFA
myristoleic acid	C14:1	0.30 - 0.53	ω-5 PUFA
palmitic acid	C16:0	14.99 - 65.1	SFA
palmitoleic acid	C16:1n-7	1.84 - 12.4	ω-7 MUFA
margaric acid	C17:0	0 - 1.2	SFA
margaroleic acid	C17:1	1.5 - 1.7	ω-8 MUFA
steric acid	C18:0	1.00 - 21.3	SFA
oleic acid	C18:1n-9	1.43 - 35.74	ω-9 MUFA
vaccenic acid	C18:1n-7	1.17 - 1.33	ω-7 MUFA
linoleic acid	C18:2n-6	10.37 - 30.7	ω-6 PUFA
γ-linoleic acid	C18:3n-6	3.1 - 35.0	ω-6 PUFA
α-linoleic acid	C18:3n-3	0-0.71	ω-3 PUFA
stearidonic acid SDA	C18:4n-3	0.57 - 0.81	ω-3 PUFA
arachidonic acid	C20:4n-6	0.34 - 0.41	ω-6 PUFA
timnodonic acid EPA	C20:5n-3	2.21 - 4.94	ω-3 PUFA
cervonic acid DHA	C22:6n-3	2.3 - 3.51	ω-3 PUFA

1.4.3 Minerals

Table 4: The mineral composition of *Arthrospira*, collected from multiple sources across the entire *Arthrospira* genus. Amounts are reported in mg/100g dry weight. Sources: [56, 58, 61].

mineral	composition (mg/100g)	mineral	composition (mg/100g)
Na	121 - 2350.0	Cr	0.09 - 1.59
Ca	110 - 2246.0	Pb	0.21 - 1.29
K	892 - 1936.0	Ni	0.0 - 1.29
P	703.4 - 1397.0	V	0.0 - 0.316
Cl	489.0 - 580.0	Co	0.03 - 0.2
Mg	67.0 - 503.0	La	0.0 - 0.183
Fe	37.6 - 201.6	Sc	0.003 - 0.0248
Mn	3.28 - 55.4	Cd	0.0 - 0.02
Zn	1.42 - 37.5	Sb	0.0 - 0.014
Br	1.79 - 7.79	Hg	0.0075 - 0.012
Cu	0.12 - 6.96	Cs	0.0021 - 0.0081
Se	0.0096 - 3.68	Eu	0.0023 - 0.0063

The mineral composition of *Arthrospira* is shown in Table 4. *Arthrospira* are a rich source of minerals, providing all essential minerals including iron (Fe), potassium (K), calcium (Ca), magnesium (Mg), and zinc (Zn) [52, 56, 58, 61]. *Arthrospira* are particularly rich in iron and zinc which are some of the worlds leading micronutrient deficiencies [14]. Furthermore, bioabsorbed zinc, iodine, and selenium in *Arthrospira* is present in the organic, bioavailable form [63]. *Arthrospira*'s bioabsorption of minerals is effected by its growth conditions and media; the cells absorb the minerals that are present in their environment, which causes different mineral profiles [52]. This bioabsorbtion is what accounts for heavy metal toxins, such as lead (Pb) and mercury (Hg), being found in some *Arthrospira*. Fortunately, when cultivated in controlled conditions, such as those during food cultivation, these heavy metal concentrations are kept at a concentration significantly below the recommended daily intake levels

[64]. Furthermore, a study evaluated the potential toxicity of *Arthrospira* in rats; rats were fed *Arthrospira* as a sole protein source for 75 weeks with no evident toxicity [65].

1.4.4   Vitamins

The vitamin composition of *Arthrospira* is shown in Table 5. *Arthrospira* are particularly high in vitamin C, E, K, and the B-vitamins, though not including vitamin B12 (cobalamin). Contrary to popular belief, *Arthrospira* are not considered a source of human-active vitamin B12; *Arthrospira* instead produces a form of B12 that humans cannot absorb [66, 67]. The lack of vitamin B12 is one major shortcoming of *Arthrospira* as a food supplement because B12 is an essential vitamin and its deficiency is extremely prevalent. B12 deficiency is common in wealthier populations but most prevalent in poorer populations. Surveys have reported deficiency or marginal status in 40% of children and adults in Latin America, 70% in Kenyan schoolchildren, 80% in Indian preschoolers, and 70% in Indian adults [68]. *Arthrospira* are an especially good source of the carotenioid, β-carotene (provitamin A), which the human body converts to vitamin A; vitamin A is one of the world's most prevalent vitamin deficiencies.

In addition to its vitamin content, *Arthrospira* is packed full of healthy pigments, including carotenoids, chlorophyll-a, and phycobiliproteins (i.e C-phycocyanin), these pigments have many therapeutic applications due to their powerful antioxidant capabilities, including anti-inflammatory, anti-tumor and anti-viral properties [69] (See Section 1.5). .

Table 5: The vitamin composition of *Arthrospira*, collected from multiple sources across the entire *Arthrospira* genus. Amounts are reported in mg/100g dry weight. Sources: [57, 60–62, 70, 71].

vitamin	composition (mg/100g)
C (ascorbic acid)	10.3 - 195.3
E (tocopherol)	1.1 - 100.0
K (phytomenadione)	2.2 - 25.5
B1 (thiamine)	1.38 - 15.4
B2 (riboflavin)	0.2 - 3.63
B3 (niacin)	11.3 - 16.62
B5 (pantothenic acid)	0.88 - 0.94
B6 (pyridoxine)	0.131 - 4.0
B7 (biotin)	0.005 - 0.01
B8 (inositol)	74.0 - 76.0
B9 (folic acid)	0.04 - 0.6
A as β-carotene (provitamin A)	22.5 - 214.0
pigments	
carotenoids	456.0 - 477.0
chlorophyll-a	1200.0 - 1300.0
phycocyanin	15600.0 - 16200.0

1.4.5 Remedying micronutrient deficiencies

Arthrospira's simple cultivation allows it to be grown in resource constrained areas, such as rural communities that suffer from undernutrition. Furthermore, it grows in extreme conditions, which minimizes the risk of contaminating mesophilic species during cultivation. A study compared the impact of nutritional rehabilitation with *A. platensis* verses vitamin and mineral supplementation with undernourished children on the Gaza strip [72]. This study concluded that *Arthrospira* was valuable and more effective in treating malnutrition and anemia when compared to conventional multi-vitamin supplementation. Researchers in Kenya noted that undernutrition affects a

substantial amount of people in Kenya, notably children and those in rural communities, and that *Arthrospira* can potentially alleviate these deficiencies because it can be feasibly cultivated in the effected communities [73]. These researchers conducted a feasibility study that evaluated the safety of *Arthrospira fusiformis* harvested from Lake Bogoria in the Kenyan Rift Valley and consulted nearby communities about the potential of incorporating *Arthrospira* into their diets [73]. The study concluded that the *Arthrospira* was safe to eat and have successfully collaborated with communities concerning *Arthrospira* consumption.

1.4.6 Concluding remarks: nutrition

Arthrospira has the ability to alleviate micronutrient deficiencies around the world. It provides nearly all essential nutrients, including all essential amino acids, fatty acids, minerals, and most essential vitamins. Currently, major shortcoming of *Arthrospira* as a nutritional supplement include a foul taste and lack of vitamins B12 and D, all of which can be remedied with synthetic biology and genetic engineering. Taste and smell molecules could be expressed in *Arthrospira* to add flavor, or pathways responsible for the foul flavors could be down regulated. To alleviate insufficient amounts of certain vitamins, the metabolic pathways for such compounds can be engineered into the *Arthrospira* genome. As the fields of synthetic biology and genetic engineering grow, so does the potential of *Arthrospira* to alleviate worldwide nutrition deficiencies.

1.5 Therapeutic properties

Table 6: Summary of the therapeutic properties of *Arthrospira* (in order of first mention. KEY: GLA = Gamma Linoleic Acid, C-pc = C-phycocyanin, Ca-SP = Calcium Spirulan.

condition	therapeutic mechanism and/or source
hyerlipidemia	GLA & C-pc [74–77]
hypertension	vasodialation; C-pc & potassium [75]
hyperglycemia	high fiber & protein content [76, 78, 79]
diabetes type 1	hypoglycemic effect; antioxidants [78]
diabetes type 2	hypolipediemic & hypoglycemic effect [76, 79]
obesity	fat-burning; C-pc & chlorophyll-a [80–82]
rheumatoid arthritis	anti-inflammatory, -oxidant, -angiogenic; C-pc [83–85]
allergic rhinitis	anti-inflammatory [86]
nephrotoxicity	antioxidant [87, 88]
cancer	antiangiogenic; C-pc [89–95]
radiation damage	antioxidant [96, 97]
HIV-1	inhibits replication; Ca-SP [98–101]
measles virus	inhibits replication; Ca-SP [101]
mumps virus	inhibits replication; Ca-SP [101]
pseudorabies virus	blocks adsorption [102]
HCMV	blocks adsorption & inhibits replication; Ca-SP [100–102]
HSV-1	blocks adsorption & inhibits replication; Ca-SP [100–102]
HSV-2	blocks adsorption [102]
HHV-6	inhibits replication; 'spirulan-like' polysaccharides [100]
influenza A virus	inhibits replication; (-) heat-unstable polysaccharides [103]
manic depression	+ serotonin, norepinephrine & dopamine; GLA [104, 105]
alcoholism	GLA [104]
schizophrenia	GLA [104]
neurotoxicity	anti-inflammatory, -ioxidant; C-pc [106, 107]
Parkinson's	anti-inflammatory, -ioxidant; C-pc [108]
Alzheimer's	antioxidant; C-pc [109]

Arthrospira have many proven medicinal properties, rendering them a diverse nutraceutical, or foods with specific medical and health benefits Table 6. Because of it's simple growth conditions, *Arthrospira* can be grown and consumed locally for its medicinal properties in addition to its nutritional benefits, which benefits rural regions that may not have access to medicines. Extracts and specific molecules from *Arthrospira* show therapeutic properties for some of the world's most prevalent

diseases, making them of particular importance for the future of medicine. With the growing field of genetic engineering, the production of therapeutic molecules may be improved in *Arthrospira*. Utilizing *Arthrospira* as a nutraceutical or as a cellular factory to produce therapeutics may provide a more sustainable method of pharmaceutical manufacturing than standard practices because *Arthrospira* has a negative carbon footprint and does not produce dangerous byproducts.

1.5.1 Reversing metabolic dysfunctions

Arthrospira provide protection against metabolic dysfunctions such as hyperlipidemia, hypertension, hyperglycemia, and obesity. With daily consumption, it is a hypolipidemic agent that reduces harmful LDL-cholesterol concentrations and fat deposition in the arteries, while boosting beneficial HDL-cholesterol [74–76]. *Arthrospira*'s hypocholesterolemic effects stem from the presence of γ-linoleic acid (GLA), an essential fatty acid, and C-phycocyanin, a pigment with antioxidant capabilities [76, 77]. In addition to its antihyperlipedemic effect, *A. maxima* was shown to have antihypertensive effects on humans, lowering systolic and diastolic blood pressure in an open sample of Mexican individuals [75]. There are many hypotheses surrounding the antihypertensive effect of *Arthrospira*, including vasoconstriction/vasodialation metabolite control, the antioxidant C-phycocyanin inhibiting platelet aggregation, and high potassium [75]. Hyperglycemia, which is excess blood glucose, is a major concern affecting those with diabetes mellitus [76]. *Arthrospira* supplementation has been shown to significantly decrease blood glucose levels in type 1 and 2 diabetic subjects, indicating that *Arthrospira* supplementation may be a beneficial factor to glycemic control [76, 78, 79]. Furthermore, *Arthrospira* supplementation in type 1 diabetic mice showed increased insulin and improved liver enzyme markers [78]. One hypothesis for the antihyperglycemic effect of *Arthrospira* is that its high fiber content leads to reduced glucose absorption; another theory suggests that the peptides resulting from protein digestion act against hyperglycemia [76]. In addition to its hantihyperglycemic effects, *Arthrospira* supplementation has been shown to reduce weight in obese subjects [80–82]. In a double-blind crossover study, *Arthrospira* ad-

ministered daily was shown to significantly reduce weight and appetite in people with obesity [80, 81]. Though partly attributed to the decrease in appetite, *Arthrospira* remedies obesity by reducing adipogenesis, or the formation of fat tissue, and increasing thermogenesis, or the 'burning' of fat [82]. Attributed to C-phycocyanin and chlorophyll, *Arthrospira* are able to make energy-storing white adipose tissue behave like the energy-using brown adipose tissue, in a process dubbed as 'browning' [82].

1.5.2 Anti-inflammatory activity

In addition to their therapeutic effects on metabolic dysfunctions, *Arthrospira* have powerful anti-inflammatory properties, which have been shown to remedy arthritis in mouse models. In multiple studies, *Arthrospira* was orally administered to mice with experimentally induced arthritis (via zymosan, adjuvant, or collagen) and various physical and biochemical arthritic symptoms were observed. In all studies, mice treated with *Arthrospira* had both physical and biochemical arthritic symptoms return to normal levels [83–85]. The anti-arthritis properties of *Arthrospira* stem from the powerful anti-inflammatory, antioxidant, and anti-angiogenic properties present in *Arthrospira* and its extracts, namely C-phycocyanin [83–85].

The anti-inflammatory effect of phycocyanin is partly due to inhibition of prostaglandin E2 and phospholipase A2, which promote inflammation in mammals [110]. Furthermore, orally administered *Arthrospira* have been shown to decrease serum levels of the inflammatory cytokines COX-2, TNF-α, IL-6, and IL-4; inflammatory cytokines are signaling molecules that promote inflammation [84, 86]. In addition to arthritis, *Arthrospira*'s anti-inflammatory effects have been shown to remedy allergic rhinitis due to the decrease of IL-4, which is a critical regulator to immunoglobulin E-mediated allergy [86].

1.5.3 Antioxidant activity

Excess reactive oxygen species (ROS) cause damage to biological systems and lead to a variety of ailments including metabolic dysfunctions (hyperlipidemia, hy-

pertension, diabetes mellitus), rheumatoid arthritis, nephrotoxicity, malignancy (see Section 1.5.4), radiation-induced tissue damage (see Section 1.5.5), and neurotoxicity/degeneration (see Section 1.5.7). *Arthrospira*'s antioxidant components, such as C-phycocyanins and β-carotene, are able to neutralize ROS and remedy these ailments. For example, *A. maxima* extract was shown to relieve oxidative stress in a type 1 diabetes model, reducing or delaying cytokine-mediated β-cell destruction and enhancing cell survival [78].

Excess ROS are among the main causes of rheumatoid arthritis, along with inflammation and angiogenicity. In both human and animal models, rheumatoid arthritis is characterized with lipid peroxidation and oxidative damage. *A. platensis* has been shown to alleviate rheumatoid arthritis by neutralizing excess ROS, characterized by a decrease in thiobarbituric acid reactive substances (TBARS), a byproduct of lipid peroxidation, and an increase in glutathione, a primary mammalian intracellular antioxidant [84]. *Arthrospira*'s free radical scavenging properties were also shown to protect against gentamicin-induced nephrotoxicity in rats [87] and mercury-induced nephrotoxicity in mice; mercury induces oxidative damage by decreasing glutathione [88].

1.5.4 Anti-angiogenic and anti-cancer activity

Along with its anti-inflammatory and antioxidant effects, *Arthrospira*'s antiangiogenic properties remedy rheumatoid arthritis by reducing vascualar endothelial growth factor (VGEF), which is highly expressed in rheumatiod arthritis [84].

In addition to rheumatoid arthritis, *Arthrospira*'s anti-angiogenic properties render them a powerful tumor suppressor and thus an anti-cancer agent. One study tested *A. platensis*'s therapeutic abilities against dibutylnitrosamine (DBN)-induced rat liver toxicity and carcinogenesis [89]. The study first tested *A. platensis* extract on HepG2 human liver cancer cells and observed inhibition of cell proliferation and induced apoptosis of the cancerous cells. These results were then tested *in vivo* and showed rats that were fed DBN supplemented with *A. platensis* had a significant decrease of liver tumor frequency (20%) compared to the DBN-only rats (80%).

Additionally, expression levels of the tumor suppressor gene, p53, and the cell proliferation marker, PCNA, were significantly reduced in the *A. platensis* supplemented mice compared to the DBN-only mice. Another study evaluated *A. platensis* extract against human non-small-cell lung carcinoma A549 cell line [90]. This 2018 study revealed that *A. platensis* cell extract significantly reduced cancer cell viability and proliferation. The extract inhibited the cell cycle in the G1 phase and induced apoptosis with no apparent cytotoxic effects. Likewise, *A. maxima*'s anti-carcinogenic effect was demonstrated in mice, showing a 51.6% protection against azoxymethane-induced aberrant colon crypts, which are biomarkers for colon cancer [91]. *A. maxima* extract has additionally been proven to inhibit human gastric cancer cell line AGS by 89.22%, human liver cancer cell line Hep3B by 85.22 %, human breast cancer cell line MCF-7 by 73.93%, and human lung cancer cell line A549 by 76.57% [92]. Furthermore, *A. fusiformis* biomass has demonstrated chemopreventative activity in humans by complete reversal of oral leukoplakia (pre oral cancer) in 45% of subjects with no apparent cytotoxic effects [93].

The role of *Arthrospira*'s antioxidant activity with cancer is subject to debate. Cancer cells have increased ROS levels, so *Arthrospira*'s ability to neutralize these ROS may inhibit cancer cell proliferation [95]. On the other hand, an increase of ROS to toxic levels within cancer cells leads to cell cycle arrest and death [95]. Therefore, it is unclear the exact role of *Arthrospira*'s ROS neutralizing properties in cancer. It is certain that *Arthrospira*'s anti-cancer effect can be largely attributed to the pigment C-phycocyanin, which has individually been shown to arrest the cell cycle and induce apoptosis in many different cancer cell lines (see Jiang *et al.* for references therein [94]). As concluded by Jiang *et al.*, C-phycocyanin has immense potential in the treatment of cancer, but the molecular mechanism by which is kills cancer cells must be better understood before clinical use [94].

1.5.5 Radioprotective

Radiation therapy is a widespread treatment of cancer that leads to toxic damage of normal tissues. Radiation treatment for cancer patients can be improved

with radio-protective therapies, which could protect the normal tissue from radiation damage. *Arthrospira* has been demonstrated as a radioprotective agent due to their antioxidant properties; oxidative stress plays a key role in tissue damage caused by radiation [96, 97]. Significant radioprotective effects of *Arthrospira* against oxidative stress and tissue injury induced by gamma radiation have been observed in rats [97] and mice [96]; gamma radiation is used in radiotherapy for cancer. Notably, mice that were treated with *Arthrospira* supplementation prior to gamma radiation showed increased total leukocyte (white blood cell), erythrocyte (red blood cell), and hemoglobin counts [96]. Leukocytes are components of the immune system that protect against infections; an increased number of leukocytes in the blood indicates a boosted immune system that is more capable of fighting infection.

1.5.6 Anti-viral

Arthrospira have powerful antiviral and antiretroviral properties, which is partly attributed to its ability to boost the immune system. A year long study observed the impact of daily *A. platensis* supplementation on the immune system of naive human immunodeficiency virus type 1 (HIV-1) patients in Cameroon [98]. After 6 months, *A. platensis* supplementation was found to significantly decrease the viral load level in patients and significantly increase CD4 cells, which are white blood cells that fight viral and bacterial infections.

In addition to their immune-boosting capabilities, *Arthrospira*'s antiviral activity stems from their polysaccharides, which have the ability to neutralize viruses. Hot water extracts of *Arthrospira* have been reported to inhibit HIV-1, pseudorabies virus, human cytomegalovirus (HCMV), and herpes simplex virus 1 and 2 (HSV), measles virus, mumps virus, whereas cold water extract inhibits influenza A viral strains [99, 101–103].

Calcium spirulan, a sulfated polysaccharide isolated from *A. platensis*, was characterized as a specific antiviral component present in *Arthrospira* hot water extracts [101]. Anti-viral activity from polysaccharide substances similar to spirulan have also been reported against a broad spectrum of enveloped viruses, including HIV-1,

HCMV, HSV-1, and human herpes virus 6 (HHV-6), suggesting that the presence of these polysaccharides in the hot water extracts are responsible for the antiviral activity [100]. One study explored the antiviral effects of both intracellular and extracellular spirulan-like polysaccharides isolated from *A. platensis* and monitored their inhibitory effect on viral replication [100]. Viral entry was not found as the primary antiviral mechanism for HIV-1, whereas both HCMV and HSV-1 were primarily inhibited during viral entry; HHV-6 is thought to have a slightly different mode of action than HCMV and HSV-1. HCMV also had a secondary inhibitory effect during intracellular steps of viral replication. This study also found that hot water extract did not have anti-viral properties against influenza.

Alternatively, a different study showed that *A. platensis* cold water extract inhibits viral plaque formation and replication for influenza A virus, whereas hot water extract did not have anti-flu properties, which agrees with the previously discussed study [103]. Influenza A virus is the only known influenza strain to cause pandemics, and the *A. platensis* cold water extract inhibited influenza A strains, including oseltamivir-resistant ones. The *Arthrospira* hot water extract in multiple studies showed no anti-flu activity, and because calcium spirulan is thermo-stable, it can be inferred that it is not responsible for the anti-viral activity against influenza A virus [100, 103]. Thus, components present in the cold water extract that are not present in the hot water extract have antiviral activities. This study concluded that a high molecular weight, negatively charged, heat-susceptible, polysaccharide is responsible for the antiviral activity in the cold water *A. platensis* extract [103]. The different antiviral modes of action present in *Arthrospira* and its extracts suggest a broad spectrum of future applications owed to robust antiviral mechanisms.

1.5.7 Physchological and neuroprotective activity

In addition to their bodily therapeutic properties, *Arthrospira* have psychological and neuroprotective effects as well. *Arthrospira* are one of the few rich sources of γ-linolenic acid (GLA); GLA deficiency has been connected to alcoholism, manic depression, and schizophrenia [104]. Therefore, consumption of *Arthrospira* may

replenish GLA levels and alleviate these ailments. The antidepressant aspect of *Arthrospira* was examined *in vivo* using carboxymethylcellulose-induced depression in mice and rats [105]. This study conducted behavior tests that are standard to measuring antidepressant activity, such as forced swim and tail suspension tests. Based on this behavioral evidence, the study found that the rodents supplemented with *Arthrospira* showed antidepressant activity via boosting serotonergic, noradrenergic, and dopaminergic systems.

Arthrospira's neuroprotective properties are partly attributed to their anti-oxidant and anti-inflammatory effects [106–109]. Using the HT-22 mouse hippocampal neuronal cell line, one study observed the neuroprotective effects of *A. maxima* extract against trimethyltin-induced neurotixicity [106]. This study observed that in addition to inhibiting ROS production, *A. maxima* extract elevated the levels of pCREB and BDNF, which are both well-studied neuroprotective proteins. A second study observed the neuroprotective properties of *A. platensis* against kainic acid-induced hippocampal damage; kainic acid is known to cause damage specifically to the CA3 hippocampal region [107]. This study administered *A. platensis* to mice for 24 days and a single dose of kainic acid on day 14. The study found that although *A. platensis* did not protect against seizures, it protected against neuronal death in CA3 hippocampal cells. Kainic acid-induced neuronal cell death is related to both oxidative stress and inflammation, including microglial activation, both of which *Arthrospira* provide protection against [107]. Microglia cells mediate immune responses in the central nervous system and their activation is thought to be associated with the development of neurodegenerative diseases such as Parkinson's disease [108]. One study observed the effects of *Arthrospira* on the inflammatory response in rats with α-synuclein induced Parkinson's disease [108]. The study found that rats fed with *Arthrospira* decreased the number of activated microglial cells, likely via increasing the expression of a fractalkine receptor, CX3CR1, on microglia. This study provides a hypothetical mechanism explaining the neuroprotective effects of *Arthrospira* against Parkinson's disease.

In addition to protecting against Parkinson's disease, *Arthrospira* have been

shown to protect against memory dysfunction, such as Alzheimer's disease. One such study administered *A. platensis* water extract to senescence-accelerated prone-8 mice, which are widely used in aging research due to their accelerated aging phenotype [109]. The mice that were fed *A. platensis* showed improved memory function attributed to significantly reduced amyloid β-protein deposition in the brain as well as significantly reduced oxidative damage. Amyloid β-protein is a key factor to the to the pathogenesis of Alzheimer's disease; the proteins make up the plaques found in the brains of Alzheimer's patients. The oxidative damage was reduced via lowering the level of lipid peroxidation (free radical induced lipid damage) and increasing catalase activity, an antioxidant. Increased lipid peroxidation and decreased endogenous enzymes are thought to contribute to the development of Alzheimer's disease. This study demonstrated the mechanisms by which *A. platensis* protects against Alzheimer's disease [109].

1.5.8 Concluding remarks: therapeutics

Arthrospira possess an immense therapeutic potential. Consumption of it's biomass or extract provides protection and therapy to some of the worlds most plaguing ailments including metabolic dysfunctions, arthritis, cancer, viral and retroviral infections, and neurological disorders. Many of *Arthrospira*'s therapeutic properties can be attributed to its powerful anti-inflammatory, antioxidant, and anti-angiogenic properties. The therapeutic potential of *Arthrospira* may be vastly improved with the recent tools of synthetic biology and genetic engineering, for example, the therapeutic molecules already present in *Arthrospira* could be upregulated or further engineered for improved efficacy, or metabolic pathways for completely new molecules may be added into the *Arthrospira* genome. Using *Arthrospira* as a tool for therapeutic production provides a sustainable and accessible method of pharmaceutical synthesis. Cultivation produces a negative carbon footprint and, because of its ease of growth, it can be grown in far reaches of the world and used therapeutically, aiding those that may not have reliable access to such pharmaceuticals. As the field of genetic engineering grows, so does the biopharmaceutical potential of *Arthrospira*.

1.6   Genetics

1.6.1   Genome

To date, eight *Arthrospira* genomes have been assembled: *Arthrospira sp.* PCC 8005, *A. platensis* NIES-39, *A. maxima* CS-328, *A. platensis* C1, *A. platensis* Paraca P0, *A. platensis* YZ, *Arthrospira* sp. TJSD091, and *Arthrospira* sp. TJSD092; the TJSD092 genome was not published in a journal at the time of this paper, but it is published via NCBI by Dong *et al.* under the NCBI accession NZ CP028914 [111–117]. A ninth genome assembly for *A. platensis* O9.13F is in progress under the NCBI accession number NZ PKGD00000000. A table of sequencing statistics and methods for each genome is summarized in Table 7.

Table 7: Summary of genome statistics for different strains of *Arthrospira* [111–117].

strain	size (bp)	sequencing technology
A. sp. 8005	6,279,260	454; Sanger
A. platensis NIES-39	6,788,435	ABI 3730
A. maxima CS-328	6,000,000	n/a
A. platensis C1	6,089,210	Sanger; 454
A. platensis Paraca P0	6,501,886	Illumina HiSeq
A. platensis YZ	6,520,772	ABI3730; Illumina GAIIx
A. sp. TJSD091	6,311,308	Illumina HiSeq
A. sp. TJSD092	6,434,389	Illumina HiSeq; Pacbio

Arthrospira's genome is organized into a single circular chromosome with no plasmid DNA; its size ranges from 6.0 Mbp to 6.78 Mbp. The total genes range from 5885 - 6646, with 807 - 935 being identified as pseudo-genes and 5032 - 5856 as protein-coding genes. The *Arthrospira* genome is highly repetitive, with one study reporting more than 300kb as tandem sequences and another study reporting 9% of the genome as highly interspersed repetitive sequences [111, 114]. Included in these repetitive sequences are an average 3-8 clustered regulatory interspaced short palindromic repeat (CRISPR) arrays, which act as defense mechanisms [111, 112, 117]. Furthermore, the genome is rich with other genes involved with defense mechanisms,

such as group II introns, phage-like sequence defenses, insertion sequences, and other repetitive elements. These defense elements in conjunction with the CRISPR arrays make up 612kb of the genome and are considered the major barrier to a stable transformation method for *Arthrospira* [111, 112, 114].

1.6.2 Genetic manipulation

Random mutagenesis *Arthrospira*'s abundant defense mechanisms have slowed the development of a stable transformation system for targeted genetic alterations. There has been successful non-specific genetic manipulations by way of random mutagenesis, and only until recently has a stable transformation system for targeted genetic edits been reported. Modifying *Arthrospira* opens the possibility of improving the strain for many biotechnological applications. Such improvements can be increasing the growth rate, broadening the growth conditions, or improving production or consumption of certain molecules.

Random mutagenesis is a tool widely used to generate mutants of an organism; it is not considered a form of targeted genetic modification. As previously discussed in Section 1.3, the growth rate and carbohydrate or lipid content of *Arthrospira* must be increased for it to be a viable source for biofuels. Fang *et al.* successfully used atmospheric and room temperature plasma (ARTP), a powerful physical mutagenesis tool, to generate *A. platensis* mutants with high carbohydrate content and high growth rate [41]. Guan *et al.* used ethyl methanesulfonate mutagenesis and low temperature screening to identify *Arthrospira* mutants that grow in lower temperature and light intensity [118]. Mutants that are both temperature and light tolerant could expand the regions suitable for cultivation, lengthen the cultivation season, and decrease production costs [118]. Furthermore, one of these mutants was screened for phytonutrient content and showed a significant increase in chlorophyll-a, carotenoids, C-phycocyanin, allophycocyanin, and phycobiliproteins, all of which have strong pharmaceutical benefits (see Section 1.5).

Transformation Transformations incorporate exogenous DNA to genetically alter a cell; this DNA induces a specific function within the transformed cell via the pro-

duction of recombinant proteins. *Arthrospira* are considered a promising organism for recombinant protein expression due to their high protein content and abundant amino acids, lipids, vitamin, and minerals [15]. There have been few reports of successful transformations within *Arthrospira* because of its abundant defense mechanisms, including cytoplasmic nucleases that cleave foreign DNA [15, 119–121]. The first report of an *Arthrospira* transformation was by Toyomizu *et al.* in 2001 where electroporation was used to transform a chloromphenicol resistance gene into *A. platensis* [119]. The transformants from this procedure did confer chloromphenicol resistance due to recombinant chloramphenicol acetyltransferase, but the resistance could not be maintained and thus the transformation was unstable.

A few years later, Kawata *et al.* modified this electroporation transformation system by implementing a Tn5 transposon, transposase, and cation liposome complex to transform *A. platensis* [120]. This procedure used a methylated chloramphenicol acetyltransferase gene to protect against restriction enzymes and reported chloromphenicol resistance up to 12 months after the transformation, but only with a low concentration of antibiotic. Because of the polyploidy nature of cyanobacteria, it is hypothesized that the chloramphenicol acetyltransferase gene was only integrated into one genomic copy. This partial integration is common with polyploidic cyanobacteria and is overcome by continuing selection pressure; after several generations the integrated element spreads to other copies of the genome [122]. If selection pressure is removed from partially transformed clones, the cells will expel the recombinant gene and return to wild-type. This selection was attempted in this study, but the researchers were unable to isolate a fully resistant *A. platensis* clone, and thus the transformation was unstable.

Jeamton *et al.* implemented a type I restriction inhibitor with the Tn5 transposon and cationic liposome electroporation technique, but showed similar results to the 2004 Kawata *et al.* paper [120, 121]. This study reported antibiotic resistance over multiple generations, albeit at a low concentration, indicating a low expression of the resistance gene; the recombinant fluorescence protein caused no visible fluorescence, presumably due to low expression as well. The study hypothesized that the low

expression was caused by either competition with an endogenous gene under the same promoter or the polyploidy nature of cyanobacteria.

Dehgani *et al.* integration of the foreign genes into the host genome, which may affect essential wild-type genes and host viability [15]. They conducted their own 2018 study, which used an *Agrobacterium*-based system to transfer foreign genes into the genome of *A. platensis*, and reported the first truly successful transformation of *Arthrospira* [15]. *Agrobacterium tumefaciens (A. tumefaciens)* is a gram-negative bacterium that has been used for the stable transformation of various cell types, including plant, fungi, microalgae, and human cells [15]. It contains protective genes against host endonucleases and can transfer its DNA into plant cells and cause tumor formation. The use of a *Agrobacterium*-based plasmid in this study allows *A. tumefaciens* to integrate the genes into the *A. platensis* nuclear genome, achieving stable transformants just 14 days after the initial transformation. Three months after transformation, this study reported a high expression of recombinant fluorescent protein and resistance to high antibiotic concentrations, indicating that the transformants are stable [15].

1.6.3   Concluding remarks: genetics

With the recent success of a stable transformation system, the biotechnological applications of *Arthrospira* can be optimized. *Arthrospira* has been considered one of the most promising hosts for the advancement of biotechnology and by use of genetic engineering and synthetic biology its full potential, which has been discussed for decades, can finally become a reality.

1.7   Future prospects

Arthrospira are among the most promising organisms for a sustainable and technologically advanced future. They harness CO_2 and sunlight to clean up waste, act a feedstock for biofuel, are the most nutrient dense organism in the world, and provide plentiful applications to medicine. These aspects of *Arthrospira* have been recognized by multiple space agencies, such as the United State's National Aeronautics

and Space Administration (NASA) and the European Space Agency (ESA). On long distance space missions, *Arthrospira* can be used to clean waste, as a food source, as a therapeutic, and to produce oxygen. In the ESA's closed-loop artificial ecosystem, The Micro-Ecological Life Support System Alternative (MELiSSA), *A. platensis* is being used as a water and air-cleaning, oxygen-producing, food supplement [123]. Back on Earth, *Arthrospira* can provide a sustainable alternative to current CO_2-producing, chemical-using, or expensive technologies used in today's world.

With the recent discovery of a stable transformation system for *Arthrospira*, its biotechnological applications can be vastly improved. With genetic engineering and synthetic biology, researchers can re-engineer the *Arthrospira* genome and improve upon its metabolic pathways or add entirely new ones. Its ability to clean and grow in wastewater can be improved; its carbohydrate or lipid content can be increased to improve its use as a biofuel feedstock; its vitamin content can be improved by upregulating or adding vitamin metabolic pathways; its therapeutic components, such as C-phycocyanin or GLA, can be upregulated to improve content within *Arthrospira*. *Arthrospira* can be used as a solar powered factory for the synthesis of entirely new molecules, the metabolic pathways of which can be engineered into the genome. By focusing on an edible cyanobacteria, these products can be produced in a food-safe, easy-to-grow photosynthetic culture. Cyanobacteria have immense manufacturing potential because as cellular "factories" they are inexpensive, environmentally friendly, and have simple growth conditions that enable people to grow their own supplies, whether on Earth or in space.

2 Induction of an axenic culture of *Arthrospira platensis* and whole-genome sequencing using Oxford Nanopore and Illumina MiSeq

2.1 Introduction

Arthrospira is a genus of cyanobacteria, which are photosynthetic prokaryotes thought to be Earth's first oxygen producers [1]. *Arthrospira* are filamentous and form multicellular cylindrical trichomes [2].

Arthrospira are alkaliphiles and halophiles, making them resistant to contamination [7]. Furthermore, their cultivation is simple, inexpensive, and fixes CO_2 [7]. These aspects make *Arthrospira* attractive for use in many biotechnological and agricultural applications, including wastewater treatment, biofuels, medicine, and nutritional supplementation.

Consumption of *Arthrospira* dates back to ancient civilizations like the Aztecs [5]. Presently, *Arthrospira* are a globally consumed nutritional supplement and are considered some of the most nutrient dense organisms in the world [6]. *Arthrospira* are commonly referred to as *Spirulina*, though these are actually two separate genera [124]. Commercially, the term *Spirulina* refers to the Food and Drug Administration (FDA) approved *Arthrospira*; the most commonly consumed strains are *A. platensis* and *A. maxima* [4].

The biotechnological applications of *Arthrospira* can be expanded through genetic engineering, a feat only made possible through the recent advances in the stability of their genetic transformation [15]. Genetic engineering requires a contaminant-free (axenic) cell culture, as well as a known (sequenced) genome. Previously, finding an axenic *Arthrospira* strain with a sequenced genome to purchase proved challenging. Furthermore, isolating *Arthrospira* from xenic cultures is difficult because contaminants, such as *Microcystis Aeruginosa*, attach to the *Arthrospira* trichomes.

Previous assemblies report the *A. platensis* genome as being highly repetitive, but all previous published genomes have been assembled using short-read technology, such as Illumina, Roche 454, Sanger, and ABI3730. This brings into question the

assembly accuracy with these repetitive regions [111–117]. One *Arthrospira* genome has been sequenced using PacBio long read technology in conjunction with Illumina, but there is no publication available detailing this genome assembly (*Arthrospira sp.* TJSD092 NCBI Reference Sequence: NZ_ CP028914.1).

Arthrospira platensis UTEX 2340 is an unsequenced, xenic strain available from the University of Texas Culture Collection of Algae. To increase accessibility to *Arthrospira* genetic engineering research, I developed a novel, simple axenicity protocol, and sequenced the genome of *A. platensis* UTEX 2340 using Oxford Nanopore MinION and Illumina MiSeq. Herein is the first *Arthrospira* genome sequenced using the Oxford Nanopore MinION long read technology, the first publication detailing the long read assembly of an *Arthrospira* genome, and the first report of a sequenced *Arthrospira* bacteriophage.

2.2 Materials and methods

2.2.1 Bacterial strain and culture conditions

A xenic culture of *A. platensis* UTEX 2340 was purchased from the University of Texas Culture Collection of Algae (UTEX). The cells were grown in modified SAG medium ranging from 1X to 3X concentrations shaking at 150 rpm in 30°C with 12 hour 80 μmol photons per m^{2}s light cycles using a 90 CRI light source with a color temperature of 3000 Kelvin.

2.2.2 Induction of an axenic *A. platensis* culture

Physical treatments To separate contaminants coagulated with *A. platensis*, 150 mL of cell culture (OD$_{750}$: 2) grown in 1X SAG media was vortexed for 15 seconds followed by 15 seconds on ice for 3 minutes. The culture was filtered using a 20 μm filter and washed with sterile SAG media to remove any contaminating species smaller than 20 μm. Cells that remained on the filter after the filtration process were suspended in 1 mL of sterile SAG and vortexed for 15 seconds. These cells were centrifuged for 10 minutes at 10000 rcf to separate contaminated *A. platensis* and pure *A. platensis* into two phases. *A. platensis* cells coagulated with other bacteria

to form a pellet at the bottom of the tube, while the free-floating *A. platensis* formed a layer on the air-liquid interface. The surface layer of *A. platensis* was collected, resuspended in sterile SAG, and centrifuged at 10000 rcf a second time. The final surface layer was examined with an optical microscope to assess contaminants, and used to inoculate *A. platensis* cultures treated with antibiotics and high pH, from which DNA was extracted and sequenced. I call this *A. platensis* cell separation technique Surface Activated Layer Extraction Method (SALEM).

Optimized technique for collecting floating cells *A. platensis* cultures were inoculated (OD_{750}:0.2) in 1X, 2X, and 3X SAG medium. Each cultures' growth was measured in 24 hour intervals via OD_{750}. Once the cells reached the log phase of growth, the cultures were allowed to settle overnight. The floating cells were collected from the liquid surface, briefly vortexed, and twice centrifuged at 10000 xg for 10 minutes and suspended in sterile SAG. The samples were examined microscopically to assess contamination, and used for a second DNA extraction.

Gas vesicle collapse pressure *A. platensis* gas vesicle collapse was investigated at various pressures. A culture of *A. platensis* settled overnight and cells were collected from the surface of the culture. The cells were centrifuged for 10 minutes at either 0 xg, 2,000 xg, 4,000 xg, 8000 xg, or 16,000 xg. Both the pellet and surface cells from each sample were microscopically examined.

Antibiotic and pH treatment Sterile SAG media was supplemented with 65 μg/mL Ampicillin, 77μg/mL Cefoxitin, and 100μg/mL Meropenem. The pH of the media was adjusted to 12.15 using 6 M HCl and 5 N NaOH. The media was re-sterilized by filtering with a 0.22 μm filter. SALEM 1 separated *A. platensis* cells were inoculated into this media and incubated in the dark for 4 days at 150 rpm and 30 °C.

After 4 days, the cells were filtered through a 1μm filter, gathered from the filter, and suspended in 1 mL sterile SAG. The cells were centrifuged and the top layer collected. A small portion of these cells were inoculated in sterile SAG adjusted to

a pH of 11.8 with HCl and NaOH. The remainder of the cells were used for DNA extraction.

2.2.3 DNA extraction and sequencing

DNA extraction   DNA was extracted from *A. platensis* using a protocol adapted from Morin *et al.* [125]. Cells were resuspended in 0.5 mL of sterile extraction buffer (0.15 M NaCl, 0.1 M EDTA, pH 8.0). The cells were subject to 3 freeze-thaw cycles using dry ice and a 37°C bath to damage the cells walls and increase the efficiency of cell lysis. The cells were then centrifuged, collected from the surface, and resuspended in CTAB buffer (75mM Tris-HCl, 2% CTAB, 1.4 M NaCl, 1 mM EDTA, H_2O, pH 8). These cells were enzymatically lysed with 50 mg of lysozyme at 37 °C for 30 minutes. The lysed cells were then incubated at 37 °C for 1 hour with 2% SDS, 5 mg/mL proteinase K, and 100 μg/mL Rnase A. Following this incubation, the lysed cells were mixed by slow inversion and incubated at 65 °C for 10 minutes to optimize the formation of CTAB -protein and -polysaccharide complexes. The sample was incubated with 1 volume of chloroform:isoamyl alcohol on ice for 30 minutes. The sample was centrifuged for 10 minutes at 3500 xg and the aqueous phase was transferred to a fresh tube using a wide-bore pipette tip. 1 volume of phenol:chloroform:isoamyl alcohol (25:24:1) was added, mixed with gentle inversion, centrifuged for 3 minutes at 3500 xg, and the aqueous phase transferred to a fresh tube. This phenol:chloroform:isoamyl wash was repeated until the interphase was cleared. The aqueous phase was gently mixed with 1 volume of chloroform:isoamyl alcohol, centrifuged for 3 minutes at 3500 xg, and transferred to a fresh tube. This chloroform:isoamyl alcohol wash was repeated 4 more times. The final aqueous phase was gently mixed with 1/10 volume 3M sodium acetate and 2.5 volumes of 100% ethanol to precipitate DNA. The sample was incubated at -20 °C overnight, then centrifuged at 3500 xg for 1 hour at 4 °C to pellet the DNA. The supernatant was removed and the DNA was washed twice with 70% ethanol and mixed with inversion. Following the last wash, the supernatant was removed and the DNA pellets were allowed to dry. The DNA was then incubated in 1X TE at 37 °C until dissolved.

The DNA purity was assessed with a Nanodrop UV/VIS spectrophotometer. The DNA length was observed on a 0.5% agarose gel alongside an NEB 1 kb extended ladder. The DNA from SALEM 2 was selected for high molecular weight DNA via gel extraction.

DNA sequencing   The extracted DNA was sequenced using an Illumina MiSeq and an Oxford Nanopore MinION. The MiSeq library was prepared and sequenced at the University of California Davis DNA Technologies & Expression Analysis Cores. The MinION library was prepared according to the Nanopore 1D Genomic DNA by Ligation (SQK-LSK109) protocol.

Genome assembly 1   The MinION reads were basecalled using Albacore [126]. The basecalled MinION reads were filtered to include fragments 15 kb and above and the reads were assembled using Canu [127]. This genome assembly was polished with signal-level data using Nanopolish [128]. Pilon was used to align the high-accuracy Illumina data to the Nanopolished genome and clean up short inserts, deletions, and SNPs [129]. RAST v 2.0 was used to annotate the genome [130] and SPAdes was used to identify potential plasmid DNA using the Illumina data [131].

Genome assembly 2   The MinION reads were basecalled using Guppy v 2.3.5. The basecalled MinION reads were filtered to include fragments 35 kb and above and the reads were assembled using Shasta [132]. This genome assembly was polished using MarginPolish [133], and polished with the Illumina data using Pilon. RAST was used annotate the genome. CRISPRfinder was used to identify CRISPR clusters [134]. PhyML with 1000 bootstrap steps was used to build a maximum-likelihood phylogenetic tree using the genes phycocyaninB & A [135]. The phylogenetic tree was visualized with Seaview4 [136].

Axenicity verification   Cultures that went through the full axenicity protocol were visually examined for contaminants using microscopy. RNAmmer 1.2 was used to predict ribosomal RNA in the sequenced reads [137]. NCBI BLAST was used to identify what organisms the ribosomal RNA belongs to.

2.3 Results

2.3.1 Axenicity protocol

SALEM 1 *A. platensis* purification via centrifugation acts as an enrichment step by separating *A. platensis* UTEX 2340 from a large portion of contaminating microbes, such as *M. aeruginosa*. Figure 3A shows the phase separation that occurs after centrifuging a mixed *A. platensis* UTEX 2340 culture, where contaminating microbes pellet and *A. platensis* UTEX 2340 forms a layer on the air-liquid interface. Figure 3B shows the first pellet of *A. platensis* UTEX 2340 cells entangled with *M. aeruginosa* (brown). Figure 3C shows the pellet after a second round of centrifugation entangled with less *M. aeruginosa* cells. Figure 3D shows cells collected from the air-liquid interface that are primarily *A. platensis* UTEX 2340. SALEM enriches the *A. platensis* UTEX 2340 purification by removing contaminating organisms with each centrifugation step.
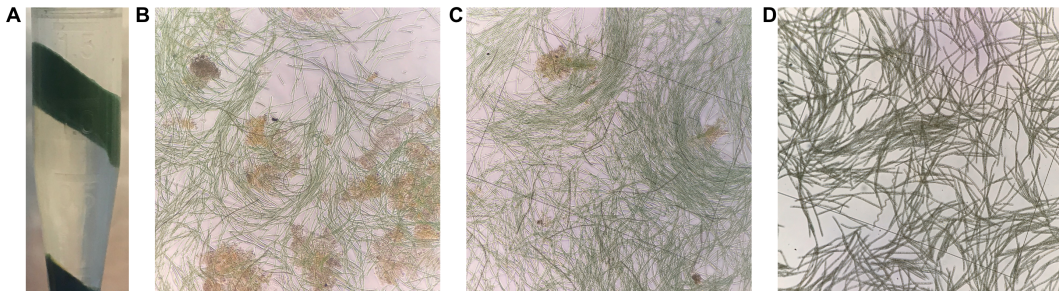
Figure 3: Images of a crude culture of *A. platensis* at various stages of SALEM. A) The phase separation of cells in a microcentrifuge tube. B) The pellet of cells after one round of centrifugation. C) The pellet of cells after two round of centrifugation. D) Cells from the liquid-air interface after two rounds of centrifugation.

SALEM 2 The cells on which SALEM was first performed had been from a mother culture that had been incubating for approximately 6 months with media replenished periodically. Therefore, we sought to expedite this method and induce SALEM in a more controlled manner. We hypothesized that the flotation in *A. platensis* UTEX 2340 was caused by gas vesicles. A previous study reported that *A. platensis* cells showed flotation in log phase of growth due to an optimal protein-to-carbon ratio [17]. Carbohydrate accumulation in the form of glycogen increases the cell density

and thus decreases the buoyancy [138]. When there is a higher protein content in the cells, the gas vesicles outcompete the carbohydrates and the cells remain buoyant.

Furthermore, it was reported that the addition of cations to a cell culture increases its buoyancy, either by increasing the media density or by reducing the negative charge on the outside of the cells that prevents aggregation [17].

To test these hypotheses, *A. platensis* UTEX 2340 cells were grown in various concentrations of SAG media and their growth was monitored. Once the cells reached log phase, they were settled at static condition overnight. The growth curves of each *A. platensis* UTEX 2340 culture in their respective culture medium are shown in Figure 4. The 1X culture grew most efficiently. The 1X, 2X, and 3X cultures showed floating cells on day 3, 4, and 5, respectively, and retained flotation for at least 5 days after. The constant increased concentration of salts in the media did not improve the buoyancy of *A. platensis* UTEX 2340.
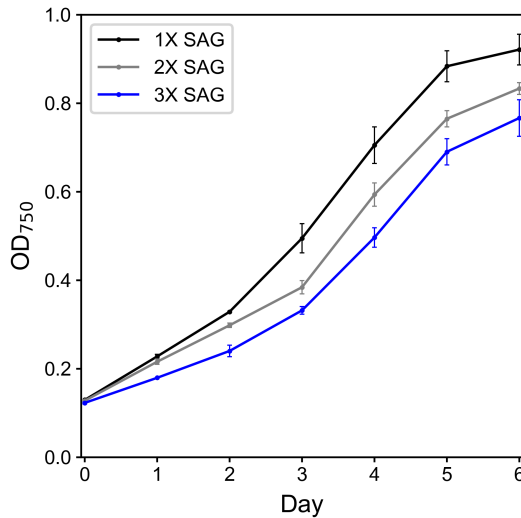
Figure 4: Growth curves of *A. platensis* UTEX 2340 in various concentrations of SAG media. Experiment was performed in triplicate.

Cells were collected from the surface of the culture and SALEM was performed. Figure 5 shows microscopy images of the *A. platensis* UTEX 2340 culture at various stages of this second SALEM. Figure 5A shows the cells collected from the surface without any treatment, it is primarily *A. platensis* UTEX 2340 with small bacteria. Figure 5B shows a pellet of primarily bacteria and some *A. platensis* UTEX 2340

and *M. aeruginosa* after one round of centrifugation. Figure 5C shows surface *A. platensis* UTEX 2340 after this round of centrifugation, with a much lower level of contaminating organisms.
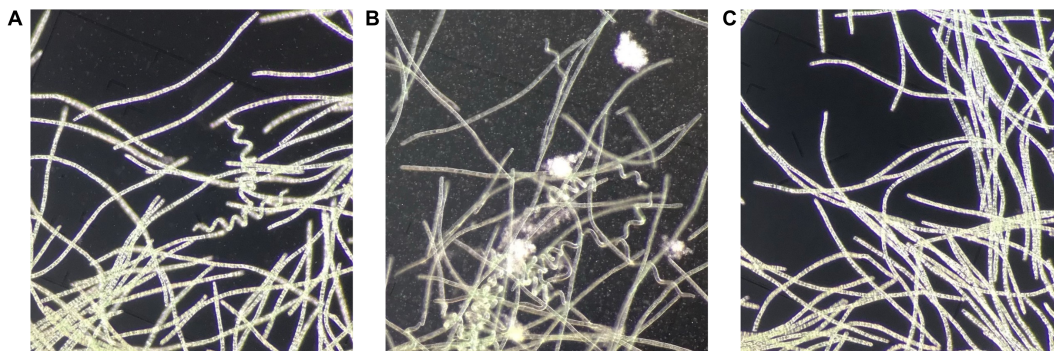
Figure 5: Images of cells at various stages of optimized SALEM 2. A) *A. platensis* floating cells and contaminating bacteria prior to centrifugation. B) Pellet following 10,000 xg centrifugation that contains,*A. platensis*, *M. aeruginosa*, and other small bacteria. C) *A. platensis* culture after SALEM.

Gas vesicle pressure collapse Under pressure, gas vesicles collapse and cells lose buoyancy [139]. I hypothesized that the *A. platensis* UTEX 2340 cells that remained buoyant after centrifugation would have intact gas vesicles, and that the cells collecting on the bottom would have deflated gas vesicles. Under phase contrast microscopy, gas vesicles appear as bright, irregular shapes within the *A. platensis* trichomes [139]. When gas vesicles collapse, they lose this bright appearance and the trichomes appear darker and more hallow [139].

A. platensis UTEX 2340 cells that were buoyant in stagnant conditions were subjected to various pressures via centrifugation to observe any changes in their gas vesicles. Bright gas vesicles are clearly seen in Figure 6A - D, which are buoyant cells collected after centrifuging at 2000 xg, 4000 xg, 8000 xg, and 16000 xg, respectively. Figure 6E - H shows the pelleted cells after their respective centrifugation pressure. With increased pressure, the *A. platensis* trichomes appear to darken, which is indicative of gas vesicle collapse.

Some of the contaminating organisms in these cultures also have gas vesicles, such as *M. aeruginosa* [140], yet they pellet from centrifugation. I hypothesize that these

organisms' gas vesicles have a lower pressure threshold for collapse. Alternatively, *A. platensis* UTEX 2340 is the most abundant species, so it is more likely to have a subpopulation of cells with hardier gas vesicles.
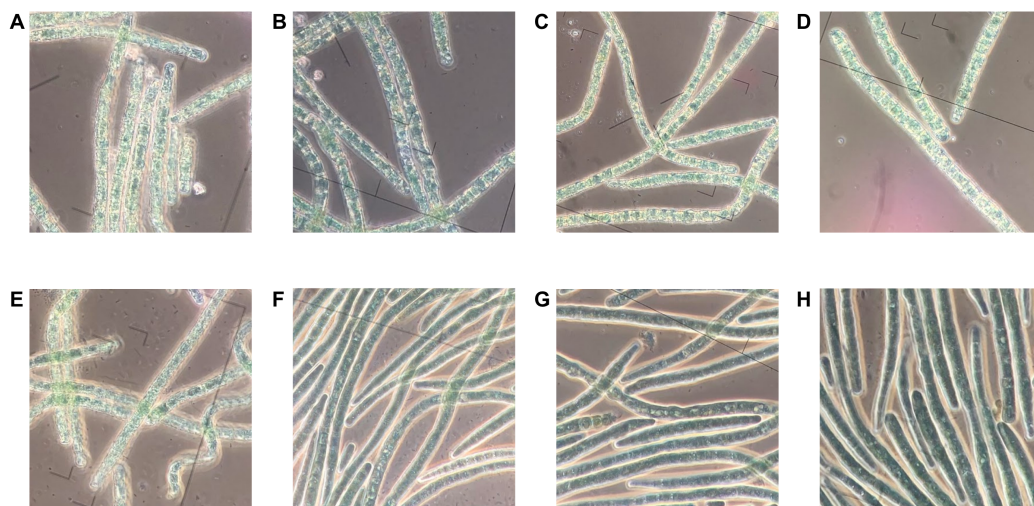
Figure 6: A-D) Floating *A. platensis* UTEX 2340 cells after centrifugation at A) 2000 xg, B) 4000 xg, C) 8000 xg, D) 16000 xg. E-H) Pelleted *A. platensis* UTEX 2340 cells after centrifugation at E) 2000 xg, F) 4000 xg, G) 8000 xg, H) 16000 xg.

pH and antibiotic treatments   The xenic *A. platensis* UTEX 2340 culture was subject to pH and antibiotic treatments following vortexing, filtering, and conducting SALEM. Based on a previous report, high pH was used to eliminate *M. aeruginosa* [141]. Figure 7A is a 1000x phase contrast microscopy image that shows a trichome of *A. platensis* surrounded by a colony of *M. aeruginosa*. Figure 7B shows lysed *M. aeruginosa* surrounding *A. platensis* UTEX 2340 after incubating at pH 12.15 for 4 days.

The antibiotic mix most effective at eliminating contaminants while keeping *A. platensis* UTEX 2340 alive was 65 μg/mL Ampicillin, 77 μg/mL Cefoxitin, and 100 μg/mL Meropenem. The antibiotic treatment was concurrent with the pH treatment. These antibiotics were used based on previous reports [141, 142]. Figure 7C shows dark field microscopy (400x) of an axenic *A. platensis* UTEX 2340 culture following the entire axenicity protocol: vortex, filter, SALEM, pH and antibiotic treatment.
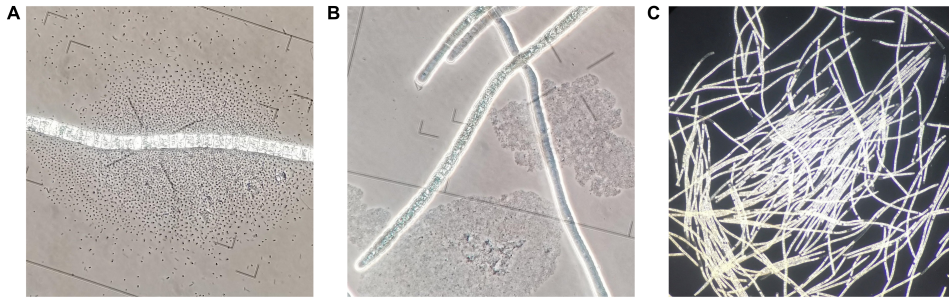
Figure 7: Images of cells at various stages of the pH and antibiotic treatments. A) *A. platensis* UTEX 2340 prior to any pH treatment, surrounded by *M. aeruginosa*. B) *A. platensis* UTEX 2340 and *M. aeruginosa* after pH treatment. C) *A. platensis* UTEX 2340 culture after SALEM, pH, and antibiotic treatment.

Axenicity   The axenicity of this culture was verified by identifying ribosomal RNA sequences within the Illumina sequencing data. Only ribosomal RNA from *A. platensis* was detected, indicating that the axenicity protocol was successful in eliminating contaminating organisms. This protocol takes just 7 days, a significant improvement over previous published *Arthrospira* axenicity methods. Shiraishi *et al.* produced an axenic *A. platensis* culture by performing a series of serial dilutions with individually-selected trichomes of *A. platensis* UTEX 1926, which were inspected for axenicity and then propagated for one month to populate an axenic culture [143]. Sena *et al.* produced an axenic A. platensis Lefevre 1963/M-132-1 strain by filtering 20 mL of contaminated culture, which were then subjected to a 72-hour, high pH treatment followed by a 48-hour antibiotic treatment. This culture was then propagated for 2 weeks to generate enough cells for serial dilutions. In total, this method took upwards of 3 weeks [141]. One method described by Choi *et al.* reported axenicity of *A. platensis* SAG 21.99 in 3 days using a washing step and an antibiotic treatment, but this method was verified only via microscopy and agar plating, which are not as reliable as molecular-level assays, such as 16s and 23s *rRNA* identification that was performed herein [142]. Furthermore, the *A. platensis* SAG 21.99 starting culture did not contain *Microcystis* and comprised an assortment of actinobacteria, γ-proteobacteria, and Firmicutes. The axenicity method presented herein addresses *Microcystis* contamination, among other bacteria, and achieves axenicity in just one week, which has been verified on the molecular level.

2.3.2 Sequencing

Classification and features A maximum-likelihood phylogenetic tree was constructed using the phycocyanin operon, which shows that the sequenced genome is *Arthrospira platensis* and its closest neighbors are *A. platensis* PCC 8005, TJSD092, CHM, and *Arthrospira maxima* [111, 113].
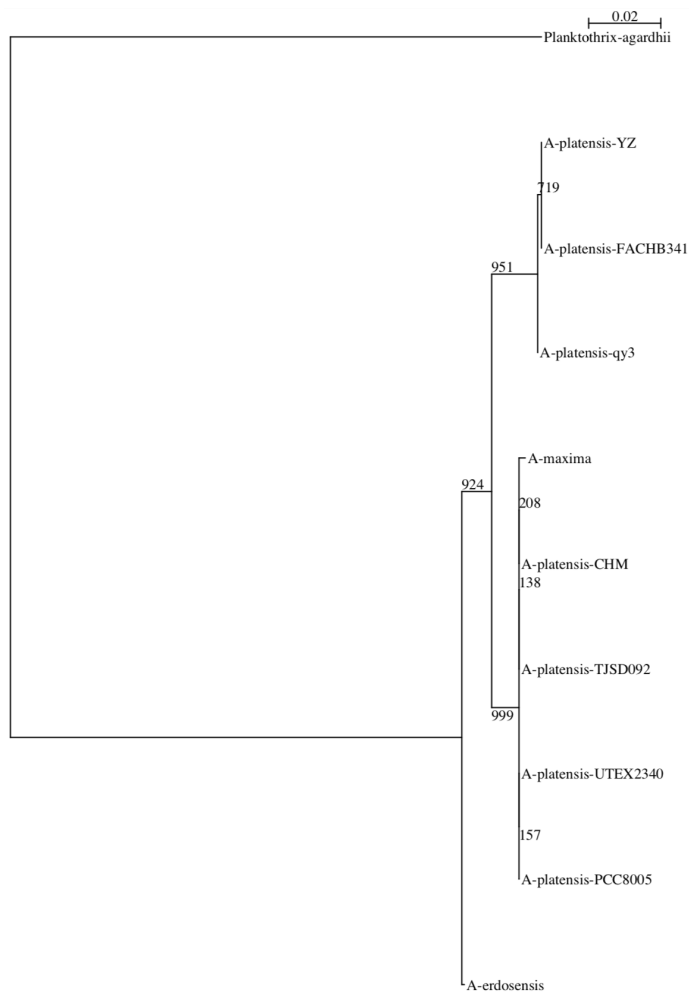
Figure 8: Bootstrapped phylogenetic tree of *A. platensis* UTEX 2340, constructed using Phyml with 1000 bootstrap steps, and visualized using Seaview4. The numbers on the branches represent the number of bootstrap steps that support this configuration, with 1000 being perfect.

Classification and general features of *Arthrospira platensis.*		
Property	**Term**	**Reference**
Current Classification	Domain	
	Bacteria	[144]
	Phylum	
	Cyanobacteria	[145]
	Class	
	Cyanophyceae	[146]
	Order	
	Oscillatoriales	[144]
	Family	
	Oscillatoriaceae	[144]
	Genus	
	Arthrospira	[145]
	Species	
	platensis UTEX 2340	
Cell Shape	Spiral	NAS
Sporulation	None	NAS
Motility	none	IDA
Temperature Range	20-40°C	[147]
Optimum temperature	30-45°C	[147]
pH	8.0-10.0	[147]
Carbon Source	Phototroph, Mixotroph	[147]
Energy Source	Phototroph	[147]
Relationship to oxygen	Aerobic	[147]
Pathogenicity	None	NAS
Origin	Natron Lake, Tanzania	[146]
Habitat	saltwater	[148]
Latitude	2.3436 S	NAS
Longitude	36.0458 E	NAS
Altitude	610 m	[149]
Obtained From	University of Texas, Strain UTEX 2340	[146]

Table 8: Classification and general features of *A. platensis* UTEX 2340 according to the MIGS recommendations [150]. Evidence codes - IDA: Inferred from Direct Assay (first time in publication); TAS: Traceable Author Statement; NAS: Non-traceable Author Statement. These evidence codes are from the Gene Ontology Project [151].

DNA extraction Figure 9 shows 0.5 μg of high molecular weight extracted DNA on a 0.5% agarose gel alongside an NEB 1 kb extended ladder. The DNA extraction yielded DNA with a 260/280 ratio of 1.92 and a 260/230 of 2.43.
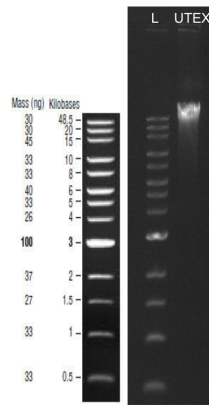
Figure 9: 0.5 μg of DNA extracted from an axenic culture of *A. platensis* UTEX 2340 visualized on a 0.5% gel alongside an NEB 1 kb extend ladder.

Axenic genome assembly   The first genome assembly used the SALEM 1 DNA extraction that underwent the entire axenicity protocol. This data was sequenced using both Illumina Miseq and Oxford Nanopore MinION. Figure 10 shows the different possible orientations that the Illumina data can be scaffolded; this genome path has a multitude of potential genome paths and is a result of using short-read data alone to assemble a genome.
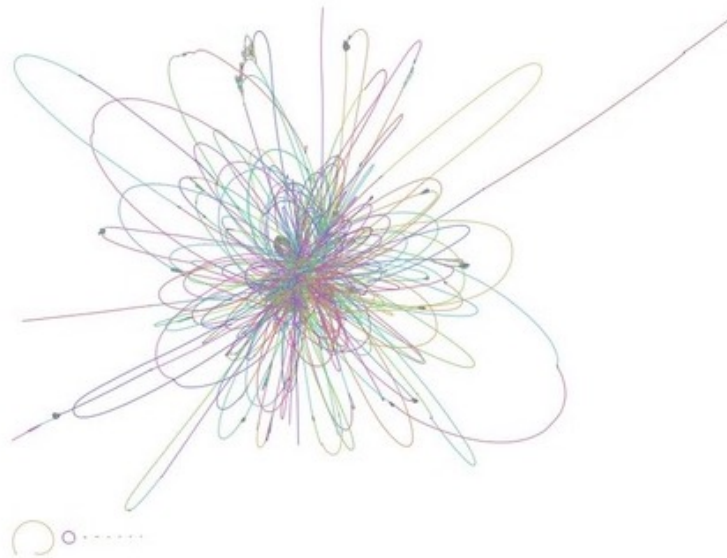
Figure 10: Genome path of an axenic culture of *A. platensis* UTEX 2340 generated with only the Illumina short-read data. Genome path generated with Bandage [152].

Instead, the long-read Nanopore data was used to assemble the genome first.

Because the MinION only has 94% accuracy for 1D sequencing [153], this assembly was polished with the Illumina data, which has over 99% accuracy. Nanopore reads greater than 15 kb were assembled with 56X coverage into 5 contigs with an N50 of 3.29 Mb. These contigs were scaffolded into a 6.465 Mb genome and polished with the Illumina data. The structure of this genome is ambiguous. Figure 11 shows this genome path with the colored contigs linked together in different possible orientations that complete the circular chromosome. Assembling the genome with long read data first was a significant improvement over a stand-alone Illumina-based assembly.
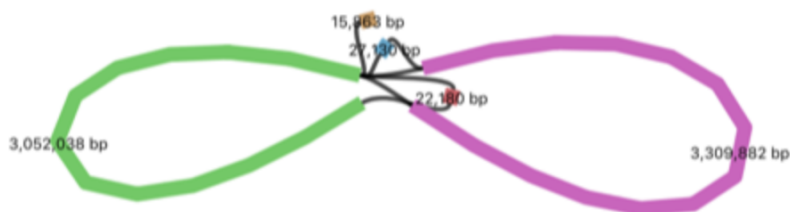
Figure 11: Genome path of an axenic culture of *A. platensis* UTEX 2340 showing a 6.465 Mb genome with an ambiguous circular structure. Genome path generated with Bandage [152].

Putative viral genome   The Illumina data sourced from the axenic DNA extraction was used to predict plasmids using SPAdes. Origin of replications in the potential plasmids were located by visualizing GC skew using Artemis [154], and identifying DnaA binding boxes. With this approach, one predicted plasmid of 11,305 bp (40.4% GC) was isolated (Figure 12). This element appears to be a bacteriophage genome, and possibly a cyanophage, which specifically infect cyanobacteria [155]. This circular construct encodes a Sp6 promoter, 3 tRNAs, an IS630 family transposase, a HNH endonuclease, a tail-fiber domain containing protein, and four hypothetical proteins, two of which have protein K and L fragments, respectively. These are all known characteristics of a viral genome.
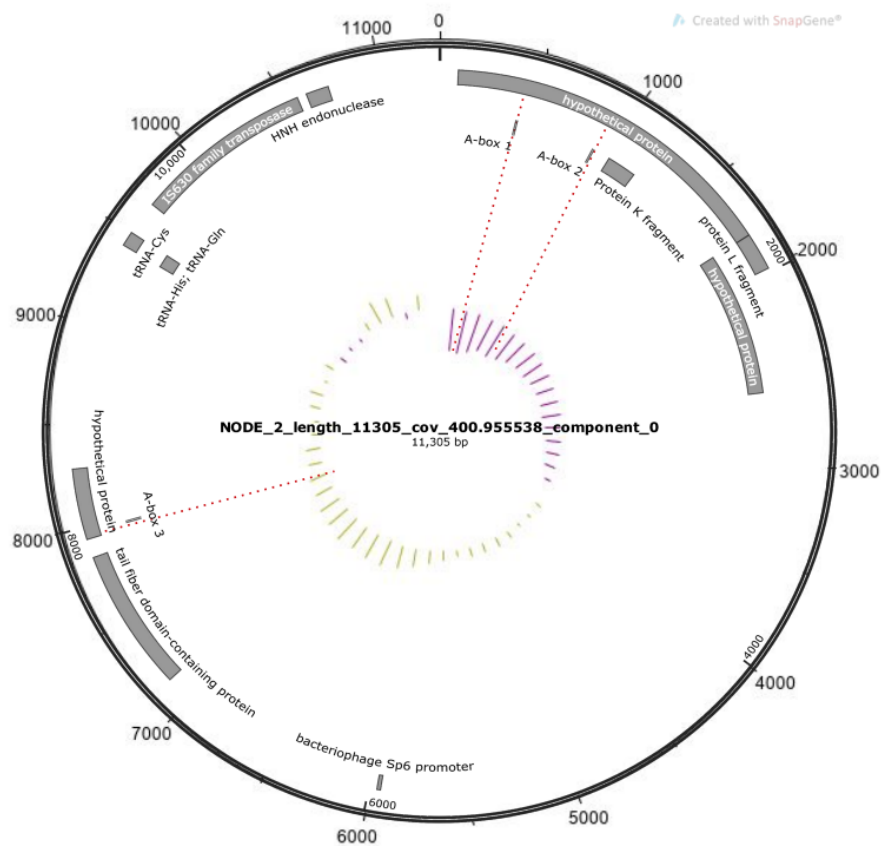
Figure 12: Putative viral genome. GC skew is shown in purple and green. DnaA binding boxes are labeled as A-box. The ori is predicted to be location at position 0, where there is visible GC skew and two DnaA boxes. This construct has components that suggest it is a viral genome.

I determined that the phage was integrated into the *A. platensis* UTEX 2340 genome via a reference-based alignment, and that the phage genome is larger than the 11,305 bp circular construct, indicated by an upstream cluster of hypothetical proteins and a DNA polymerase, shown in pink in Figure 13. The phage genome is roughly 25 kb when the hypothetical protein cluster and DNA polymerase are included. Most encoded genes in bacteriophage genomes are unrelated to known proteins and have unknown functions [156]. A BLAST search on Virus Pathogen Resource (ViPR) showed no significant similarity to already sequenced viral genomes, which expected because bacteriophage genomes are incredibly diverse and rarely have extensive nucleotide sequence similarity to other entries [156].

There have been two reports of *Arthrospira* phages: one in *A. platensis* and

another in *A. fusiformis* [155, 157]. The *A. platensis* cyanophage was determined to be a narrow, host specific virus. The *A. fusiformis* cyanophage study observed infected biomass and its associated affect on flamingos [157]. It is worth noting that the *A. fusiformis* was isolated from an African Soda Lake, a similar habitat to that of *A. platensis* UTEX 2340. According to the KEGG Virus-Host Database, only 20 cyanophage genomes have been sequenced, and an *Arthrospira* phage is not among them; presented herein is the first sequenced *Arthrospira* bacteriophage genome. A BLASTx search of the Phage Tail Fiber Protein downstream of the Sp6 promoter showed that this viral protein is conserved across multiple *Arthrospira* genomes Figure 13. Because Arthrospira is a widely-distributed commercial product, it is crucial to identify and characterize potential sources of disease that may be detrimental to crop health. Further studies must be conducted to characterize this phage.
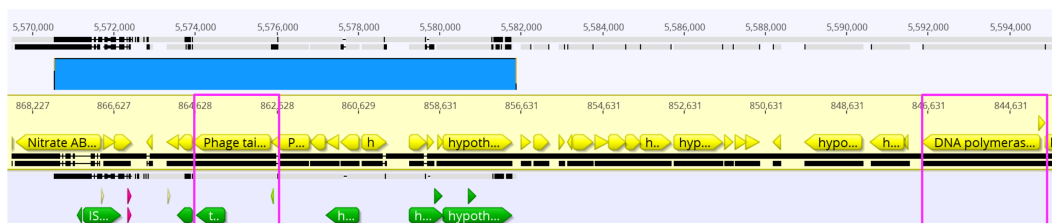
Figure 13: Viral genome integrated into the *A. platensis* genome.

Genome assembly 2   We performed a second sequencing run using high molecular weight selected DNA to obtain reads that elucidate the regions of ambiguity in the first genome assembly. This DNA was only purified via two rounds of SALEM centrifugation and sequenced on an Oxford Nanopore MinION and Illumina MiSeq. The genome was assembled using fragments 35 kb and above from the Nanopore data, and polished with the high accuracy Illumina data. Table 9 contains relevant project information. This assembly produced a 6.44 Mb circular genome in a single contig (44.9% GC). The genome statistics can are summarized in Table 11, and Table 10. A genome path is shown in Figure 14.

A. platensis UTEX 2340 is a non-nitrogen fixing cyanobacterium. The genome

contains type I, II, and III restriction modification systems and abundant CRISPRs, which are some of the main defense mechanisms that inhibit the stable transformation of *arthrospira* [114]. *A. platensis* UTEX 2340 possesses no motility genes, unlike *A. platensis* NIES-39 [112].
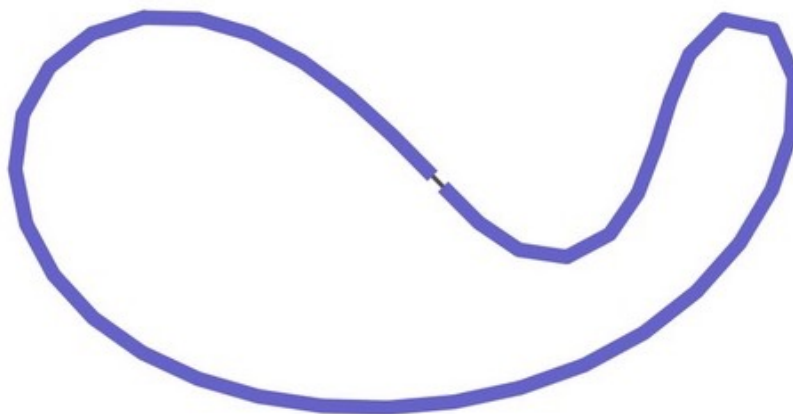
Figure 14: Genome path of the second genome assembly, producing one 6.44 Mb circular contig. Genome path generated with Bandage [152].

Project Information	
Property	**Term**
Finishing Quality	Draft
Libraries Used	Nanopore 1D genomic DNA by Ligation SQK-LSK109
Sequencing Platforms	Oxford Nanopore MinION, Illumina MiSeq
Fold Coverage	87x using fragments > 35 kb
Assemblers	Shasta
Gene Calling Method	RAST, GLIMMER
Genome Database Release	Genbank
Genbank ID	1236701.5
Project relevance	Biotechnology

Table 9: Summary of project information.

Summary of genome		
Label	**Size(bp)**	**Topology**
Chromosome	6,436,916	circular

Table 10: Summary of genome organization

Genome Statistics		
Property	**Term**	**% total**
Genome size(bp)	6,438,226	100.00%
DNA coding region(bp)	5,439,720	84.49%
DNA G+C content(bp)	2,888,727	44.9%
Total genes	7379	100%
Protein coding genes	7335	99.4%
RNA genes	44	0.60%
rRNA operons	2	
tRNAs	37	
CRISPR arrays	5	

Table 11: Summary of genome statistics gathered from RAST and CRISPR finder.

2.4 Conclusion and future directions

The novel axenicity protocol herein provides a simple method to efficiently isolate *Arthrospira platensis* from contaminating organisms, which is crucial in its genetic engineering. *A. platensis* UTEX 2340 is available for purchase from The University of Texas Culture Collection of Algae, and with its genome sequenced, it is an accessible strain for a multitude of applications. This study may help drive forward the development of *Arthrospira* biotechnology, which has been enabled by the recent stable genetic transformation of *A. platensis* [15]. The novel bacteriophage identified in this genome assembly is the first of its kind and plans to further characterize this phage are underway.

3 Engineering photosynthetic bacterium *Synechococcus elongatus* to produce mammalian-active vitamin B12

3.1 Introduction

Cobalamin, more commonly known as vitamin B12, is an essential vitamin that is critical for many bodily functions, such as nucleotide synthesis, metabolism of branched amino acids and odd-chain fatty acids, and methionine and succinyl-CoA synthesis [158]. Furthermore, it is considered an essential prenatal vitamin for nervous system development [159]. Inadequate vitamin B12 consumption is a leading global vitamin deficiency, and the vitamin itself is difficult to naturally acquire, especially for vegetarians [160]. Surveys have reported fully or marginally deficient status in 40% of children and adults in Latin America, and in smaller studies, 70% of Kenyan schoolchildren, 80% of Indian preschoolers, and 70% of Indian adults [68, 160]. Vitamin B12 deficiency can lead to health problems such as megaloblastic anemia and demyelinating nervous system disease [161].

Vitamin B12 chemical synthesis is roughly 70 steps, the most of any other commercially produced B vitamin, and also the most expensive [162]. Microbes can produce vitamin B12 in significantly fewer steps, but current biosynthesis approaches are still costly due to the price of media and lack of genetic tools [162]. Cyanobacteria are a promising host for biosynthesis of vitamin B12 because of their relatively low media cost. They require only water, sunlight, air and a mix of salts, and grow efficiently in seawater and wastewater [7, 13]. Furthermore, cyanobacteria are well-studied organisms for genetic engineering, notably *Synechococcus elongatus* PCC 7942 (hereby referred to as PCC 7942) [163]. Genetically engineering a cyanobacteria to produce vitamin B12 could be more cost effective than other biosynthesis methods because it would not require an added carbon source or vitamin B12 precursor, unlike other approaches [162].
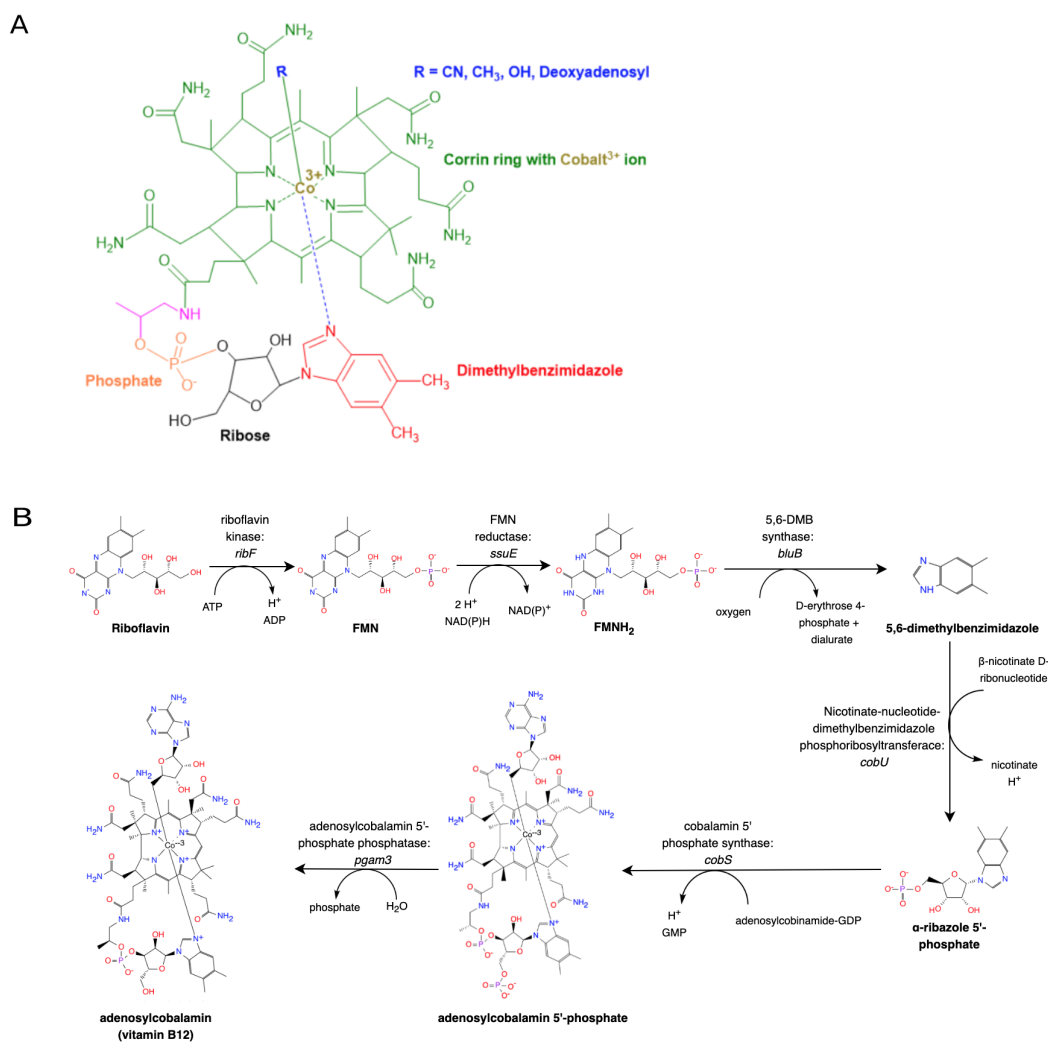
Figure 15: A) The different components of the cobalamin (vitamin B12) molecule. B)The final steps of the vitamin B12 metabolic pathway, which involve the creation and attachment of the lower ligand to cobinamide to make cobalamin. 5,6-DMB is synthesized and then used to make the lower ligand, α-ribazole 5'-phosphate. The lower ligand is attached to make cobalamin 5'-phosphate, which gets dephosphorylated to make cobalamin.

As seen in Figure 15A, vitamin B12 contains upper (blue) and lower (orange, black, & red) ligands [158, 164]. The lower ligand, α-ribozole (orange, black, & red), determines whether a vitamin B12 molecule can be absorbed by mammals into the gastrointestinal tract – it must contain a 5,6-dimethylbenzimidazole (5,6-DMB) base (red) [158, 161]. In the absence of 5,6-DMB, most cyanobacteria instead use cellular adenine as the base in the α-ribozole lower ligand, which makes vitamin B12 inactive in mammals [67, 158]. This inactive form of vitamin B12 is cobamide, which is more commonly known as pseudo-B12.

Figure 15B shows the synthesis of 5,6-DMB from flavin mononucleotide (FMN) using proteins encoded by the genes *ssuE* and *bluB* [158, 165–167]. The lower ligand, α-ribazole 5' phosphate (orange, black, & red), is constructed with either 5,6-DMB (red) or adenine using the gene *cobU* [66, 158, 167, 168]. This lower ligand attaches to cobinamide (green) using the gene *cobS*, making cobalamin 5' phosphate, which is dephosphorylated using the gene *cobC* (or the homologue *pgam3*) to make vitamin B12 [66].

Some organisms, such as *Rhodobacter sphaeroides* and *Dehalococcoides mccartyi*, are capable of remodeling intracellular pseudo-B12 into active vitamin B12 by replacing the adenine base in α-ribozole with 5,6-DMB with exogenously supplemented 5,6-DMB [169, 170]. A previous study by Helliwell *et al.* highlighted that certain microalgal species, *Pavlova lutheri* and *Chlamydomonas reinhardtii*, are capable of remodeling pseudo-B12, but *Synechococcus* is not [66]. This specific conclusion is flawed because it makes a general assumption about all *Synechococcus* strains based on results from strains WH8102 and WH7803 that may not have the molecular machinery needed to construct the lower ligand, α-ribozole, using a 5,6-DMB base. If this were the case, then providing 5,6-DMB to these strains would not be sufficient for α-ribozole synthesis, and thus would not be capable of remodeling pseudo-B12 into active vitamin B12, which is consistent with the study's findings [66].

This uncertainty with WH8102 and WH7803 is rooted in the confusion surrounding the final steps of vitamin B12 synthesis, in which the proteins encoded by *cobC* and *cobS* attach the lower ligand to the cobamide molecule, remove a phosphate group, and make vitamin B12. In one model, the CobC phosphatase acts on α-ribazole 5' phosphate to generate α-ribazole, which is then attached as the lower ligand to produce cobalamin [165]. In the second model, α-ribazole 5' phosphate is first added to cobinamide, generating cobalamin 5'-phosphate, which is then dephosphorylated to generate vitamin B12 [171]. A study from 1991 found that the cobalamin synthase enzyme isolated from *Pseudomonas denitrificans* accepts both α-ribazole and α-ribazole 5' phosphate as substrates [172]. It was generally accepted that the assembly followed the first proposed model in which α-ribazole is attached,

until studies using *Salmonella enterica* showed that the true substrate for the cobalamin synthase is α-ribazole 5'-phosphate and not α-ribazole [171]. This finding was documented in *Propionibacterium freudenreichii* shermanii as well [173]. Thus, the evidence suggests that vitamin B12 synthesis follows the second model, in which cobalamin 5'-phosphate is dephosphorylated (Figure 15).

The CobC protein present in WH8102 is not predicted to have phosphatase activity with cobalamin 5'-phosphate, but rather only with α-ribazole 5'-phosphate [165]. With the current model, therefore,WH8102 would not be able to synthesize vitamin B12 when provided exogenous 5,6-DMB, which is consistent with previous findings [66].

WH7803 only contains the cobalamin salvage pathway, which allows for cobalamin synthesis from exogenous cobalamin, which is imported into the cell, or cob(I)inamide, which is synthesized intracellularly [174, 175]. There is no evidence that WH7803 synthesizes its own cob(I)inamide, and it does not have the cobalamin transporter gene, *btuB*, according to a NCBI BLASTp search [176]. Therefore, WH7803 would likely not be capable of remodeling active vitamin B12 with exogenous 5,6-DMB and pseudo-B12, which is consistent with previous findings [66].

Unlike strains WH8102 and WH7803, PCC 7942 is annotated to have the machinery required to assemble vitamin B12 in the presence of 5,6-DMB: CobU synthesizes α-ribazole 5' phosphate with a 5,6-DMB base, CobS attaches it to cobalamin, and Pgam3 dephosphorylates the complex in iron deficient conditions.

I hypothesize that PCC 7942 can remodel vitamin DMB-B12 with 5,6-DMB, which can be done without exogenous supplementation by engineering the biosynthetic pathway for 5,6-DMB into its genome. PCC 7942 contains flavin mononucleotide (FMN), a precursor to 5,6-DMB, which can be converted to 5,6-DMB via two enzymes: FMN reductase, encoded by *ssuE*, and 5,6-DMB synthase, encoded by *bluB* (Figure 15). The addition of these genes to the PCC 7942 genome could render PCC 7942 an optimal factory for vitamin B12 synthesis.

In this study, this vitamin B12 remodeling hypothesis was proved correct through exogenous 5,6-DMB supplementation of PCC 7942 in iron deficient conditions. A

plasmid was constructed for the stable integration of *ssuE* and *bluB* into Neutral Site I (NSI) of the PCC 7942 genome. This work has the potential to make vitamin B12 production more affordable and environmentally friendly. It also provides a proof of concept for further vitamin B12 engineering in other cyanobacteria, such as a the edible and nutrient dense *Arthrospira platensis* (Spirulina).

3.2   Materials and methods

Materials   All restriction enzymes, polymerase, and competent *E. coli* were purchased from New England Biolabs. Gene blocks were purchased from Integrated DNA Technologies. pAM2991 was generously provided by the Golden Lab at University of California San Diego. 5,6-DMB was purchased from Acros Organics. Adenosylcobalamin standard was purchased from Toronto Research Chemicals. Hydroxocobalamin and methylcobalamin standards were purchased from Spectrum Chemical MFG Corp. Mini-prep kits were purchased from Zymo Research. Gel extraction kits were purchased from Quiagen. DNA ladders were purchased from NEB.

Bacterial strain and culture conditions   *Synechococcus elongatus* PCC 7942 was generously provided by the Golden Lab at University of California San Diego. Cultured cells were grown in BG-11 medium shaking at 150 rpm in 30^oC with 12 hour 80 μmol photons per m^2s light cycles using a 90 CRI light source with a color temperature of 3000 Kelvin [177]. Cells on agar plates were grown in 24 hour light cycles under the same conditions. BG-11(Fe-) medium is made by omitting ferric ammonium citrate from the recipe.

Vitamin B12 remodeling with 5,6-DMB   *S. elongatus* cells were grown in BG-11 media until early log phase (3 days). Then, the cells were centrifuged, washed once with sterile water, and resuspended in fresh BG-ll(Fe-) media. Three of the BG-11(Fe-) cultures were supplemented with 10 uM DMB and the other three remained unsupplemented. The cells grew for 5 more days, then were condensed via centrifugation. Sucrose was added to the medium to a final concentration of 12% and the cells were lyophilized.

Microbiological assay of vitamin B12 Lyophilized cells were assayed for vitamin B12 at Exact Scientific Services Incorporated via the AOAC certified kit: R-BioPharm AG VitaFast® B12 Microbiological Microtiter Plate Test for the determination of Vitamin B12 [178]. Vitamin B12 was extracted from 1g of lyophilized cells and converted to cyanocobalamin by boiling with a 1% NaCN solution. The samples were serial diluted and added to the wells of a microtiter plate coated with *Lactobacillus delbrueckii subsp. lactis (leichmannii)* (*L. delbrueckii*). The plate was incubated at 37°C for 48 hours in the dark and absorbance of each well was measured at 650 nm. Vitamin B12 concentration was determined by comparing to a standard curve of *L. delbrueckii* cells grown in known vitamin B12 concentrations.

Vitamin B12 purification for HPLC Lyophilized cells were suspended in sterile water in an opaque container and autoclaved at 121 °C for 10 minutes [179]. The extract was cooled at 4°C for 30 minutes and centrifuged at 1000 xg for 20 minutes. All subsequent steps were performed in a dark room. The supernatant was transferred to a clean, opaque tube and diluted with 20 mL sterile PBS. The pH was adjusted to pH 7, and the extract was passed through a 0.22μm filter into an Eagle Biosciences Vitamin B12 Immunoaffinity Column. The vitamin B12 was eluted in methanol and concentrated in a dark fume hood.

HPLC analysis of vitamin B12 Vitamin B12 was analyzed on an Agilent 1260 Infinity LC System using an Agilent Poroshell 120 EC-C18 column (4.6 x 100mm 2.7μm). Sample analysis was conducted using Agilent ChemStation software.

Separate 100 μg/mL standards of hydroxocobalamin, methylcobalamin, and adenosylcobalamin were prepared in methanol from 1mg/ml water stocks. A standard curve was generated with samples containing all three standards from 100μg/mL to 1μg/mL. Additionally, a methanol blank was created, a sample of vitamin B12 extract from the cells supplemented with 5,6-DMB, and sample from extract from the cells not supplemented with 5,6-DMB. All samples were prepared in a dark room equipped with a red light to prevent sample degradation.

The sample sequences adhered to Agilent's published protocol for multivitamin

tablets [180], which I found to efficiently separate the different forms of vitamin B12. Samples were detected at a spectral range of 200 - 235 nm.

Plasmid design Geneious 11.0.5 was used to visualize and design the plasmid. Plasmid SYNB12 was designed with a pAM2991 vector backbone, which has an *E. coli* origin of replication, ptrc IPTG inducible promoter, spectinomycin resistance gene (SpR), and Neutral Site I left(-) and right(+) arms for homologous recombination into NSI of PCC 7942 (Figure 16) [181].
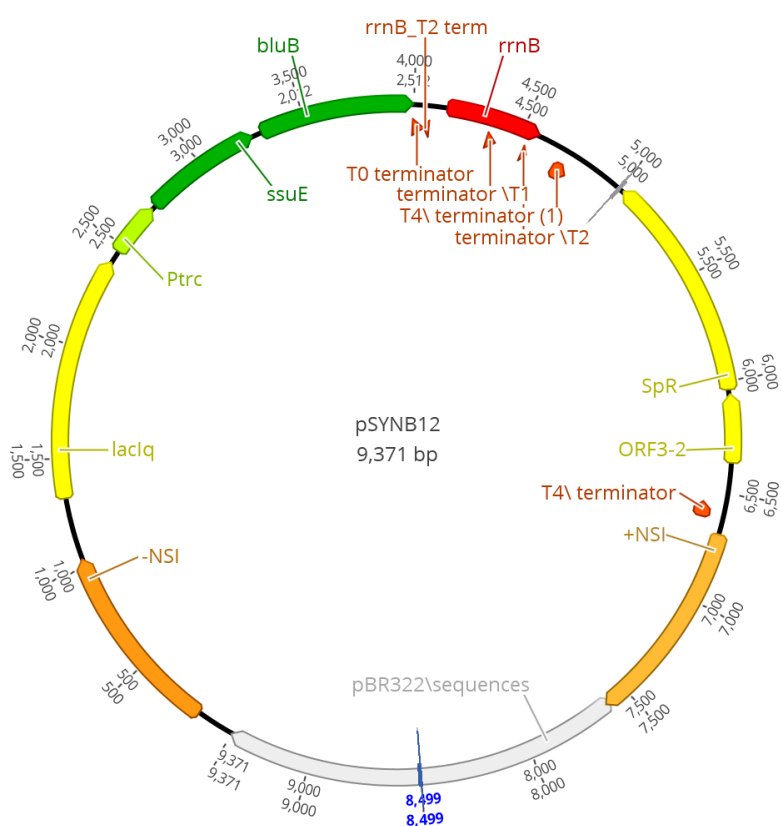
Figure 16: pSYNB12 design. Plasmid map generated with Geneious 11.0.5.

The genes used to produce vitamin B12 were *ssuE*, which encodes for FMN reductase, and *bluB*, which encodes for 5,6-dimethylbenzimidazole synthase. The sequence for *ssuE* was sourced from *S. elongatus* PCC 7002 and the sequence for *bluB* was sourced from *Sinorhizobium meliloti* 1021. The genes were codon optimized for PCC 7942 with DNAworks [182] using the PCC 7942 codon table generated by the

Kasuza website [183]. The gene blocks were designed with overhangs compatible with Gibson Assembly and ordered from IDT. *SsuE* and *bluB* were inserted downstream of the ptrc promoter.

Plasmid construction   PAM2991 was linearized via inverse PCR and confirmed on a gel. Gene blocks were assembled into pAM2991 via Gibson Assembly. Assembly reactions were treated with DpnI, transformed into NEB *E. coli* DH5α cells, and plated on spectinomycin (Spc) selective plates. Colonies were screened via colony PCR with OneTaq DNA Polymerase and visualized on an agarose gel. Plasmids from positive colonies were confirmed via Sanger Sequencing at UC Berkeley DNA Sequencing Facility or at Sequetech DNA Sequencing Service.

Plasmids missing +NSI were repaired via restriction digest using SapI and BlpI enzymes, which excised +NSI from pAM2991, and digested pSYNB12 at the intended NSI insertion site; fragments used to assemble the repaired fragment are shown in pink Figure 17. Fragments were analyzed on a gel, extracted, ligated, and transformed into NEB *E. coli* DH5α cells. Colonies were screened via colony PCR and plasmids were confirmed with Sanger sequencing at Sequetech DNA Sequencing Service.
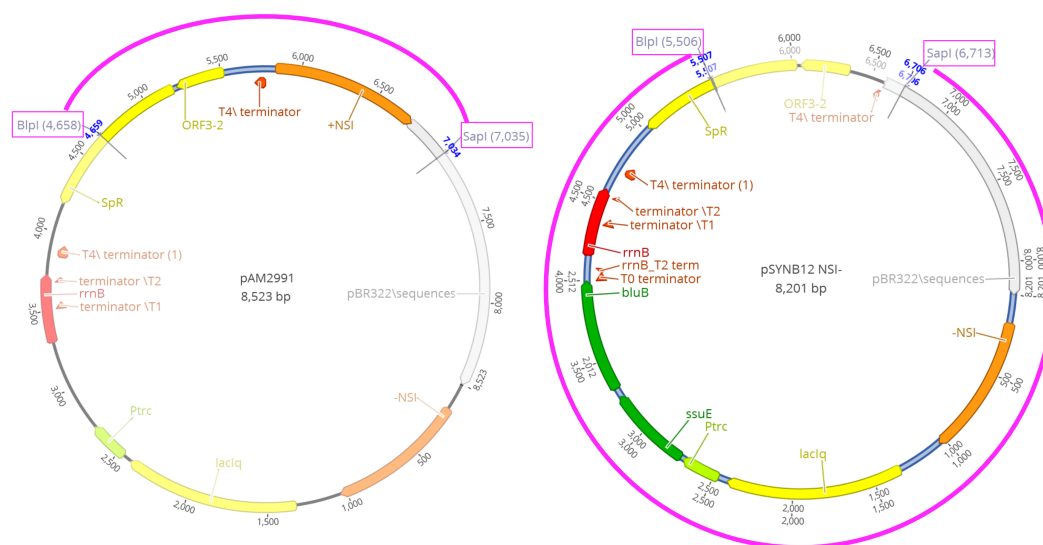
Figure 17: Restriction digests used to repair the pSYNB12 plasmid that was lacking +NSI.

Synechococcus elongatus **PCC 7942 transformation**   10 mL of PCC 7942 cell culture was pelleted, washed once with 10 mM NaCl, and resuspended in 2 mL sterile BG-11 media. 1 μg of DNA was added to 300 μL of cells and incubated in the dark at 30°C for 16 hours at 150 rpm. Transformants were plated on BG-11 plates with 25 μg/ml Spc. Plates were incubated at 30°C in 80 μmol photons per m^{2}s. Cells were restreaked weekly onto fresh BG-11 plates, and were transferred to 50 μg/ml Spc plates after 3 weeks. Gene inserts were confirmed via colony PCR with primers that annealed to NSI and the gene construct.

3.3   Results and Discussion

3.3.1   Vitamin B12 remodeling with 5,6-DMB

The remodeling of pseudo-B12 into active vitamin B12 has been tested only in *Synechococcus* strains that may not have the machinery needed to assemble vitamin B12, which is likely why past attempts have failed [66]. PCC 7942 synthesizes only psuedo-B12, and has the genes *cobU*, *pgam3*, and *cobS*, which are responsible for synthesizing the lower ligand, attaching it to cobinamide to make cobalamin, and performing a dephosphorylation of the vitamin B12 molecule [66, 168]. *Pgam3* is a homologue of *cobC* that is expressed only under iron deficient conditions [184]. I hypothesized that the presence of these genes should allow the construction of vitamin DMB-B12 when 5,6-DMB is present in iron deficient conditions. I first tested this hypothesis with exogenously supplemented 5,6-DMB.

Microbiological assay   *L. delbrueckii* requires exogenous vitamin B12 to survive and is an Association of Official Agricultural Chemists (AOAC) approved method for quantifying vitamin B12 [178, 185]. *L. delbrueckii* predominantly uses active vitamin DMB-B12, but may still use some inactive pseudo-B12 [185]. PCC 7942 was grown in iron deficient BG-11 media both with and without 10 μM exogenous 5,6-DMB, referred to as media+DMB and media-DMB, respectively. The PCC 7942 sample in media+DMB was expected to remodel its native pseudo-B12 into active vitamin B12. The PCC 7942 sample grown in media-DMB was expected to only produce

pseudo-B12 and acted as a control for the inactive pseudo-B12 that *L. delbrueckii* may metabolize. All forms of vitamin B12 present in the cells were converted to cyanocobalamin, the most stable cobalamin, which allowed for total vitamin B12 quantification [186].
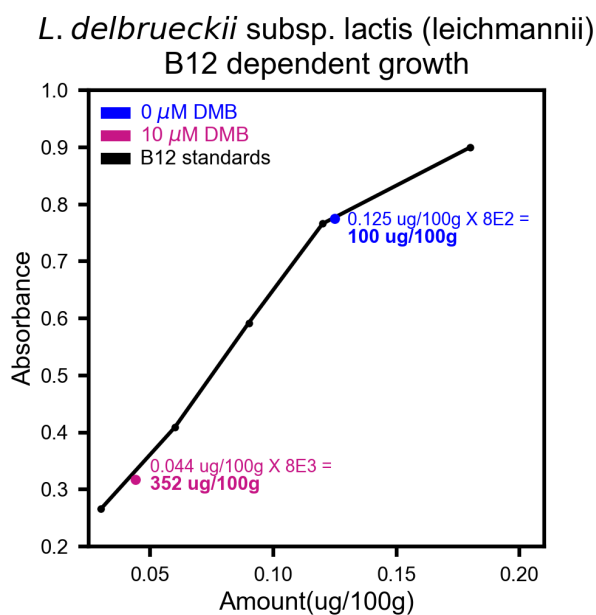
Figure 18: Growth response of B12 dependent *Lactobacillus delbrueckii subsp. lactis (leichmannii)* to known B12 standards (black), B12 extract from PCC 7942 grown in media-DMB (blue), and B12 extract from PCC 7942 grown in media+DMB The samples were diluted to a concentration that was within the range of the standard curve. Each sample's concentration is calculated.

Figure 18 shows the results from this growth assay. The black line represents the standard curve generated with known vitamin B12 concentrations, shown on the X axis. The samples were serially diluted from 8E1 to 8E4 and used in the growth assay. Absorbances that were within the values of the standard curve were used for quantification. The colored points are the absorbances from the different vitamin B12 extracts fitted onto the standard curve, which is used to estimate concentration. The vitamin B12 extract from PCC 7942 media-DMB produced an absorbance of 0.775, which corresponds to 0.125 μg vitamin B12 /100g dry cell weight. This sample was diluted 8E2, so in correcting for that dilution, this extract is estimated to have 100μg of vitamin B12/100g dry cell weight. Since PCC 7942 only produces pseudo-B12, this

is the expected amount of pseudo-B12 that *L. delbrueckii* produces a response with [66]. The vitamin B12 extract from PCC 7942 media+DMB produced an absorbance of 0.317, which corresponds to 0.044μg vitamin B12 /100g dry cell weight. This sample was diluted 8E3, so this extract is estimated to have 352 μg vitamin B12 /100g dry cell weight. Subtracting the pseudo-B12 that *L. delbrueckii* responds to, this corresponds to 2.52 μg of vitamin B12/ 1g of dry cell weight, which is just under the 2.4 μg recommended daily value for adults according to the National Institute of Health.

HPLC The HPLC analysis identified the different forms of vitamin B12 present in the cell extract. The three forms tested were hydroxocobalamin, adenosylcobalamin, and methylcobalamin, which are the three natural forms of vitamin B12. All forms of vitamin B12 are converted to either adenosylcobalamin or methylcobalamin intracellularly [187]. Adenosylcobalamin and methylcobalamin are converted to hydroxocobalamin within seconds of UVA exposure [186].

Figure 19 shows the standards and controls used in this experiment. HPLC samples and standards are typically prepared in a solvent similar to the mobile phase, but this B12 extraction requires an elution in methanol. Figure 19 A shows the signal generated from a methanol blank when ran analyzed in the sodium phosphate and acetonitrile mobile phase. Figure 19 B - D shows that hydroxocobalamin, adenosylcobalamin, and methylcobalamin have distinct retention times when ran in these conditions. Hydroxocobalamin's most prominent peak is at 14.24 minutes, but this peak is not a distinct as adenosylcobalamin, which has a retention time of 15.371 minutes, and methylcobalamin, which has a retention time of 17 minutes. The best wavelength for detecting both adenosylcobalamin and methylcobalamin appears to be 205 nm, shown in orange.

Figure 19 F shows 100μg/mL of hydroxocobalamin, adenosylcobalamin, and methylcobalamin. Panels G and H are the same standards at 10 μg/mL and 1 μg/mL, respectively. A standard curve was generated for methylcobalamin using Agilent ChemStation, which plots the area of these peaks against their concentrations and calculates correlation and the formula of the line generated (Figure 19 E).

This standard curve had a correlation of 1.000, with the fit equation $y = mx + b$, where $m = 38.245$, $b = 2.894$, x is amount in ng/μL, and y is area of the peak.
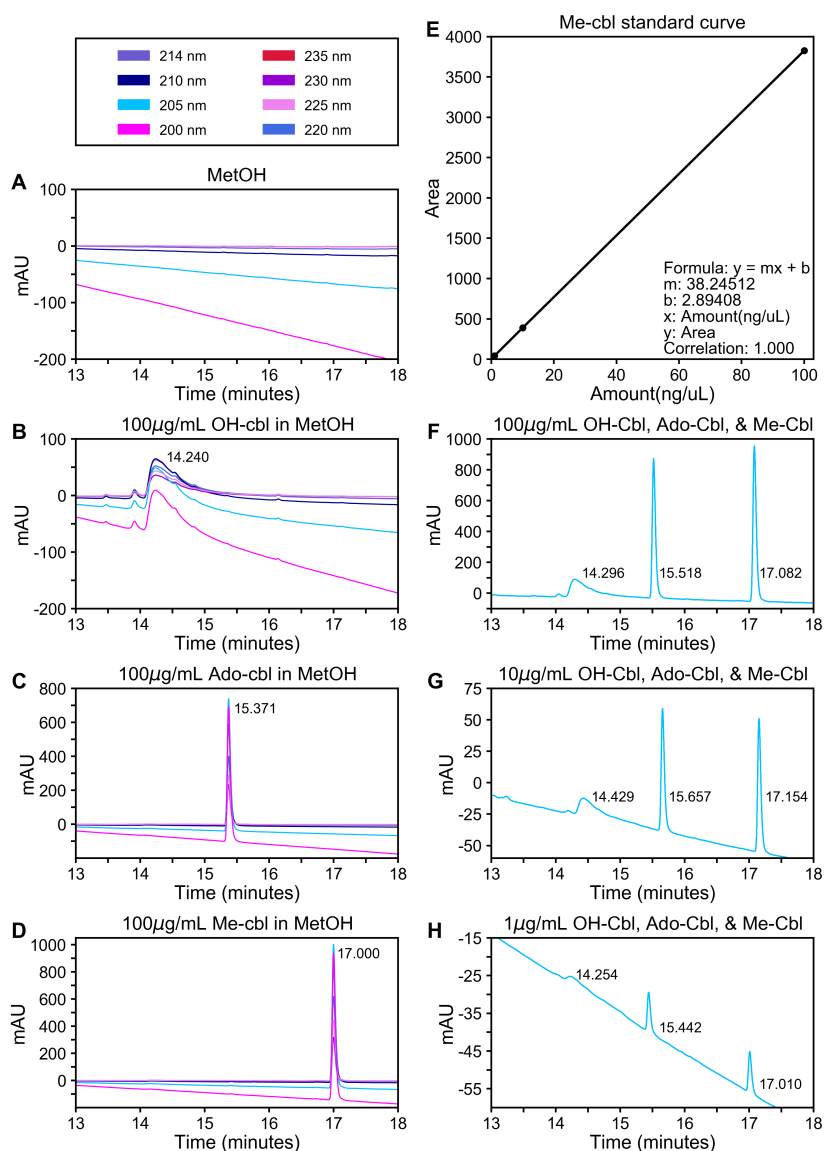
Figure 19: Standards and controls used to detect and quantify B12 in the cell extract. A) Methanol blank B) 100μg/mL hydroxocobalamin (OH-cbl) standard in methanol. C) 100μg/mL adenosylcobalamin (Ado-cbl) standard in methanol. D) 100μg/mL methylcobalamin (Me-cbl) standard in methanol. E) Methylcobalamin standard curve calibrated using standards ranging from 1μg/mL to 100μg/mL. F) 100μg/mL OH-cbl, Ado-cbl, and Me-cbl standards in methanol. G) 10μg/mL OH-cbl, Ado-cbl, and Me-cbl standards in methanol. H) 1μg/mL OH-cbl, Ado-cbl, and Me-cbl standards in methanol.

The B12 extracts from PCC 7942 media-DMB and PCC 7942 media+DMB were analyzed via HPLC (Figure 20). The 205 nm signal was used because it produced the

most prominent peaks for both adenosylcobalamin and methycobalamin. Samples were each measured three times. PCC 7942 media-DMB consistently produced no peaks near the methycobalamin retention time, whereas PCC 7942 media+DMB consistently produced a small peak at the expected methycobalamin retention time. This data suggests that PCC 7942 media+DMB was able to remodel pseudo-B12 into methylcobalamin. The other cobalamins were not detected, likely because the peaks were too small to detect, considering that methylcobalamin had the largest peak at 205 nm, followed by adenosylcobalamin, and then hydroxocobalamin with a much smaller peak.
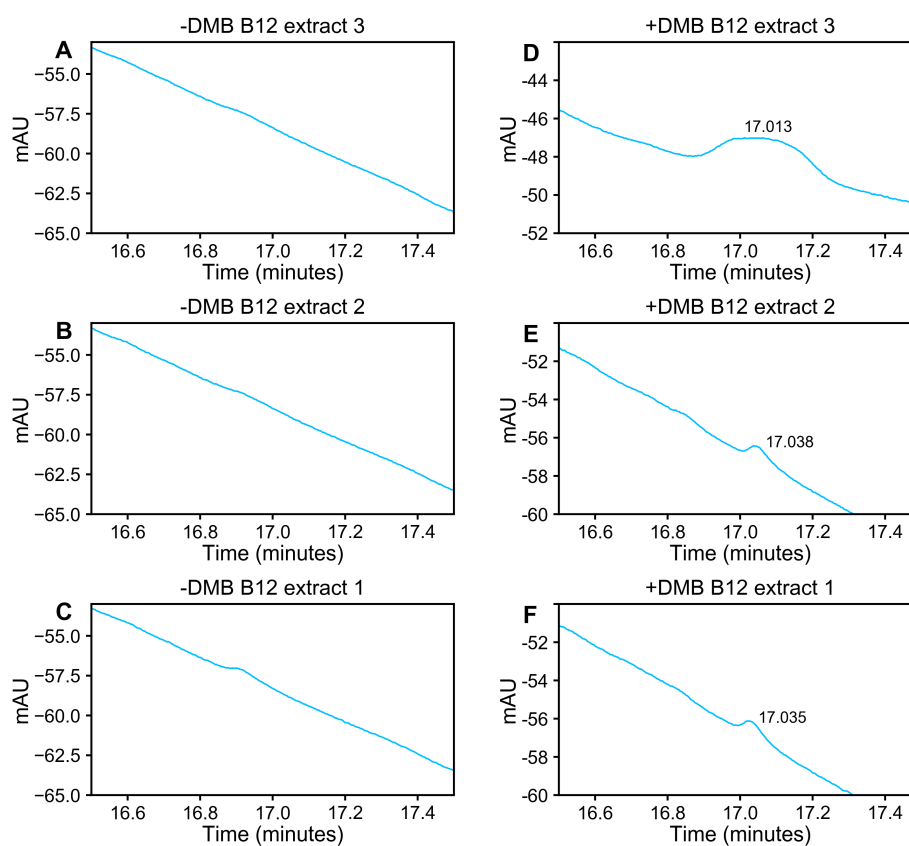
Figure 20: A-C) PCC 7942 cultured in media-DMB show no peaks that resemble methylcobalamin. D-F) PCC 7942 cultured in media+DMB show peaks that resemble methylcobalamin, suggesting that PCC 7942 is capable of remodeling pseudo-B12 into cobalamin when provided 5,6-DMB.

The areas of the methylcobalamin peaks were calculated to be 10.17, 36.45, 27.6 for extracts 1,2, and 3, respectively. This corresponds to respective concentrations

63

of 0.1902 ,0.8774, and 0.646 ng/uL, which averages to 0.571 ng/uL. The extract is suspended in 1.5mL methanol, was sourced from 0.9g of cells, and the immunoaffinity column expects an 85% recovery, so this concentration corresponds to 1.12μg of methylcobalamin per gram of dry cell weight.

This vitamin B12 quantification is lower than the 2.52μg calculated in the microbiological assay, though this is expected. The microbiological assay converted all forms of vitamin B12 to cyanocobalamin, thereby stabilizing all cobalamins and allowing for an accurate total B12 quantification. The B12 extraction procedure used for the HPLC did not convert all forms to cyanocobalamin to preserve the different forms of vitamin B12. Methylcobalamin and adenosylcobalamin degrade into hydroxocobalamin within seconds of UVA exposure. It is extremely likely that a portion of the methylcobalamin and adenosylcobalamin present in B12 extract was degraded into hydroxocobalamin from unintended light exposure. If this were the case, the hydroxocobalamin would be undetectable with this HPLC protocol because its peak was significantly lower than both adenosylcobalamin and methylcobalamin and the expected concentration is too small to accurately detect.

3.3.2 *S. elongatus* PCC 7942 genetic engineering

Plasmid assembly 1   Plasmid SYNB12 was assembled in two steps. The first step cloned 600bp *ssuE* into pAM2991 using Gibson assembly. Figure 21 Panel A shows an *E. coli* colony PCR with two positive colonies for this assembly. The next step cloned 815 bp *bluB* into pAM2991-*ssuE* using Gibson assembly. Figure 21 Panel B shows an *E. coli* colony PCR with three possible positive assemblies of pSYNB12. Sanger sequencing confirmed that the genes were assembled into pAM2991 correctly without mutations.

Figure 21: *E. coli* colony PCRs alongside a plasmid backbone control and an NEB 2-log ladder. A) Gibson assembly of *ssuE* into pAM2991. B) Gibson assembly of *bluB* into pAM2991-*ssuE*.

S. elongatus PCC 7942 transformation pSYNB12 is a suicide vector designed for homologous recombination into NSI of the PCC 7942 genome; a neutral site is an area of a genome that allows permanent genetic alterations [177, 188]. pSYNB12 was transformed into PCC 7942 and the cells were restreaked onto fresh agar plates for approximately 6 weeks. PCC 7942 has up to eight copies of its single chromosome [189], so transformants must be grown under selection until all eight copies of the chromosome are transformed.
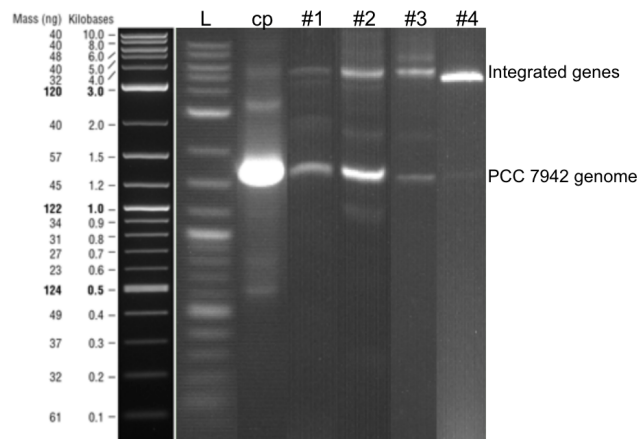
Figure 22: Previous integration of *ssuE* into NSI of PCC 7942. Over time, the genomic copies converge to all have the integrated gene cassette.

A colony PCR was performed on transformed PCC 7942 using primers that annealed to NSI and amplified the gene construct. This PCR produces an erratic banding pattern at first, and over the weeks of restreaking the gene construct is in-

serted into all chromosomal copies and produces a single band; Figure 22 shows an example of this pattern from a previous NSI integration.

Figure 23 shows an NSI colony PCR of multiple cell lines alongside a wildtype PCC 7942 control; the gene insert is expected to produce a band at 7.3kb. After 6 weeks, it appeared that the PCR never converged to the gene insert size, indicating that the genes were not present within NSI. The cells were growing on 50 μg/ml Spc, which is well above the standard concentration used for PCC 7942 [177], indicating that at least part of the genetic construct was present somewhere in the genome.
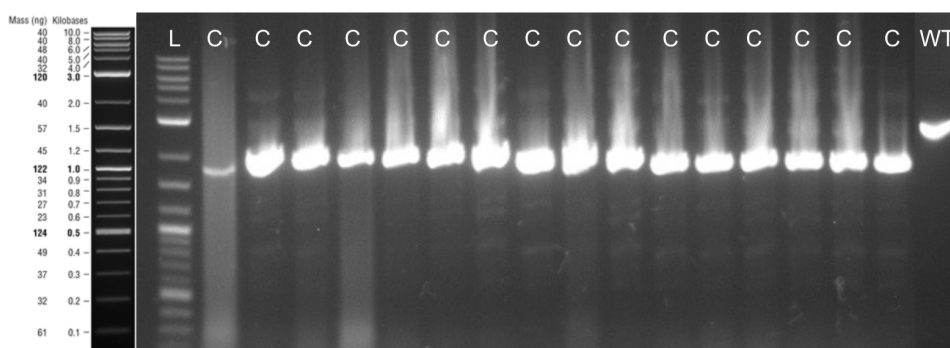
Figure 23: PCC 7942 colony PCRs of NSI suggest that the *ssuE* and *bluB* gene cassette was not integrated into NSI. The gene cassette was expected to produce a band at 7.3kb.

Because pSYNB12 is a suicide vector, its contents would not amplify in a PCR unless they were present somewhere in the genome. I performed a PCR with primers specific to the gene cassette that annealed to the ptrc promoter and SpR. The gel suggested that some of the cell lines had this portion of the gene construct present in the genome and matched that of the pSYNB12 plasmid control (Figure 24). Wildtype PCC 7942 did not show amplification with these gene specific primers, as expected. These transformants are named PCC 7942-B12a.
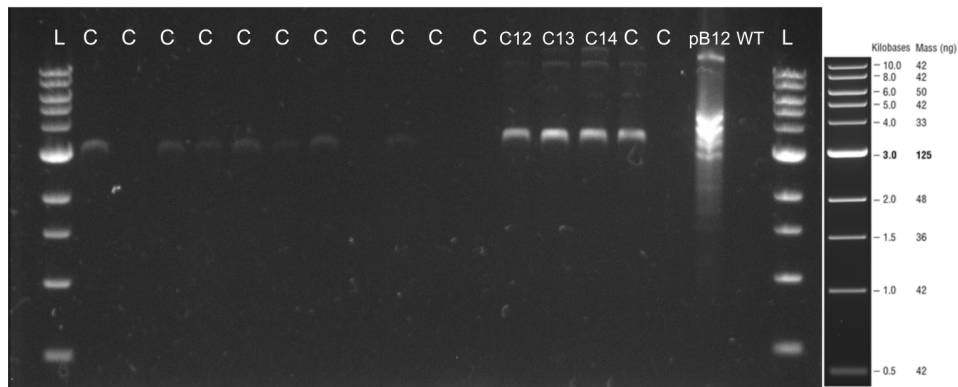
Figure 24: PCC 7942 colony PCR with primers that anneal to the ptrc promoter and SpR. Cell lines showed amplification that resembles that of the pSYNB12 control, indicating gene integration into PCC 7942.

Multiple PCR attempts with pSYNB12 using primers that annealed to NSI produced no results or erratic bands. I hypothesized that a portion of NSI must be missing from pSYNB12, which also explains why the genetic construct would not have been integrated into NSI of the PCC 7942-B12a genome. Sanger sequencing of NSI in pSYNB12 showed that +NSI was deleted from the pSYNB12 plasmid, likely due to a cloning error. Figure 25 panel A shows pSYNB12 aligned to its reference and a misalignment starting in the middle of the T4 terminator. Figure 25 panel B show the same chromatogram aligned with no mismatches to a pSYNB12 reference with a portion deleted–this portion contained +NSI.
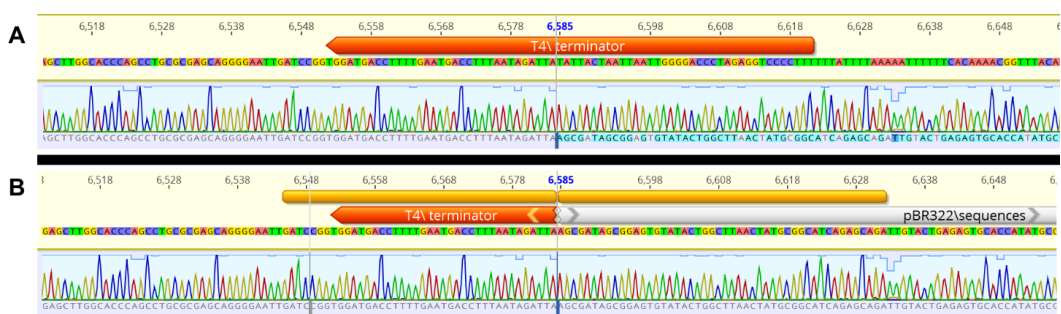
Figure 25: +NSI is not present in pSYNB12. A) Misalignment of pSYNB12 to its reference. B) Perfect alignment of pSYNB12 to a altered reference in which +NSI was deleted.

PCC 7942-B12a colonies 12,13, and 14 were inoculated into liquid BG-11 with 5ug/ml Spc and grown for vitamin B12 testing. Subsequent colony PCRs with the same primers that anneal to ptrc and SpR showed that the genes were ejected from

67

the PCC 7942-B12a genome. Figure 26 shows these colonies alongside a pSYNB12 control; the expected amplicon size is 2.8kb. The cells likely ejected the genes due to being in low antibiotic concentration, and which did not provide enough selective pressure to retain the genetic construct. When grown on plates, PCC 7942 were re-streaked on agar with increasing antibiotic concentration, but this pattern was not repeated in liquid culture. Moreover, if the genes were not integrated into NSI, the construct may have been placed in an alternative position in the genome that disrupts normal cellular function, which renders the construct unfavorable to the cell and more likely to be excised.
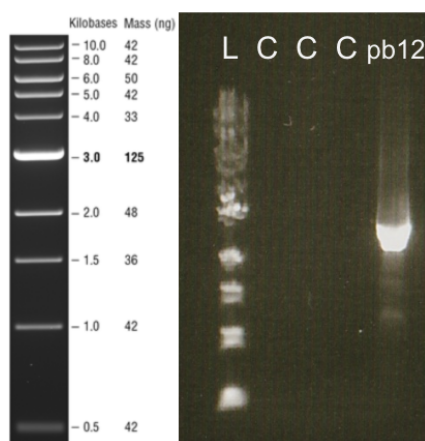
Figure 26: PCC 7942-B12a colony PCRs alongside pSYNB12 suggesting that the genetic construct was ejected from the genome.

Plasmid assembly 2 A restriction digest was used to repair pSYNB12. One digest excised the deleted +NSI fragment from pAM2991, the second digest cut pSYNB12 in the same positions. The pSYNB12 backbone was ligated with the +NSI fragment to produce pSYNB12v2 Figure 28. The success of this ligation was confirmed with PCR and Sanger sequencing. One PCR used primers that annealed on either side of the +NSI insert, which produces an 800bp fragment when absent and a 2kb fragment when present. The two screened colonies produced a 2kb fragment that matched that of the pAM2991 positive control, and the pSYNB12v1 negative control producing a fragment of 800bp (Figure 27). The second PCR confirmed that the genes were still assembled correctly and used primers annealed to ptrc and SpR, producing a 2.8bp

fragment. The two screened colonies produced amplicons that matched that of the pSYNBb12v1 positive control, which has correctly assembled genes; the pAM2991 negative control worked as expected (Figure 27). The gene inserts and +NSI insert ligation was Sanger sequenced and aligned to the reference, indicating that +NSI was successfully inserted Figure 28.
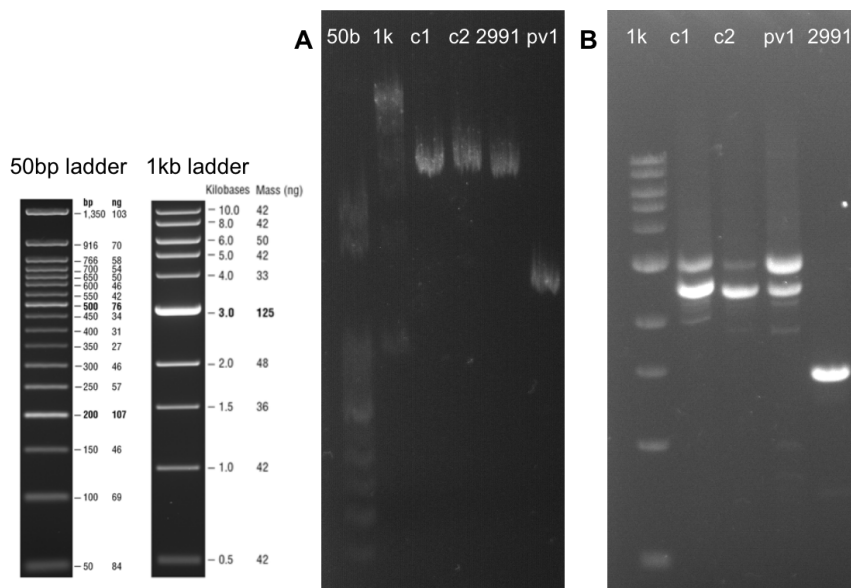
Figure 27: Successful ligation repair of pSYNB12. A) PCR of two screened colonies, a pAM2991 + control, and a pSYNB12 - control, that amplifies the inserted +NSI fragment. B) PCR of two screened colonies, a pSYNB12v1 + control, and a pAM2991 - control, that amplifies the gene inserts.
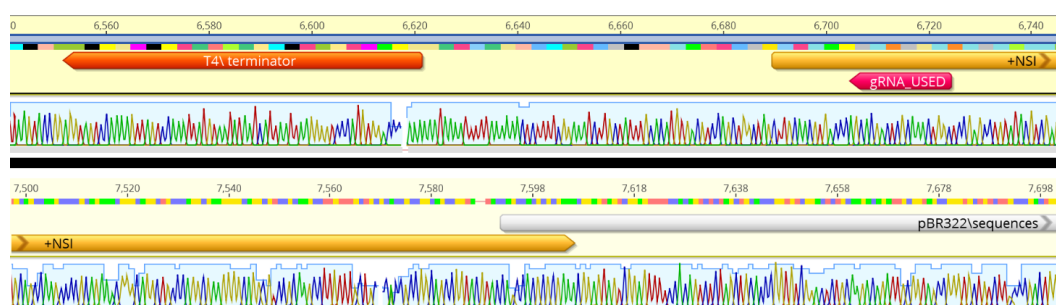
Figure 28: Successful ligation repair of pSYNB12. Sanger sequencing of ligation reactions aligned against the pSYNB12vs reference showing successful insert ligation of +NSI.

3.4   Conclusion and future directions

PCC 7942 is able to remodel its native pseudo-B12 into vitamin B12 with exogenous 5,6-DMB. PCC 7942 synthesized roughly 2.52 μg of vitamin B12 per gram

of dry cell weight, which is just over the 2.4 μg recommended daily value for adults according to the National Institute of Health. This finding is the first report of a *Synechococcus* strain performing this corrinoid remodeling. This concentration is on the lower end of vitamin B12 production in commercial microbiological fermentation processes, with the highest output being 206 μg/mL and the lowest being 1.1 μg/mL [190]. All of these microbes, however, require media additives such as 5,6-DMB, glucose, or sucrose.

The next steps of this work are to engineer PCC 7942 to synthesize 5,6-DMB, thereby producing vitamin B12 without any media additives. The plasmid to transform PCC 7942, pSYNB12v2, has been created for stable genetic integration of *ssuE* and *bluB* into NSI of the PCC 7942 genome. The metabolic engineering with these genes will complete the pathway for 5,6-DMB synthesis within PCC 7942, giving it the ability to produce vitamin B12 without any external supplementation. The engineered PCC 7942 will be assayed for vitamin B12 using the same methods presented herein, and if the concentration is still low, routes for optimization will be explored. It is feasible that over-expressing the genes responsible for riboflavin production, which is the precursor to 5,6-DMB, could drive up the production titer of vitamin B12 in PCC 7942.

Cyanobacteria could be useful factories for vitamin B12 production, because they use sunlight as their energy, water as an electron donor, and air as their carbon source [191]. They can grow in seawater or non-potable water, and with access to sunlight and air, produce vitamin B12.

This work has implications for consistent access to nutrition around the world. An estimated 2 billion people are micronutrient deficient [192]. Transferral of this work into the edible cyanobacteria, *A. platensis*, more commonly known as Spirulina, would extend its impact range. A widely consumed food for its many nutritional and health benefits [72, 104, 193], *A. platensis* contains nearly all essential vitamins, minerals, amino acids, and lipids, but lacks vitamin B12 [66, 67]. Engineering *A. platensis* to produce vitamin B12 could create a vegetarian multivitamin supplement that is cultivated with minimal materials, making it accessible to regions that

may struggle with access to nutrition. The 2.5 μg vitamin B12 per gram dry cell weight concentration observed here with PCC 7942 would be sufficient for vitamin supplementation if the cell mass were being consumed directly, as one would with *A. platensis*.

4 Engineering the photosynthetic bacterium *Synechococcus elongatus* PCC 7942 to produce acetaminophen

4.1 Introduction

Paracetamol, more commonly known as acetaminophen, is a common mild analgesic and antipyretic recognized by the WHO as an essential medicine [51]. Acetaminophen is often used in conjunction with opioid pain medications postoperatively to enhance pain relief, thus reducing reliance upon opioid pharmaceuticals [194].

Acetaminophen is one of the most commonly-used pain relievers in the world, and is projected to reach a global market value of 999.4 million in 2020 [195], with over 143 kilo metric tons produced annually [196]. The industrial synthesis of acetaminophen can begin either with phenol, chlorobenzene, nitrobenzene, or 4-hydroxyacetophenone oxime [197]. The first two methods present environmental concerns because of unsafe byproducts, such as salts or isomers [197]. The second two methods require the use of mineral acids, strong acids, and severe reaction conditions [197]. The processes of acetaminophen synthesis involve multiple steps, high temperatures, and various harmful chemicals. Developing processes that mitigate the concomitant byproducts of acetaminophen production is crucial to ensuring the sustainability of the volume at which it is currently manufactured.

With the immediate concern of climate change, there has been a movement to decrease sources of pollution and waste in favor of conservation-minded methods. Arisen among this movement is the concept of green chemistry, which aims to develop procedures that limit waste accumulation and protect the environment through the limitation of hazardous reagents and energy consumption [198]. In particular, there has been special interest in the green synthesis of acetaminophen [197, 199, 200], since its use is so commonplace that an environmentally-friendly synthesis method could have a major impact on sustaining environmental health.

Presented herein is a proposed method for biosynthesis of acetaminophen in the photosynthetic cyanobacterium, *Synechococcus elongatus* PCC 7942 (hereby referred

to as PCC 7942) using a previously engineered pathway in *E. coli* as a model [201]. This pathway converts chorismate, an abundant amino acid precursor of tryptophan, phenylalanine, and tyrosine, into acetaminophen with the addition of the *4ABH* gene from *Agaricus bisporus*, an edible mushroom, and *nhoA* from *E. coli* (Figure 29).
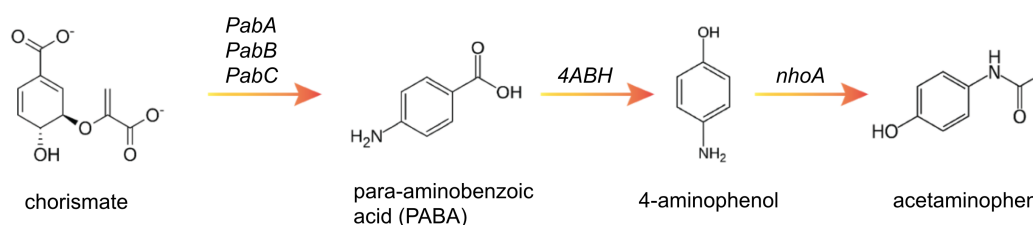
Figure 29: Previously described pathway for acetaminophen biosynthesis from the abundant precursor, chorismate [201]. Acetaminophen synthesis is induced in PCC 7942 with the addition of the genes *4ABH* and *nhoA*.

This method of biosynthesis could reduce the environmental impact of acetaminophen production, because cyanobacteria use sunlight as their energy, water as an electron donor, and air as their carbon source [191]. They can grow in seawater or non-potable water, and with access to sunlight and air, produce acetaminophen. This biosynthesis would fix atmospheric CO_2, require no harmful chemicals or media additives, and have low temperature and energy requirements.

The genes for acetaminophen production, *4ABH* and *nhoA*, have been integrated into the PCC 7942 genome. Acetaminophen has been detected in a range of 1.04 - 3.3 μg/mL cell media. These concentrations are lower than what has been previously reported in *E. coli* [201], but methods for optimization in PCC 7942 have yet to be explored. Though this concentration is not yet industrially feasible, this work paves the way for solar-powered pharmaceutical synthesis.

4.2   Materials and methods

Materials   All restriction enzymes, polymerases, competent *E. coli*, and DNA ladders were purchased from New England Biolabs. Mini-prep kits were purchased from Zymo Research. Gene blocks were purchased from Integrated DNA Technologies. pAM2991 was generously provided by the Golden Lab at University of California San

Diego. pAM1573 was purchased from Addgene. Acetaminophen and 4-aminophenol standards were purchased from Alfa Aesar. HPLC solvents were purchased from VWR.

Bacterial strain and culture conditions *Synechococcus elongatus* PCC 7942 was provided by the Golden Lab at University of California San Diego. Cultured cells were grown in BG-11 medium shaking at 150 rpm in 30°C with 12 hour 80 μmol photons per m^{2}s light cycles using a 90 CRI light source with a color temperature of 3000 Kelvin [177]. Cells on agar plates were grown in 24 hour light under the same conditions.

Plasmid designs Geneious 11.0.5 was used to visualize and design the plasmids. Plasmid AM2991-*4ABH* was designed with a pAM2991 vector backbone containing an *E. coli* origin of replication, ptrc IPTG inducible promoter, spectinomycin resistance gene (SpR), and Neutral Site I left(-) and right(+) arms for homologous recombination into NSI of PCC 7942 (Figure 30 A) [181]. The gene used to synthesize 4-aminophenol from chorismate, *4ABH* was placed downstream of the ptrc promoter. The sequence for *4ABH* was sourced from *Agaricus bisporus*.

Plasmid AM1573-*nhoA* was designed with a pAM1573 vector backbone containing an *E. coli* origin of replication, rop, ptrc IPTG inducible promoter, rrnB T1 and T2 terminators, chloramphenicol resistance gene (CmR), ampicillin resistance gene (AmpR), and Neutral Site II left(-) and right(+)arms for homologous recombination into NSII of PCC 7942 (Figure 30 B) [202]. The gene used to synthesize acetaminophen from 4-aminophenol, *nhoA*, was placed downstream of the ptrc promoter and upstream of a T0 terminator. The sequence for *nhoA* was sourced from *E. coli.*

The genes were codon optimized for PCC 7942 with DNAworks [182] using the PCC 7942 codon table generated by the Kasuza website [183]. The gene blocks were designed with overhangs compatible with Gibson Assembly and ordered from IDT.
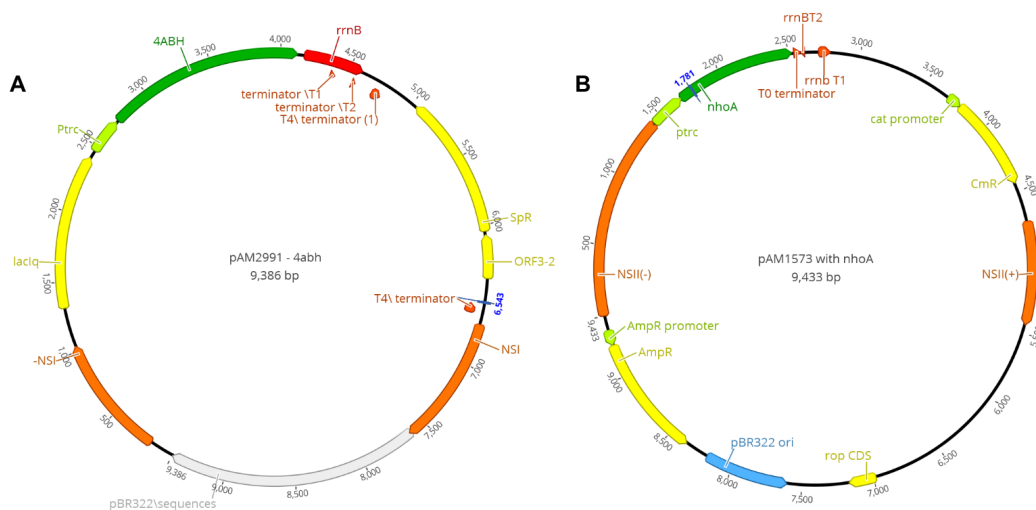
Figure 30: A) pAM2991-*4ABH*. B) pAM1573-*nhoA*. Plasmid map generated with Geneious 11.0.5.

Plasmid construction   PAM2991 and pAM1573 were linearized via inverse PCR and confirmed on a gel. Gene blocks were assembled into pAM2991 and pAM1573 via Gibson Assembly. Assembly reactions were treated with DpnI, transformed into NEB *E. coli* DH5α cells, and plated on spectinomycin (Spc) or chloramphenicol (Cm) selective plates. Colonies were screened via colony PCR with OneTaq DNA Polymerase, and visualized on an agarose gel. Plasmids from positive colonies were confirmed via Sanger Sequencing at the UC Berkeley DNA Sequencing Facility.

PCC 7942 transformation   10 mL of PCC 7942 cell culture was pelleted, washed once with 10 mM NaCl, and resuspended in 2 mL sterile BG-11 media. 500 g of pAM2991-*4ABH* and pAM1573-*nhoA* were each added to 300 μL of cells and incubated in the dark at 30°C for 16 hours at 150 rpm. Transformants were plated on BG-11 plates with 2 μg/ml Spc and 5 μg/ml Cm, based on previous reports [203]. Plates were incubated at 30°C in 80 μmol photons per m^{2}s. Cells were re-streaked weekly onto fresh BG-11 plates, and were transferred to 10 μg/ml Spc and 15 μg/ml Cm plates after 3 weeks. Gene inserts were confirmed via colony PCR with primers that annealed to NSI, NSII, and the pAM2991-*4ABH* gene contruct. PCC 7942 transformed with both constructs, PCC 7942 zxx::*4ABH* NSII::*nhoA*, are hereby referred to as Se4n.

Colorimetric assay of acetaminophen   The acetaminophen concentration within the culture media was analyzed following a previously-described colorimetric assay [204]. A series of acetaminophen standards were prepared in PCC 7942 wild type (WT) media at the following concentrations: 0.5, 1, 5, 25, 50, 100, 200, 300, and 400 μg/mL. These standards were used to generate a standard curve with the described method. WT cells were inoculated in BG-11 and Se4n cell culture was inoculated in BG-11 with 2μg/mL Spc, 5μg/mL Cm, and 1mM IPTG [205]. The cultures were grown until log phase and the media was used to estimate acetaminophen concentration with the described method by comparing against the standard curve.

0.5 mL of sample was mixed with 1 mL of 15% trichloroacetic acid. This mix was vortexed, centrifuged, and the supernatant was added to 0.5mL 6N HCl. 0.4 mL of sodium nitrite was added to the solution, creating nitrous acid, and allowed to sit for 2 minutes, after which 1.0 mL of 15% sulfamic acid was added to neutralize any excess nitrous acid. Lastly, 2.5 mL of 15% NaOH was added to the solution. The absorbance of each sample at 430 nm was measured against a WT method blank. The method was performed in triplicate for each sample.

HPLC analysis of acetaminophen   Acetaminophen and 4-aminophenol were analyzed on an Agilent 1260 Infinity LC System using an Agilent Poroshell 120 EC-C18 column (4.6 x 100 mm 2.7 μm). Sample analysis was conducted using Agilent ChemStation software.

Separate 100 μg/mL standards of 4-aminophenol and acetaminophen were prepared in WT media from 1 mg/ml water stocks. A standard curve was generated with samples containing both standards at 100 μg/mL, 10 μg/mL, and 1 μg/mL. Additionally, WT and WT + IPTG blanks were created. Media from Se4n + IPTG was examined for acetaminophen. All samples were prepared immediately prior to measurement to avoid degradation.

The samples were run according to Agilent's published protocol to detect acetaminophen and its impurities [206]. Samples were detected at a range of 225 - 235 nM.

DNA extraction and sequencing A DNA extraction was performed on Se4n colonies 8 and 5 as described in Section 2.3.3. Samples were sequenced for 10 gb of data on an Illumina NovaSeq at the QB3 Vincent J. Coates Genomics Sequencing Laboratory, Berkeley.

4.3 Results and discussion

4.3.1 Plasmid construction

Gibson assembly of pAM2991-*4ABH* was successful. Colony PCR showed gene integration into pAM2991, with an expected amplicon size of 2800 bp alongside a pAM2991 control (1383 bp) (Figure 31A). This integration was confirmed with Sanger sequencing. Gibson assembly of pAM1573-*nhoA* was also successful; Figure 31B shows a colony PCR of four *E. coli* colonies alongside a pAM1573 control. The expected amplicon for an *nhoA* insert is 4 kb and without is 3.1 kb. This integration was confirmed with Sanger sequencing.
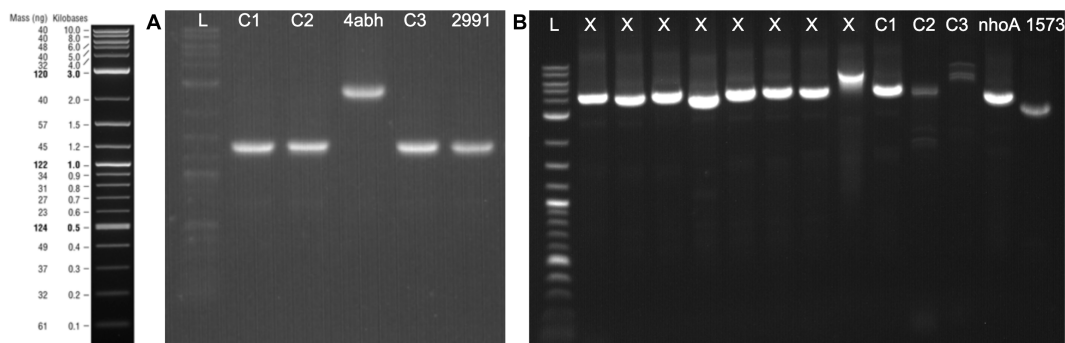
Figure 31: A)*E. coli* colony PCR showing successful Gibson assembly of pAM2991-*4ABH*. B) *E. coli* colony PCR showing successful assembly of pAM1573-*nhoA*.

4.3.2 PCC 7942 transformation

Both pAM2991-4ABH and pAM1573-*nhoA* are suicide vectors designed for homologous recombination into NSI and NSII of the PCC 7942 genome, respectively. Both plasmids were simultaneously transformed into PCC 7942 and the cells were re-streaked onto fresh agar plates for approximately 6 weeks. A colony PCR was performed on transformed PCC 7942 using primers that annealed to NSI and NSII

and amplified each gene construct.

Each colony in the NSII PCR produced amplicons larger than the pAM1573 and WT PCC 7942 (2kb) controls Figure 32. The expected size for WT PCC 7942 was 2kb, pAM1573 was 4.5kb, and pAM1573-*nhoA* was 5.3kb. The plasmid controls produced amplicons about 1 kb smaller than expected, but some of the transformed PCC 7942 produced amplicons near the expected size. These results indicate that the cassette may have been incorrectly integrated into NSII, but that it is nonetheless present.
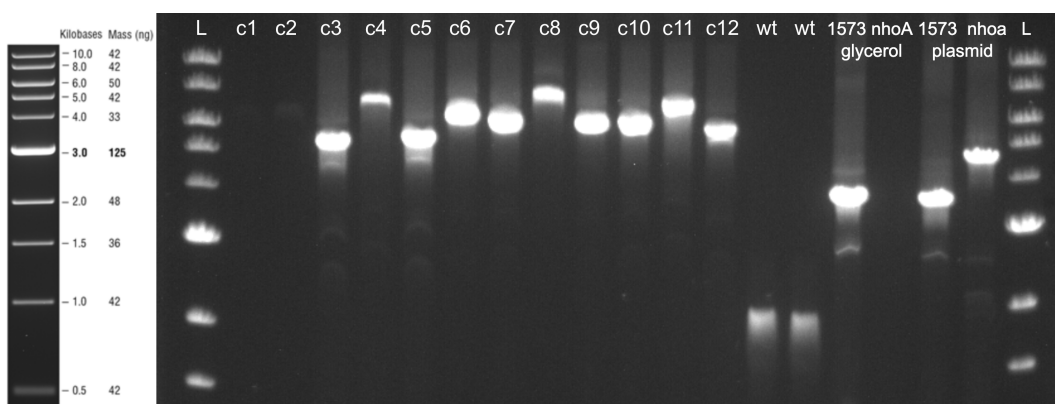
Figure 32: PCC 7942 colony PCR of NSII indicating one or more*nhoA* integrations. Colonies produced amplicons greater than that of WT PCC 7942 or the plasmid controls.

Figure 33 shows an NSI colony PCR of multiple cell lines alongside a WT PCC 7942 control; the gene insert is expected to produce a band at 7.4 kb. After 6 weeks, it appears that the PCR never converged to the gene insert size, indicating that the genes were not present within NSI. The cells were growing on 10 μg/ml Spc and 15 μg/ml Cm, which is higher than standard concentrations used for PCC 7942 [177], indicating that at least part of the genetic construct was present somewhere in the genome. This result mirrors the one discussed in Section 3.2.2 Figure 23.
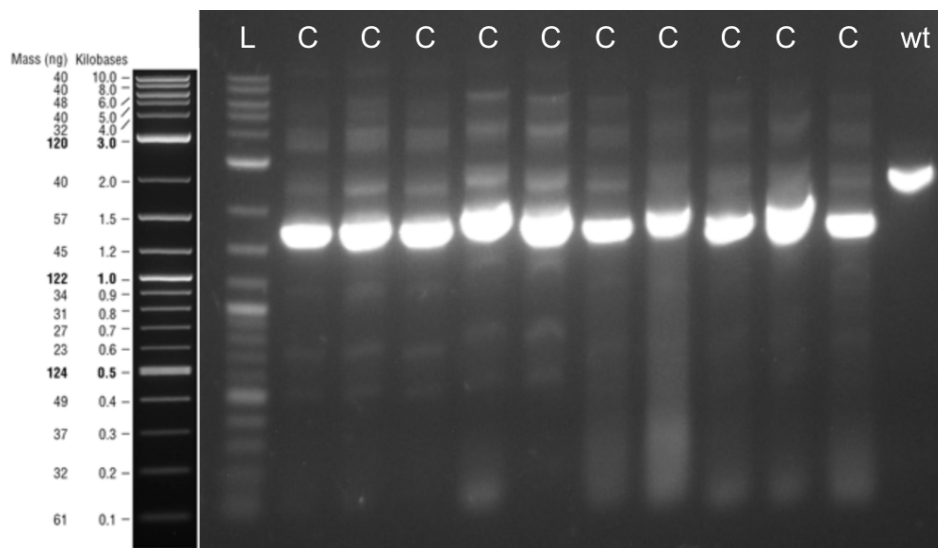
Figure 33: PCC 7942 colony PCRs of NSI suggest that the *4ABH* gene cassette was not integrated into NSI. The gene cassette was expected to produce a band at 7.3 kb.

Because pAM2991-*4ABH* is a suicide vector, its contents would not amplify in a PCR unless they were present somewhere in the genome. I performed a PCR with primers specific to the gene cassette that annealed to the ptrc promoter and SpR. This PCR was run alongside pAM2991-*4ABH*, pAM2991, and WT PCC 7942 controls (Figure 34). Many colonies produced amplicons larger than those of the controls, indicating that the genetic construct may be inserted, but in an ambiguous orientation. These transformants are named PCC 7942 zxx::*4ABH* NSII::*nhoA*, abbreviated as Se4n. Sequencing of pAM2991-*4ABH* revealed that +NSI was missing, which explains why the genes weren't integrating properly.

Because the amplicons for the PCRs in Figure 34 differed in size between colonies, multiple colonies were selected for further screening. While growing the cells for screening, pAM2991-*4ABH* was repaired by digesting +NSI from pAM2991 and ligating it into pAM2991-*4ABH*, which is the same approach as discussed in Section 3.3.2. Ligation repairs were confirmed via colony PCR and Sanger sequencing.
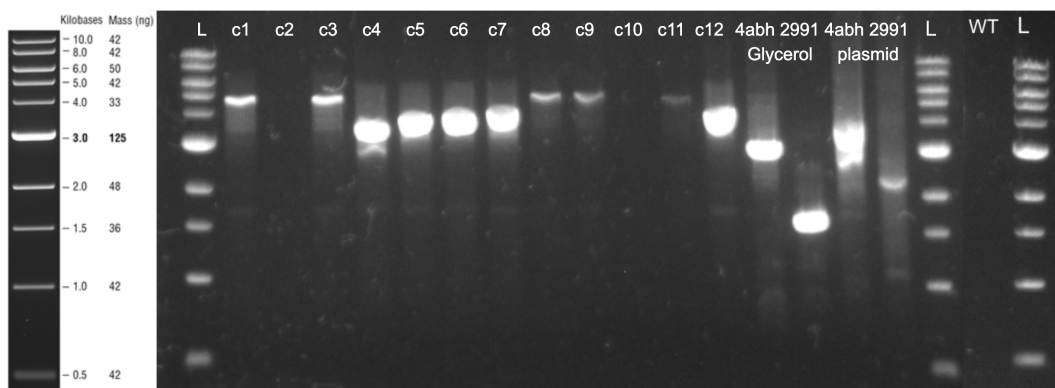
Figure 34: PCC 7942 colony PCRs of gene cassette specific primers suggests that the *4ABH* gene cassette was integrated in an unknown location of the PCC 7942 genome. These transformants are named Se4n.

4.3.3 Colorimetric assay for acetaminophen

The colorimetric assay for acetaminophen was first described for plasma samples by Glynn and Kendall in 1975 [207]. The method is based on the reaction of paracetamol (acetaminophen) with nitrous acid, which produces the chromophore, 2-nitro-4-acetamidophenol [208]. This method is specific to acetaminophen, with no interference by its conjugates or other drugs [209]. An optimized method with decreased volumes and less generated nitrous gas was used[204]. This method was tested on clinical plasma samples and was reported to have a correlation with HPLC of $r^2 = 0.9758$.

A standard curve was built by performing the colorimetric method with 0.5 μg/mL to 400 μg/mL acetaminophen in WT spent media and measuring their absorbance at 430 nmFigure 35. The standard samples were performed in triplicate and blanked against a WT method blank, producing an r^2 of 0.9992.

Biosynthesis of acetaminophen has previously been performed in *E. coli*, and the acetaminophen was reported to be exported into the culture medium [201]. A 500 mL culture of Se4n colony 5 was inoculated in BG-11 with 1 mM IPTG, 2 μg/mL Spm, and 5 μg/mL Cm. Once in log phase (4 days), the cell media was collected and prepared according to the method. The sample was prepared in triplicate, as was a WT negative control. Se4n colony 5 media had an absorbance that roughly correlates to 3.3μg/mL acetaminophen; the WT control was below the standard curve

and thus treated as 0 (Figure 35). This concentration of acetaminophen is below the 50 μg/mL that was previously reported in *E. coli* . The difference may be caused by the haphazard integration *4ABH*, which may not include all parts of the genetic construct or may be inserted in a genomic location that disrupts the cells normal function. Despite the low concentration, this evidence does suggest that PCC 7942 is capable of synthesizing acetaminophen.
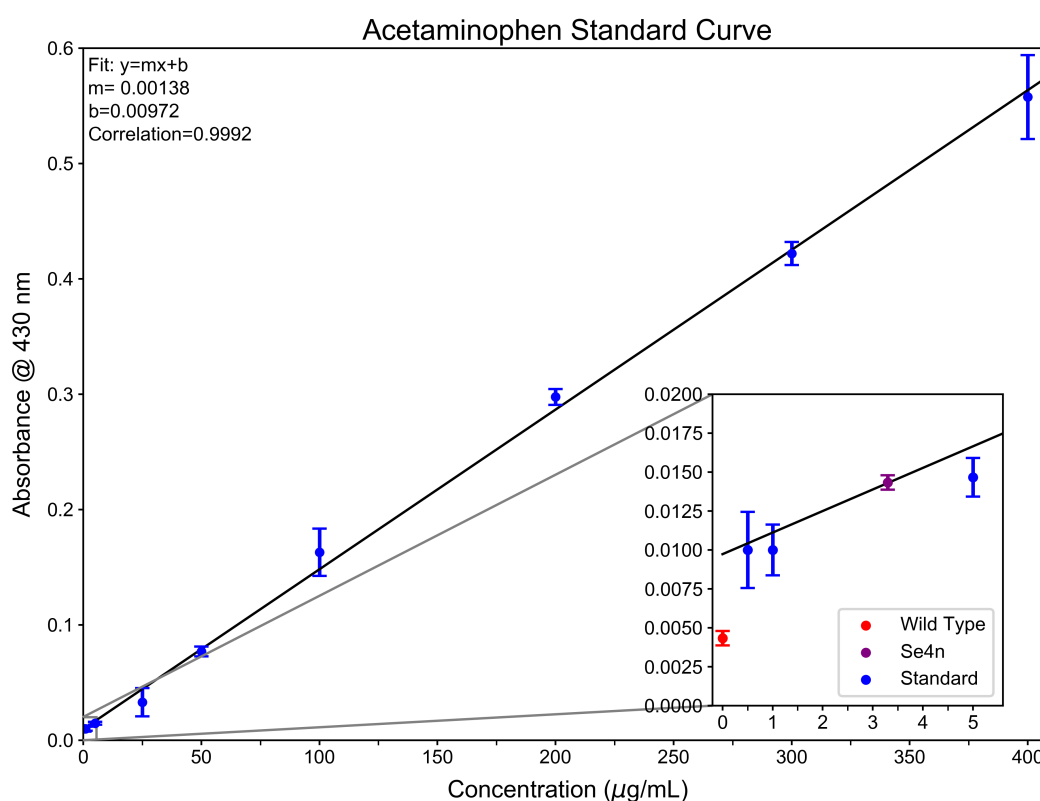
Figure 35: Colorimetric assay of acetaminophen. A standard curve was built (blue) and used to estimate the concentration of acetaminophen in Se4n cell medium (purple). These results indicate 3.3 μg/mL acetaminophen in the cell medium.

4.3.4 HPLC analysis of acetaminophen

Cell media was analyzed via HPLC for acetaminophen and its precursor, 4-aminophenol, which is the principal impurity in pharmaceutical acetaminophen, and is caused by both its synthesis and degradation [210] Figure 36. A WT blank and WT + 1 mM IPTG blank was analyzed to determine expected background signals. WT produced a peak at 0.709 minutes (Figure 36 G), which is present in the rest of

the signals observed. WT+ 1 mM IPTG produced two peaks, one at 0.710 minutes and another at 0.814 minutes (Figure 36 H). 100 μg/mL standards of 4-aminophenol and acetaminophen were prepared in WT media and observed to have distinct retention times of 0.992 and 1.207 minutes, respectively (Figure 36 A & B). Both 4-aminophenol and acetaminophen were measured at 100 μg/mL, 10 μg/mL, and 1 μg/mL and used to generate an acetaminophen standard curve with $r^2 = 0.99997$ and fit equation $y = mx + b$, where y is the peak integration area, x is the concentration in ng/μL, $m = 12.02615$, and $b = 7.03328$ (Figure 36 C-F).

The Se4n colony 5 cell media + 1 mM IPTG showed a peak at 1.225 minutes, which corresponds to acetaminophen (Figure 36 I). This peak was not present in either of the blanks, indicating that Se4n colony 5 was producing acetaminophen. The area of this acetaminophen peak was calculated to be 19.5, which corresponds to 1.0366 μ/mL of acetaminophen. This concentration differs from that of the colorimetric assay, which may be due to natural fluctuation between the two assays; the correlation between the two methods was previously reported as $r^2 = 0.9758$ [204].
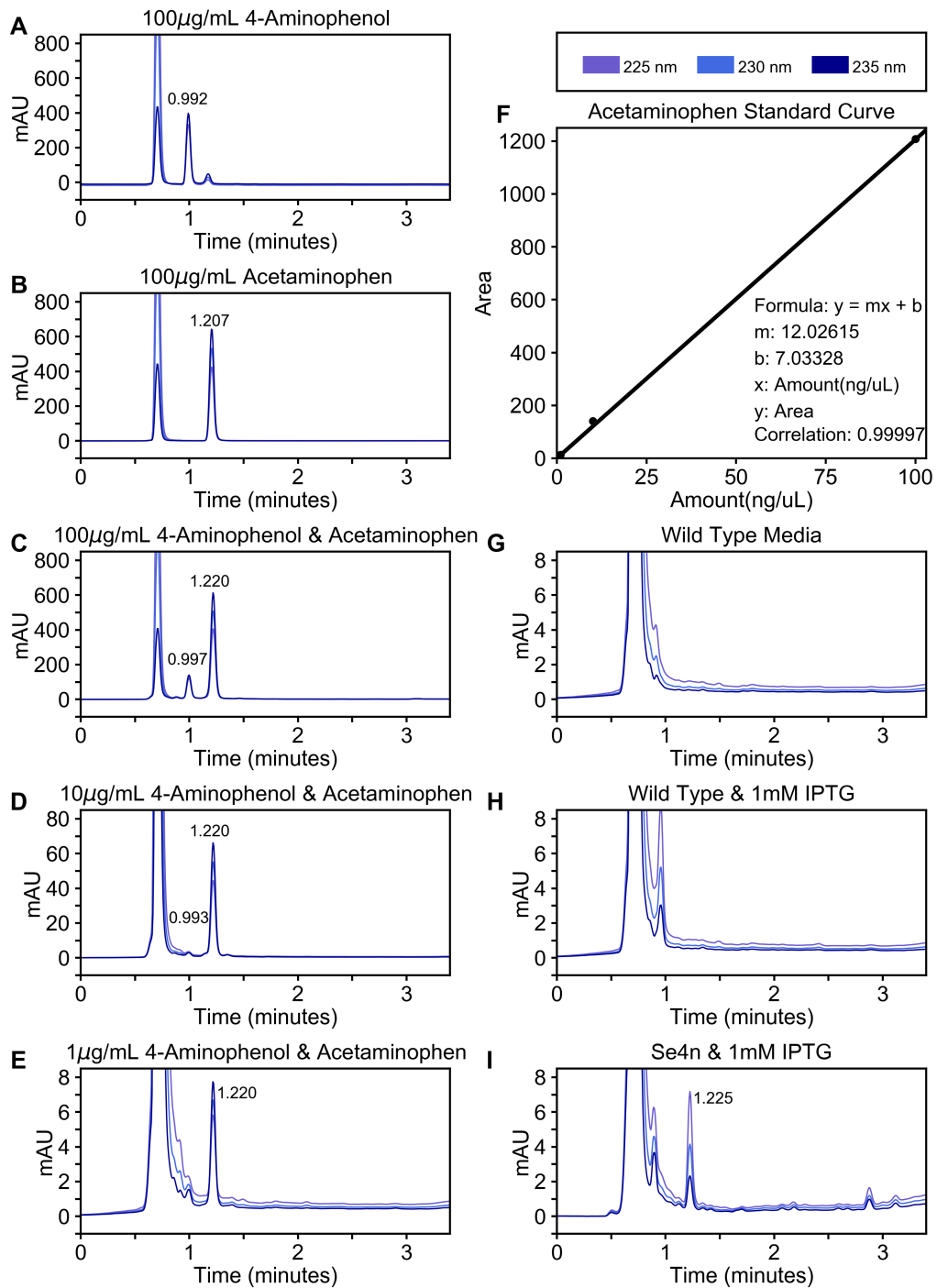
Figure 36: HPLC data indicating Se4n colony 5 produces acetaminophen. A) 100 μg/mL 4-aminophenol in WT media. B)100 μg/mL acetaminophen in WT media. C) C) 100 μg/mL 4-aminophenol & acetaminophen. D) 10 μg/mL 4-aminophenol & acetaminophen. E) 1 μg/mL 4-aminophenol & acetaminophen. F) Acetaminophen standard curve built from the standards in Panels C-E. G) Wildtype PCC 7942 media H) Wildtype PCC 7942 media with 1 mM IPTG I) Engineered Se4n colony 5 with 1 mM IPTG showing a peak that indicates acetaminophen presence.

4.3.5 DNA extraction and sequencing

In the neutral site PCRs, Figure 32 Figure 34, colony 5 produced amplicons close to the expected values, whereas colony 8 had amplicons larger than expected. DNA was extracted from each of these colonies, and 10 gb of data were sequenced on an Illumina NovaSeq. This sequencing was performed to elucidate where in the genome *4ABH* was integrated, and why the amplicons were larger than expected. Unfortunately, the data for this has not yet been received.

4.4 Conclusion and future directions

Acetaminophen biosynthesis in a cyanobacteria is an environmentally friendly method of production. Cyanobacteria harness the power of the sun to fix CO_2 and drive cellular processes. Engineered acetaminophen production in PCC 7942, enabled with the genes *4ABH* and *nhoA*, allows for solar-powered synthesis of the compound, naturally driven by the host organism. This synthesis does not require harmful chemicals, media additives, or stringent energy requirements.

The Se4n colony 5 produced acetaminophen in a range of 1.04-3.3 μg/mL, proving that PCC 7942 is compatible with this engineered pathway. This acetaminophen titer is lower than expected, likely due to the ambiguous integration of the *4ABH* and *nhoA* genetic constructs. It is possible that the gene blocks had their parts assembled incorrectly, conceivably with some parts missing or disrupted by a double integration event, as is suggested by the colony PCRs (Figure 32, Figure 34). Furthermore, *4ABH* is integrated in an unknown location of the genome that may be disrupting normal cellular function, which would lower the synthesis efficiency. The ambiguity of the gene integrations will be solved with the Illumina sequencing data, and appropriate steps will be taken to optimize acetaminophen production in PCC 7942.

Although this acetaminophen titer is below industrial feasibility, it shows that cyanobacteria are capable of synthesizing acetaminophen via an engineered pathway. Upon further optimization, this system could provide a truly green synthesis of acetaminophen and have a profound impact on the pharmaceutical synthesis industry.

References

[1] Stefan V. Lalonde and Kurt O. Konhauser. "Benthic perspective on Earth's oldest evidence for oxygenic photosynthesis". In: *Proceedings of the National Academy of Sciences* 112.4 (2015), pp. 995–1000. ISSN: 0027-8424. DOI: `10.1073/pnas.1415718112`. eprint: `http://www.pnas.org/content/112/4/995.full.pdf`. URL: `http://www.pnas.org/content/112/4/995`.

[2] Gershwin M et al. *Spirulina in Human Nutrition and Health*. Boca Raton: CRC Press, 2007.

[3] Qinghua Wu et al. "The antioxidant, immunomodulatory, and anti-inflammatory activities of Spirulina: an overview". In: *Archives of Toxicology* 90.8 (2016), pp. 1817–1840. ISSN: 1432-0738. DOI: `10.1007/s00204-016-1744-5`. URL: `https://doi.org/10.1007/s00204-016-1744-5`.

[4] Y. H. Hui and E. Özgül Evranuz. *Handbook of Plant-Based Fermented Food and Beverage Technology, Second Edition*. en. Google-Books-ID: 4kBqVku9B4YC. CRC Press, May 2012. ISBN: 978-1-4398-4904-0.

[5] Dan Wan, Qinghua Wu, and Kamil Kuča. "Chapter 42 - Spirulina". In: *Nutraceuticals*. Ed. by Ramesh C. Gupta. Boston: Academic Press, 2016, pp. 569 –583. ISBN: 978-0-12-802147-7. DOI: `https://doi.org/10.1016/B978-0-12-802147-7.00042-5`. URL: `http://www.sciencedirect.com/science/article/pii/B9780128021477000425`.

[6] Udayasree V., Manjula K., and Sowjanya M. "Effect of Spirulina as a Nutritional Supplement in Malnourished Children". In: *International Journal of Scientific Research* 2.5 (2013), pp. 2277 –8179.

[7] Elizabeth Kebede and Gunnel Ahlgren. "Optimum growth conditions and light utilization efficiency of Spirulina platensis (= Arthrospira fusiformis) (Cyanophyta) from Lake Chitu, Ethiopia". In: *Hydrobiologia* 332.2 (1996), pp. 99–109. ISSN: 1573-5117. DOI: `10.1007/BF00016689`. URL: `https://doi.org/10.1007/BF00016689`.

[8] Jai Pandey, Amit Tiwari, and R M. Mishra. "Evaluation of Biomass Production of Spirulina maxima on Different Reported Media". In: 1 (Jan. 2010), pp. 70–81.

[9] Florian Delrue et al. "Optimization of Arthrospira platensis (Spirulina) Growth: From Laboratory Scale to Pilot Scale". In: 3 (Jan. 2017).

[10] Jun Zhai et al. "Optimization of biomass production and nutrients removal by Spirulina platensis from municipal wastewater". In: *Ecological Engineering* 108 (2017), pp. 83 –92. ISSN: 0925-8574. DOI: `https://doi.org/10.1016/j.ecoleng.2017.07.023`. URL: `http://www.sciencedirect.com/science/article/pii/S0925857417304391`.

[11] Wu Z. Feng D. "Culture of Spirulina platensis in human urine for biomass production and O2 evolution". In: 7 (1 2006), pp. 34–37. DOI: `doi:10.1631/jzus.2006.B0034`.

[12] Fedekar Fadel Madkour, Abd El-Wahab Kamil, and Hoda Shafik Nasr. "Production and nutritive value of Spirulina platensis in reduced cost media". In: *The Egyptian Journal of Aquatic Research* 38.1 (2012), pp. 51 –57. ISSN: 1687-4285. DOI: `https://doi.org/10.1016/j.ejar.2012.09.003`. URL: `http://www.sciencedirect.com/science/article/pii/S168742851200009X`.

[13] Mario R. Tredici, Teresa Papuzzo, and Luisa Tomaselli. "Outdoor mass culture of Spirulina maxima in sea-water". In: *Applied Microbiology and Biotechnology* 24.1 (1986), pp. 47–50. ISSN: 1432-0614. DOI: `10.1007/BF00266284`. URL: `https://doi.org/10.1007/BF00266284`.

[14] International Micronutrient Malnutrition Prevention and Control (IMMPaCt). "Micronutrient Facts". In: *CDC* (). URL: `https://www.cdc.gov/immpact/micronutrients/index.html`.

[15] Jaber Dehghani et al. "Stable transformation of Spirulina (Arthrospira) platensis: a promising microalga for production of edible vaccines". In: *Applied Microbiology and Biotechnology* (2018). ISSN: 1432-0614. DOI: `10.1007/s00253-018-9296-7`. URL: `https://doi.org/10.1007/s00253-018-9296-7`.

[16] Siew-Moi Phang, Wan-Loy Chu, and Reza Rabiei. "Phycoremediation". In: *The Algae World*. Ed. by Dinabandhu Sahoo and Joseph Seckbach. Dordrecht: Springer Netherlands, 2015, pp. 357–389. ISBN: 978-94-017-7321-8. DOI: `10.1007/978-94-017-7321-8_13`. URL: `https://doi.org/10.1007/978-94-017-7321-8_13`.

[17] S.-G. Kim et al. "Harvesting of Spirulina platensis by cellular flotation and growth stage determination". In: *Letters in Applied Microbiology* 40.3 (), pp. 190–194. DOI: `10.1111/j.1472-765X.2005.01654.x`. eprint: `https://onlinelibrary.wiley.com/doi/pdf/10.1111/j.1472-765X.2005.01654.x`. URL: `https://onlinelibrary.wiley.com/doi/abs/10.1111/j.1472-765X.2005.01654.x`.

[18] Xia L et al. "Effective harvesting of microalgae by coagulation–flotation". In: 4 (11 2017). DOI: `10.1098/rsos.170867`.

[19] Luv Mehan et al. "Illumination wavelengths effect on Arthrospira platensis production and its process applications in River Yamuna water treatment". In: *Journal of Water Process Engineering* 23 (2018), pp. 91 –96. ISSN: 2214-7144. DOI: `https://doi.org/10.1016/j.jwpe.2018.03.010`. URL: `http://www.sciencedirect.com/science/article/pii/S2214714417307110`.

[20] Weizhi Zhou et al. "Nutrients removal and recovery from saline wastewater by Spirulina platensis". In: *Bioresource Technology* 245 (2017), pp. 10 –17. ISSN: 0960-8524. DOI: `https://doi.org/10.1016/j.biortech.2017.08.160`. URL: `http://www.sciencedirect.com/science/article/pii/S0960852417314748`.

[21] S. Balaji et al. "Removal of heavy metals from tannery effluents of Ambur industrial area, Tamilnadu by Arthrospira (Spirulina) platensis". In: *Environmental Monitoring and Assessment* 187.6 (2015), p. 325. ISSN: 1573-2959. DOI: `10.1007/s10661-015-4440-7`. URL: `https://doi.org/10.1007/s10661-015-4440-7`.

[22] Inga Zinicovscaia et al. "Metal Uptake from Complex Industrial Effluent by Cyanobacteria Arthrospira platensis". In: *Water, Air, & Soil Pollution* 229.7 (2018), p. 220. ISSN: 1573-2932. DOI: 10.1007/s11270-018-3873-3. URL: https://doi.org/10.1007/s11270-018-3873-3.

[23] Lakhveer Singh et al. *Metals Cd, As, Cu, and Zn Transfer through Dry to Rehydrated Biomass of Spirulina Platensis from Wastewater*. Apr. 2014.

[24] Inga Zinicovscaia et al. "Spirulina platensis as biosorbent of chromium and nickel from industrial effluents". In: *Desalination and Water Treatment* 57.24 (2016), pp. 11103–11110. DOI: 10.1080/19443994.2015.1042061. eprint: https://doi.org/10.1080/19443994.2015.1042061. URL: https://doi.org/10.1080/19443994.2015.1042061.

[25] Inga Zinicovscaia et al. "Application of Arthrospira (Spirulina) platensis biomass for silver removal from aqueous solutions". In: *International Journal of Phytoremediation* 19.11 (2017). PMID: 28441036, pp. 1053–1058. DOI: 10.1080/15226514.2017.1319332. eprint: https://doi.org/10.1080/15226514.2017.1319332. URL: https://doi.org/10.1080/15226514.2017.1319332.

[26] Inga Zinicovscaia et al. "Zinc removal from model solution and wastewater by Arthrospira (Spirulina) Platensis biomass". In: *International Journal of Phytoremediation* 20.9 (2018). PMID: 29873533, pp. 901–908. DOI: 10.1080/15226514.2018.1448358. eprint: https://doi.org/10.1080/15226514.2018.1448358. URL: https://doi.org/10.1080/15226514.2018.1448358.

[27] K. Phengrit and S. Iamtham. "Cultivation of Arthrospira platensis using discharge water from Thai shrimp farm for algal production and wastewater treatment." In: *Journal of ISSAAS (International Society for Southeast Asian Agricultural Sciences)* 24.1 (2018), pp. 27–40.

[28] Sara Monaliza Sousa Nogueira et al. "Use of Spirulina platensis in treatment of fish farming wastewater". In: 49 (Jan. 2018).

[29] Cai Xiao-Bo et al. "[Cultivation of Spirulina platensis in Digested Piggery Wastewater Pretreated by SBR with Operating Conditions Optimization]". In: *Huan jing ke xue= Huanjing kexue* 38.7 (2017), 2910—2916. ISSN: 0250-3301. DOI: 10.13227/j.hjkx.201612168. URL: https://doi.org/10.13227/j.hjkx.201612168.

[30] Ratana Chaiklahan et al. "Cultivation of Spirulina platensis using pig wastewater in a semi-continuous process". In: *J. Microbiol. Biotechnol* 20.3 (2010), 609—614.

[31] S. Hena et al. "Dairy farm wastewater treatment and lipid accumulation by Arthrospira platensis". In: *Water Research* 128 (2018), pp. 267 –277. ISSN: 0043-1354. DOI: https://doi.org/10.1016/j.watres.2017.10.057. URL: http://www.sciencedirect.com/science/article/pii/S0043135417309004.

[32] Mesfin M. Mekonnen and Arjen Y. Hoekstra. "Four billion people facing severe water scarcity". In: *Science Advances* 2.2 (2016). DOI: 10.1126/sciadv.1500323. eprint: http://advances.sciencemag.org/content/2/2/e1500323.full.pdf. URL: http://advances.sciencemag.org/content/2/2/e1500323.

[33] International Energy Agency. *Global Energy & CO2 Status Report*. 2018. URL: http://www.iea.org/geco/.

[34] K. Kaygusuz. "Bioenergy as a Clean and Sustainable Fuel". In: *Energy Sources, Part A: Recovery, Utilization, and Environmental Effects* 31.12 (2009), pp. 1069–1080. DOI: `10.1080/15557030801909839`. eprint: `https://doi.org/10.1080/15557030801909839`. URL: `https://doi.org/10.1080/15557030801909839`.

[35] Naira Quintana et al. "Renewable energy from Cyanobacteria: energy production optimization by metabolic pathway engineering". In: *Applied Microbiology and Biotechnology* 91.3 (2011), pp. 471–490. ISSN: 1432-0614. DOI: `10.1007/s00253-011-3394-0`. URL: `https://doi.org/10.1007/s00253-011-3394-0`.

[36] Piyushi Nautiyal, K.A. Subramanian, and M.G. Dastidar. "Production and characterization of biodiesel from algae". In: *Fuel Processing Technology* 120 (2014), pp. 79 –88. ISSN: 0378-3820. DOI: `https://doi.org/10.1016/j.fuproc.2013.12.003`. URL: `http://www.sciencedirect.com/science/article/pii/S037838201300372X`.

[37] H. I. El-Shimi et al. "Biodiesel Production from Spirulina-Platensis Microalgae by In-Situ Transesterification Process". In: *Journal of Sustainable Bioenergy Systems* 3 (2013), pp. 224–233. DOI: `http://dx.doi.org/10.4236/jsbs.2013.33031`.

[38] Katsuhiro Aoyama et al. "Fermentative metabolism to produce hydrogen gas and organic compounds in a cyanobacterium, Spirulina platensis". In: *Journal of Fermentation and Bioengineering* 83.1 (1997), pp. 17 –20. ISSN: 0922-338X. DOI: `https://doi.org/10.1016/S0922-338X(97)87320-5`. URL: `http://www.sciencedirect.com/science/article/pii/S0922338X97873205`.

[39] Gennady Ananyev, Damian Carrieri, and G. Charles Dismukes. "Optimization of Metabolic Capacity and Flux through Environmental Cues To Maximize Hydrogen Production by the Cyanobacterium "Arthrospira (Spirulina) maxima"". In: *Applied and Environmental Microbiology* 74.19 (2008), pp. 6102–6113. ISSN: 0099-2240. DOI: `10.1128/AEM.01078-08`. eprint: `https://aem.asm.org/content/74/19/6102.full.pdf`. URL: `https://aem.asm.org/content/74/19/6102`.

[40] Lingkan Ding et al. "Three-stage gaseous biofuel production combining dark hydrogen, photo hydrogen, and methane fermentation using wet Arthrospira platensis cultivated under high CO2 and sodium stress". In: *Energy Conversion and Management* 148 (2017), pp. 394 –404. ISSN: 0196-8904. DOI: `https://doi.org/10.1016/j.enconman.2017.05.079`. URL: `http://www.sciencedirect.com/science/article/pii/S0196890417305435`.

[41] Mingyue Fang et al. "Rapid Mutation of Spirulina platensis by a New Mutagenesis System of Atmospheric and Room Temperature Plasmas (ARTP) and Generation of a Mutant Library with Diverse Phenotypes". In: *PLOS ONE* 8.10 (Oct. 2013). DOI: `10.1371/journal.pone.0077046`. URL: `https://doi.org/10.1371/journal.pone.0077046`.

[42] Katsunori Yoshikawa et al. "Construction of a Genome-Scale Metabolic Model of Arthrospira platensis NIES-39 and Metabolic Design for Cyanobacterial Bioproduction". In: *PLOS ONE* 10.12 (Dec. 2015), pp. 1–16. DOI: `10.1371/journal.pone.0144430`. URL: `https://doi.org/10.1371/journal.pone.0144430`.

[43]   Shimpei Aikawa et al. "Direct conversion of Spirulina to ethanol without pretreatment or enzymatic hydrolysis processes". In: *Energy Environ. Sci.* 6 (2013), pp. 1844–1849. DOI: `10.1039/C3EE40305J`.

[44]   Shimpei Aikawa et al. "Direct and highly productive conversion of cyanobacteria Arthrospira platensis to ethanol with CaCl2 addition". In: *Biotechnology for Biofuels* 11.1 (2018), p. 50. ISSN: 1754-6834. DOI: `10.1186/s13068-018-1050-y`. URL: `https://doi.org/10.1186/s13068-018-1050-y`.

[45]   Giorgos Markou, Iordanis Chatzipavlidis, and Dimitris Georgakakis. "Carbohydrates production and bio-flocculation characteristics in cultures of Arthrospira (Spirulina) platensis: Improvements through phosphorus limitation process". In: (Apr. 2012).

[46]   Giorgos Markou. "Alteration of the biomass composition of Arthrospira (Spirulina) platensis under various amounts of limited phosphorus". In: *Bioresource Technology* 116 (2012), pp. 533 –535. ISSN: 0960-8524. DOI: `https://doi.org/10.1016/j.biortech.2012.04.022`. URL: `http://www.sciencedirect.com/science/article/pii/S0960852412006244`.

[47]   Orily Depraetere et al. "Harvesting carbohydrate-rich Arthrospira platensis by spontaneous settling". In: *Bioresource Technology* 180 (2015), pp. 16 –21. ISSN: 0960-8524. DOI: `https://doi.org/10.1016/j.biortech.2014.12.084`. URL: `http://www.sciencedirect.com/science/article/pii/S0960852414018306`.

[48]   Philipp Savakis and Klaas J Hellingwerf. "Engineering cyanobacteria for direct biofuel production from CO2". In: *Current Opinion in Biotechnology* 33 (2015). Environmental biotechnology ● Energy biotechnology, pp. 8 –14. ISSN: 0958-1669. DOI: `https://doi.org/10.1016/j.copbio.2014.09.007`. URL: `http://www.sciencedirect.com/science/article/pii/S0958166914001670`.

[49]   Amornpan Klanchui et al. "i AK692: A genome-scale metabolic model of Spirulina platensis C1". In: *BMC Systems Biology* 6.1 (2012), p. 71. ISSN: 1752-0509. DOI: `10.1186/1752-0509-6-71`. URL: `https://doi.org/10.1186/1752-0509-6-71`.

[50]   Hannah Ritchie and Max Roser. *Micronutrient Deficiency.* 2018. URL: `https://ourworldindata.org/micronutrient-deficiency`.

[51]   World Health Organization, ed. *The Selection and Use of Essential Medicines: report of the WHO Expert Committee, 2007 ; (including the 15th model list of essential medicines).* eng. WHO Technical Report Series 946. OCLC: 254437808. Geneva: World Health Organization, 2007. ISBN: 978-92-4-120946-5.

[52]   M. Ahsan B. Habib et al. "A review on culture, production and use of spirulina as food for humans and feeds for domestic animals and fish". In: *FAO Fisheries and Aquaculture Circular* 1034 (), p. 33. ISSN: 2070-6065. URL: `http://www.fao.org/docrep/pdf/011/i0424e/i0424e00.pdf`.

[53]   C.E.N. Sassano et al. "Evaluation of the composition of continuously-cultivated Arthrospira (Spirulina) platensis using ammonium chloride as nitrogen source". In: *Biomass and Bioenergy* 34.12 (2010). Current and Potential Capabilities of Wood Production Systems in the Southeastern U.S., pp. 1732 –1738. ISSN: 0961-9534. DOI: `https://doi.org/10.1016/j.biombioe.2010.`

07.002. URL: http://www.sciencedirect.com/science/article/pii/S0961953410002072.

[54] Ana Paula Batista et al. "Comparison of microalgal biomass profiles as novel functional ingredient for food products". In: *Algal Research* 2.2 (2013), pp. 164 –173. ISSN: 2211-9264. DOI: https://doi.org/10.1016/j.algal.2013.01.004. URL: http://www.sciencedirect.com/science/article/pii/S2211926413000210.

[55] Giuseppe Torzillo et al. "Production of Spirulina biomass in closed photobioreactors". In: 11 (Dec. 1986), pp. 61–74.

[56] O. Tokusoglu and M.K. Unal. "Biomass Nutrient Profiles of Three Microalgae: Spirulina platensis, Chlorella vulgaris, and Isochrisis galbana". In: *Journal of Food Science* 68.4 (), pp. 1144–1148. DOI: 10.1111/j.1365-2621.2003.tb09615.x. eprint: https://onlinelibrary.wiley.com/doi/pdf/10.1111/j.1365-2621.2003.tb09615.x. URL: https://onlinelibrary.wiley.com/doi/abs/10.1111/j.1365-2621.2003.tb09615.x.

[57] Hidenori Shimamatsu. "Mass production of Spirulina, an edible microalga". In: *Hydrobiologia* 512.1 (2004), pp. 39–44. ISSN: 1573-5117. DOI: 10.1023/B:HYDR.0000020364.23796.04. URL: https://doi.org/10.1023/B:HYDR.0000020364.23796.04.

[58] J. J. Ortega-Calvo et al. "Chemical composition ofSpirulina and eukaryotic algae food products marketed in Spain". In: *Journal of Applied Phycology* 5.4 (1993), pp. 425–435. ISSN: 1573-5176. DOI: 10.1007/BF02182735. URL: https://doi.org/10.1007/BF02182735.

[59] Harriet Volkmann et al. "Cultivation of Arthrospira (spirulina) platensis in desalinator wastewater and salinated synthetic medium: protein content and amino-acid profile". en. In: *Brazilian Journal of Microbiology* 39 (Mar. 2008), pp. 98 –101. ISSN: 1517-8382. URL: http://www.scielo.br/scielo.php?script=sci_arttext\&pid=S1517-83822008000100022\&nrm=iso.

[60] G. Clément, C. Giddey, and R. Menzi. "Amino acid composition and nutritive value of the alga Spirulina maxima". In: *Journal of the Science of Food and Agriculture* 18.11 (), pp. 497–501. DOI: 10.1002/jsfa.2740181101. eprint: https://onlinelibrary.wiley.com/doi/pdf/10.1002/jsfa.2740181101. URL: https://onlinelibrary.wiley.com/doi/abs/10.1002/jsfa.2740181101.

[61] L. Campanella, G. Crescentini, and P. Avino. "Chemical composition and nutritional evaluation of some natural and commercial food products based on Spirulina". In: *Analusis* 27 (1999), pp. 533–540. URL: http://dx.doi.org/10.1051/analusis:1999130.

[62] A. S. Babadzhanov et al. "Chemical Composition of Spirulina platensis Cultivated in Uzbekistan". In: *Chemistry of Natural Compounds* 40.3 (2004), pp. 276–279. ISSN: 1573-8388. DOI: 10.1023/B:CONC.0000039141.98247.e8. URL: https://doi.org/10.1023/B:CONC.0000039141.98247.e8.

[63] Szabolcs Molnar Attila Kiss. "Comparative Studies on Accumulation of Selected Microelements by Spirulina Platensis and Chlorella Vulgaris with the Prospects of Functional Food Development". In: 04 (Jan. 2013).

[64] Al-Dhabi NA. "Heavy metal analysis in commercial Spirulina products for human consumption." In: 20 (4 2013), pp. 383–388. DOI: `doi:10.1016/j.sjbs.2013.04.006`.

[65] C Boudène, E Collas, and C Jenkins. "[Determination of various toxic minerals in spiruline algae of different origins, and evaluation of long-term toxicity in the rat of a lot of spiruline algae of Mexican origin]". In: 29 (Feb. 1975), pp. 577–88.

[66] Katherine Emma Helliwell et al. "Cyanobacteria and Eukaryotic Algae Use Different Chemical Variants of Vitamin B12". eng. In: *Current biology: CB* 26.8 (Apr. 2016), pp. 999–1008. ISSN: 1879-0445. DOI: `10.1016/j.cub.2016.02.041`.

[67] V. Karuppiah, W. Sun, and Z. Li. "Natural Products of Actinobacteria Derived from Marine Organisms". en. In: *Studies in Natural Products Chemistry*. Vol. 48. DOI: 10.1016/B978-0-444-63602-7.00013-8. Elsevier, 2016, pp. 417–446. ISBN: 978-0-444-63602-7. URL: `http://linkinghub.elsevier.com/retrieve/pii/B9780444636027000138` (visited on 07/27/2017).

[68] Lindsay H Allen. "How common is vitamin B-12 deficiency?" In: *The American Journal of Clinical Nutrition* 89.2 (2009), 693S–696S. DOI: `10.3945/ajcn.2008.26947A`. eprint: `/oup/backfile/content_public/journal/ajcn/89/2/10.3945_ajcn.2008.26947a/6/693s.pdf`. URL: `http://dx.doi.org/10.3945/ajcn.2008.26947A`.

[69] Emmanuel Manirafasha et al. "Phycobiliprotein: Potential microalgae derived pharmaceutical and biological reagent". In: *Biochemical Engineering Journal* 109 (2016), pp. 282 –296. ISSN: 1369-703X. DOI: `https://doi.org/10.1016/j.bej.2016.01.025`. URL: `http://www.sciencedirect.com/science/article/pii/S1369703X16300262`.

[70] K. Iwata, T. Inayama, and Kato. "Effects of Spirulina Platensis on Plasma Lipoprotein Lipase Activity in Fructose-Induced Hyperlipidemic Rats". In: *Journal of Nutritional Science and Vitaminology* 36.2 (1990), pp. 165–171. DOI: `10.3177/jnsv.36.165`.

[71] Edis Koru. "Earth Food Spirulina (Arthrospira): Production and Quality Standarts". In: *IntechOpen* (2012). DOI: `DOI:10.5772/31848`.

[72] Abed and AN Ihab. "Impact of Spirulina on Nutritional Status, Haematological Profile and Anaemia Status in Malnourished Children in the Gaza Strip: Randomized Clinical Trial". In: 2016.

[73] Yin C et al. "TACKLING COMMUNITY UNDERNUTRITION AT LAKE BOGORIA, KENYA: THE POTENTIAL OF SPIRULINA (ARTHROSPIRA FUSIFORMIS) AS A FOOD SUPPLEMENT". In: *Afr. J. Food Agric. Nutr. Dev.* 17 (2017), pp. 11603–11615.

[74] Luciane Maria Colla, Ana Luiza Muccillo-Baisch, and Jorge Alberto Vieira Costa. "Spirulina platensis effects on the levels of total cholesterol, HDL and triacylglycerols in rabbits fed with a hypercholesterolemic diet". en. In: *Brazilian Archives of Biology and Technology* 51 (Apr. 2008), pp. 405 –411. ISSN: 1516-8913. URL: `http://www.scielo.br/scielo.php?script=sci_arttext\&pid=S1516-89132008000200022\&nrm=iso`.

[75] Patricia V. Torres-Duran, Aldo Ferreira-Hermosillo, and Marco A. Juarez-Oropeza. "Antihyperlipemic and antihypertensive effects of Spirulina maxima in an open sample of mexican population: a preliminary report". In: *Lipids in Health and Disease* 6.1 (2007), p. 33. ISSN: 1476-511X. DOI: 10.1186/1476-511X-6-33. URL: https://doi.org/10.1186/1476-511X-6-33.

[76] Panam Parikh, Uliyar Mani, and Uma Iyer. "Role of Spirulina in the Control of Glycemia and Lipidemia in Type 2 Diabetes Mellitus". In: *Journal of Medicinal Food* 4.4 (2001). PMID: 12639401, pp. 193–199. DOI: 10.1089/10966200152744463. eprint: https://doi.org/10.1089/10966200152744463. URL: https://doi.org/10.1089/10966200152744463.

[77] Nagaoka Satoshi et al. "A Novel Protein C-Phycocyanin Plays a Crucial Role in the Hypocholesterolemic Action of Spirulina platensis Concentrate in Rats". In: *The Journal of Nutrition* 135.10 (2005), pp. 2425–2430. DOI: 10.1093/jn/135.10.2425. eprint: /oup/backfile/content_public/journal/jn/135/10/10.1093_jn_135.10.2425/4/z4w01005002425.pdf. URL: http://dx.doi.org/10.1093/jn/135.10.2425.

[78] Jiyeong Lee et al. "Spirulina Extract Enhanced a Protective Effect in Type 1 Diabetes by Anti-Apoptosis and Anti-ROS Production". In: *Nutrients*. 2017.

[79] L. Anitha and K. Chandralekha. "Effect of supplementation of Spirulina on blood glucose, glycosylated hemoglobin and lipid profile of male non-insulin dependent diabetics." In: *Asian Journal of Experimental Biological Sciences* 1.1 (2010), pp. 36–46.

[80] Becker E.W. et al. "c". In: (1986).

[81] Reihaneh Zeinalian et al. "The effects of Spirulina Platensis on anthropometric indices, appetite, lipid profile and serum vascular endothelial growth factor (VEGF) in obese individuals: a randomized double blinded placebo controlled trial". In: *BMC complementary and alternative medicine*. 2017.

[82] Seo Young-Jin et al. "Spirulina maxima Extract Reduces Obesity through Suppression of Adipogenesis and Activation of Browning in 3T3-L1 Cells and High-Fat Diet-Induced Obese Mice". In: 10 (June 2018), p. 712.

[83] Diadelis Remirez et al. "Inhibitory effects of Spirulina in zymosan-induced arthritis in mice". In: *Mediators of Inflammation* 11.2 (2002), pp. 75–79. DOI: https://doi.org/10.1080/09629350220131917.

[84] Eman A. I. Ali, Bassant M. Barakat, and Ranya Hassan. "Antioxidant and Angiostatic Effect of Spirulina platensis Suspension in Complete Freund's Adjuvant-Induced Arthritis in Rats". In: *PLOS ONE* 10.4 (Apr. 2015), pp. 1–13. DOI: 10.1371/journal.pone.0121523. URL: https://doi.org/10.1371/journal.pone.0121523.

[85] Narendra Kumar et al. "Evaluation of protective efficacy of Spirulina platensis against collagen-induced arthritis in rats". In: *Inflammopharmacology* 17.3 (2009), pp. 181–190. ISSN: 1568-5608. DOI: 10.1007/s10787-009-0004-1. URL: https://doi.org/10.1007/s10787-009-0004-1.

[86] T.K. Mao, J. Van de Water, and M.E. Gershwin. "Effects of a Spirulina-Based Dietary Supplement on Cytokine Production from Allergic Rhinitis Patients". In: *Journal of Medicinal Food* 8.1 (2005). PMID: 15857205, pp. 27–30. DOI: 10.1089/jmf.2005.8.27. eprint: https://doi.org/10.1089/jmf.2005.8.27. URL: https://doi.org/10.1089/jmf.2005.8.27.

[87] Ali Karadeniz et al. "Spirulina platensis protects against gentamicin-induced nephrotoxicity in rats". In: *Phytotherapy Research* 22.11 (), pp. 1506–1510. DOI: 10.1002/ptr.2522. eprint: https://onlinelibrary.wiley.com/doi/pdf/10.1002/ptr.2522. URL: https://onlinelibrary.wiley.com/doi/abs/10.1002/ptr.2522.

[88] Mukesh Kumar Sharma et al. "Evaluation of protective efficacy of Spirulina fusiformis against mercury induced nephrotoxicity in Swiss albino mice". In: *Food and Chemical Toxicology* 45.6 (2007), pp. 879 –887. ISSN: 0278-6915. DOI: https://doi.org/10.1016/j.fct.2006.11.009. URL: http://www.sciencedirect.com/science/article/pii/S0278691506003383.

[89] Mohamed Fouad Ismail et al. "Chemoprevention of rat liver toxicity and carcinogenesis by Spirulina". In: *International Journal of Biological Sciences* 5 (2009), pp. 377 –387.

[90] Arkadiusz Czerwonka et al. "Anticancer effect of the water extract of a commercial Spirulina (Arthrospira platensis) product on the human lung cancer A549 cell line". In: *Biomedicine & Pharmacotherapy* 106 (2018), pp. 292 – 302. ISSN: 0753-3322. DOI: https://doi.org/10.1016/j.biopha.2018.06.116. URL: http://www.sciencedirect.com/science/article/pii/S0753332218332931.

[91] Antonio Morales-González Jose et al. "Inhibitory Effect of Spirulina maxima on the Azoxymethane-induced Aberrant Colon Crypts and Oxidative Damage in Mice". In: 11 (Dec. 2015), pp. 619–624.

[92] Oh Sung-Ho et al. "The Effect of Ultrasonificated Extracts of Spirulina maxima on the Anticancer Activity". In: *Marine Biotechnology* 13.2 (2011), pp. 205–214. ISSN: 1436-2236. DOI: 10.1007/s10126-010-9282-2. URL: https://doi.org/10.1007/s10126-010-9282-2.

[93] Babu Mathew et al. "Evaluation of chemoprevention of oral cancer with spirulina fusiformis". In: *Nutrition and Cancer* 24.2 (1995). PMID: 8584455, pp. 197–202. DOI: 10.1080/01635589509514407. eprint: https://doi.org/10.1080/01635589509514407. URL: https://doi.org/10.1080/01635589509514407.

[94] Jiang Liangqian et al. "Phycocyanin: A Potential Drug for Cancer Treatment". In: 8 (Sept. 2017), pp. 3416–3429.

[95] Geou-Yarh Liou and Peter Storz. "Reactive oxygen species in cancer". In: *Free Radical Research* 44.5 (2010). PMID: 20370557, pp. 479–496. DOI: 10.3109/10715761003667554. eprint: https://doi.org/10.3109/10715761003667554. URL: https://doi.org/10.3109/10715761003667554.

[96] Shekhar Verma, Ravindra Samarth, and Meenakshi Panwar. "Evaluation of Radioprotective Effects of Spirulina in Swiss Albino Mice". In: *Asian J. Exp. Sci.* 20.1 (2006), pp. 121–126. URL: http://www.ajesjournal.com/PDFs/06-1/Shekhar\%20Verma.pdf.

[97] Rehab Makhlouf and Ibrahim Makhlouf. *Evaluation of the effect of Spirulina against Gamma irradiation induced oxidative stress and tissue injury in rats.*

[98] Marthe-Elise Ngo-Matip et al. "Impact of daily supplementation of Spirulina platensis on the immune system of naïve HIV-1 patients in Cameroon: a 12-months single blind, randomized, multicenter trial". In: *Nutrition Journal* 14.1 (2015), p. 70. ISSN: 1475-2891. DOI: 10.1186/s12937-015-0058-4. URL: https://doi.org/10.1186/s12937-015-0058-4.

[99] S Ayehunie et al. "Inhibition of HIV-1 replication by an aqueous extract of Spirulina platensis (Arthrospira platensis)". In: *Journal of acquired immune deficiency syndromes and human retrovirology : official publication of the International Retrovirology Association* 18.1 (1998), 7—12. ISSN: 1077-9450. DOI: 10.1097/00042560-199805010-00002. URL: https://doi.org/10.1097/00042560-199805010-00002.

[100] Sabine Rechter et al. "Antiviral activity of Arthrospira-derived spirulan-like substances". In: *Antiviral Research* 72.3 (2006), pp. 197 –206. ISSN: 0166-3542. DOI: https://doi.org/10.1016/j.antiviral.2006.06.004. URL: http://www.sciencedirect.com/science/article/pii/S0166354206001902.

[101] KYOKO HAYASHI, TOSHIMITSU HAYASHI, and ICHIRO KOJIMA. "A Natural Sulfated Polysaccharide, Calcium Spirulan, Isolated from Spirulina platensis: In Vitro and ex Vivo Evaluation of Anti-Herpes Simplex Virus and Anti-Human Immunodeficiency Virus Activities". In: *AIDS Research and Human Retroviruses* 12.15 (1996). PMID: 8893054, pp. 1463–1471. DOI: 10.1089/aid.1996.12.1463. eprint: https://doi.org/10.1089/aid.1996.12.1463. URL: https://doi.org/10.1089/aid.1996.12.1463.

[102] Armida Hernández-Corona et al. "Antiviral activity of Spirulina maxima against herpes simplex virus type 2". In: *Antiviral Research* 56.3 (2002), pp. 279 – 285. ISSN: 0166-3542. DOI: https://doi.org/10.1016/S0166-3542(02)00132-8. URL: http://www.sciencedirect.com/science/article/pii/S0166354202001328.

[103] Chen Yi-Hsiang et al. "Well-tolerated Spirulina extract inhibits influenza virus replication and reduces virus-induced mortality". In: 6 (Apr. 2016), p. 24253.

[104] Amha Belay et al. "Current knowledge on potential health benefits of Spirulina". In: *Journal of Applied Phycology* 5.2 (1993), pp. 235–241. ISSN: 1573-5176. DOI: 10.1007/BF00004024. URL: https://doi.org/10.1007/BF00004024.

[105] Suresh D et al. "ANTIDEPRESSANT ACTIVITY OF Spirulina Platensis IN EXPERIMENTALLY INDUCED DEPRESSED MICE". In: *International Journal of Pharmaceutical Archive* 3 (2 2014), pp. 317–326. ISSN: ISSN 2319-7226. URL: http://ijpaonline.info/index.php/ijpaonline/article/view/77.

[106] Chei Sungwoo et al. "Neuroprotective Effect of Spirulina maxima Extract against Trimethyltin-Induced Neuronal Damage in HT-22 Cells". In: *The FASEB Journal* 31.1_supplement (2017), pp. 636.17–636.17. DOI: 10.1096/fasebj.31.1_supplement.636.17. eprint: https://www.fasebj.org/doi/pdf/10.1096/fasebj.31.1_supplement.636.17. URL: https://www.fasebj.org/doi/abs/10.1096/fasebj.31.1_supplement.636.17.

[107] Angélica Pérez-Juárez et al. "Neuroprotective effect of Arthrospira (Spirulina) platensis against kainic acid-neuronal death". In: *Pharmaceutical Biology* 54.8 (2016). PMID: 26799655, pp. 1408–1412. DOI: 10.3109/13880209.2015.1103756. eprint: https://doi.org/10.3109/13880209.2015.1103756. URL: https://doi.org/10.3109/13880209.2015.1103756.

[108] Pabon Mibel M. et al. "A Spirulina-Enhanced Diet Provides Neuroprotection in an α-Synuclein Model of Parkinson's Disease". In: *PLOS ONE* 7.9 (Sept. 2012), pp. 1–7. DOI: 10.1371/journal.pone.0045256. URL: https://doi.org/10.1371/journal.pone.0045256.

[109] Juen-Haur HWANG et al. "<i>Spirulina</i> Prevents Memory Dysfunction, Reduces Oxidative Stress Damage and Augments Antioxidant Activity in Senescence-Accelerated Mice". In: *Journal of Nutritional Science and Vitaminology* 57.2 (2011), pp. 186–191. DOI: 10.3177/jnsv.57.186.

[110] Cheyla Romay, Nuris Ledón, and Ricardo Gonzalez. "Effects of Phycocyanin Extract on Prostaglandin E2 Levels in Mouse Ear Inflammation Test". In: *Drug Research* 50.12 (2000), pp. 1106–1109. DOI: DOI:10.1055/s-0031-1300340.

[111] Janssen P. J. et al. "Genome Sequence of the Edible Cyanobacterium Arthrospira sp. PCC 8005". In: *Journal of Bacteriology* 192.9 (2010), pp. 2465–2466. ISSN: 0021-9193. DOI: 10.1128/JB.00116-10. eprint: https://jb.asm.org/content/192/9/2465.full.pdf. URL: https://jb.asm.org/content/192/9/2465.

[112] Fujisawa T et al. "Genomic Structure of an Economically Important Cyanobacterium, Arthrospira (Spirulina) platensis NIES-39". In: *DNA Research: An International Journal for Rapid Publication of Reports on Genes and Genomes.* 47 (2010), pp. 85–103.

[113] Carrieri Damian et al. "Contribution of a Sodium Ion Gradient to Energy Conservation during Fermentation in the Cyanobacterium Arthrospira (Spirulina) maxima CS-328". In: *Applied and Environmental Microbiology* 77.20 (2011), pp. 7185–7194. ISSN: 0099-2240. DOI: 10.1128/AEM.00612-11. eprint: https://aem.asm.org/content/77/20/7185.full.pdf. URL: https://aem.asm.org/content/77/20/7185.

[114] Cheevadhanarak S et al. "Draft genome sequence of Arthrospira platensis C1 (PCC9438)". In: *Standards in Genomic Sciences* 6.1 (2012), pp. 43–53.

[115] Lefort Francois et al. "Whole-Genome Shotgun Sequence of Arthrospira platensis Strain Paraca, a Cultivated and Edible Cyanobacterium". In: *Microbiology Resource Announcements* 2.4 (2014). DOI: 10.1128/genomeA.00751-14. eprint: https://mra.asm.org/content/2/4/e00751-14.full.pdf. URL: https://mra.asm.org/content/2/4/e00751-14.

[116] Teng et al Xu. "Whole Genomic DNA Sequencing and Comparative Genomic Analysis of Arthrospira Platensis: High Genome Plasticity and Genetic Diversity." In: *DNA Research: An International Journal for Rapid Publication of Reports on Genes and Genomes.* 23 (2016), pp. 325–338.

[117] Shirui Dong et al. "Draft genome sequence of cyanobacteria Arthrospira sp. TJSD091 isolated from seaside wetland". In: *Marine Genomics* 24 (2015), pp. 197 –198. ISSN: 1874-7787. DOI: https://doi.org/10.1016/j.margen.2015.05.008. URL: http://www.sciencedirect.com/science/article/pii/S1874778715000859.

[118] Jian Guan et al. "Biomass and terpenoids produced by mutant strains of Arthrospira under low temperature and light conditions". In: *World Journal of Microbiology and Biotechnology* 33.2 (2017), p. 33. ISSN: 1573-0972. DOI: 10.1007/s11274-016-2199-9. URL: https://doi.org/10.1007/s11274-016-2199-9.

[119] Masaaki Toyomizu et al. "Effective transformation of the cyanobacterium Spirulina platensis using electroporation". In: *Journal of Applied Phycology* 13.3 (2001), pp. 209–214. ISSN: 1573-5176. DOI: 10.1023/A:1011182613761. URL: https://doi.org/10.1023/A:1011182613761.

[120] Yoshikazu Kawata et al. "Transformation of Spirulina platensis Strain C1 (Arthrospira sp. PCC9438) with Tn5 Transposase–Transposon DNA–Cation Liposome Complex". In: *Marine Biotechnology* 6.4 (2004), pp. 355–363. ISSN: 1436-2236. DOI: 10.1007/s10126-003-0037-1. URL: https://doi.org/10.1007/s10126-003-0037-1.

[121] Wattana Jeamton et al. "Overcoming Intrinsic Restriction Enzyme Barriers Enhances Transformation Efficiency in Arthrospira platensis C1". In: *Plant and Cell Physiology* 58.4 (2017), pp. 822–830. DOI: 10.1093/pcp/pcx016. eprint: /oup/backfile/content_public/journal/pcp/58/4/10.1093_pcp_pcx016/1/pcx016.pdf. URL: http://dx.doi.org/10.1093/pcp/pcx016.

[122] J Labarre, F Chauvat, and P Thuriaux. "Insertional mutagenesis by random cloning of antibiotic resistance genes into the genome of the cyanobacterium Synechocystis strain PCC 6803." In: *Journal of Bacteriology* 171.6 (1989), pp. 3449–3457. ISSN: 0021-9193. DOI: 10.1128/jb.171.6.3449-3457.1989. eprint: https://jb.asm.org/content/171/6/3449.full.pdf. URL: https://jb.asm.org/content/171/6/3449.

[123] Larissa Hendrickx et al. "Microbial ecology of the closed artificial ecosystem MELiSSA (Micro-Ecological Life Support System Alternative): Reinventing and compartmentalizing the Earth's food and oxygen regeneration system for long-haul space exploration missions". In: 157 (Feb. 2006), pp. 77–86.

[124] Y Wu, S Wang, and S Dong. "Phylogenetic comparison between Spirulina and Arthrospira based on 16S rRNA and rpoC1 gene". In: 56 (Feb. 2016), pp. 232–240.

[125] Nicolas Morin et al. "An efficient DNA isolation protocol for filamentous cyanobacteria of the genus Arthrospira". In: *Journal of microbiological methods* 80 (Dec. 2009), pp. 148–54. DOI: 10.1016/j.mimet.2009.11.012.

[126] OmicX. *Albacore*. URL: https://omictools.com/albacore-tool.

[127] Sergey Koren et al. "Canu: scalable and accurate long-read assembly via adaptive k-mer weighting and repeat separation." In: *Genome research* 27 5 (2017), pp. 722–736.

[128] Nicholas J. Loman, Joshua Quick, and Jared T. Simpson. "A complete bacterial genome assembled de novo using only nanopore sequencing data". In: *bioRxiv* (2015). DOI: 10.1101/015552. eprint: `https://www.biorxiv.org/content/early/2015/03/11/015552.full.pdf`. URL: `https://www.biorxiv.org/content/early/2015/03/11/015552`.

[129] Bruce J. Walker et al. "Pilon: An Integrated Tool for Comprehensive Microbial Variant Detection and Genome Assembly Improvement". In: *PLOS ONE* 9.11 (Nov. 2014), pp. 1–14. DOI: 10.1371/journal.pone.0112963. URL: `https://doi.org/10.1371/journal.pone.0112963`.

[130] Thomas Brettin et al. "RASTtk: A modular and extensible implementation of the RAST algorithm for building custom annotation pipelines and annotating batches of genomes". In: *Scientific reports* 5 (Feb. 2015), p. 8365. DOI: 10.1038/srep08365.

[131] Anton Bankevich et al. "SPAdes: A New Genome Assembly Algorithm and Its Applications to Single-Cell Sequencing". In: *Journal of computational biology : a journal of computational molecular cell biology* 19 (Apr. 2012), pp. 455–77. DOI: 10.1089/cmb.2012.0021.

[132] *Shasta long read assembler*. URL: `https://github.com/chanzuckerberg/shasta`.

[133] *MarginPolish*. URL: `https://github.com/UCSC-nanopore-cgl/MarginPolish`.

[134] Pourcel C. Grissa I Vergnaud G. "CRISPRFinder: a web tool to identify clustered regularly interspaced short palindromic repeats". In: *Nucleic Acids Research* (35 2007), W52–57. DOI: 10.1093/nar/gkm360.

[135] Stéphane Guindon et al. "New Algorithms and Methods to Estimate Maximum-Likelihood Phylogenies: Assessing the Performance of PhyML 3.0". In: *Systematic Biology* 59.3 (May 2010), pp. 307–321. ISSN: 1063-5157. DOI: 10.1093/sysbio/syq010. eprint: `http://oup.prod.sis.lan/sysbio/article-pdf/59/3/307/24207259/syq010.pdf`. URL: `https://doi.org/10.1093/sysbio/syq010`.

[136] Manolo Gouy, Stéphane Guindon, and Olivier Gascuel. "SeaView Version 4: A Multiplatform Graphical User Interface for Sequence Alignment and Phylogenetic Tree Building". In: *Molecular Biology and Evolution* 27.2 (Oct. 2009), pp. 221–224. ISSN: 0737-4038. DOI: 10.1093/molbev/msp259. eprint: `http://oup.prod.sis.lan/mbe/article-pdf/27/2/221/2916333/msp259.pdf`. URL: `https://doi.org/10.1093/molbev/msp259`.

[137] Karin Lagesen et al. "RNAmmer: consistent and rapid annotation of ribosomal RNA genes". In: *Nucleic Acids Research* 35.9 (Apr. 2007), pp. 3100–3108. ISSN: 0305-1048. DOI: 10.1093/nar/gkm160. eprint: `http://oup.prod.sis.lan/nar/article-pdf/35/9/3100/16760567/gkm160.pdf`. URL: `https://doi.org/10.1093/nar/gkm160`.

[138] Colin S. Reynolds, Rod L. Oliver, and Anthony E. Walsby. "Cyanobacterial dominance: The role of buoyancy regulation in dynamic lake environments". In: *New Zealand Journal of Marine and Freshwater Research* 21.3 (1987), pp. 379–390. DOI: 10.1080/00288330.1987.9516234. URL: `https://doi.org/10.1080/00288330.1987.9516234`.

[139] Germaine Cohen-Bazire, Riyo Kunisawa, and Norbert Pfennig. "Comparative Study of the Structure of Gas Vacuoles". In: *Journal of Bacteriology* 100.2 (1969), pp. 1049–1061. ISSN: 0021-9193. eprint: `https://jb.asm.org/content/100/2/1049.full.pdf`. URL: `https://jb.asm.org/content/100/2/1049`.

[140] Alyssa Mlouka et al. "The Gas Vesicle Gene Cluster from Microcystis aeruginosa and DNA Rearrangements That Lead to Loss of Cell Buoyancy". In: *Journal of Bacteriology* 186.8 (2004), pp. 2355–2365. ISSN: 0021-9193. DOI: `10.1128/JB.186.8.2355-2365.2004`. eprint: `https://jb.asm.org/content/186/8/2355.full.pdf`. URL: `https://jb.asm.org/content/186/8/2355`.

[141] Lucia Lamounier Sena et al. "A strategy to obtain axenic cultures of Arthrospira spp. cyanobacteria". In: *World journal of microbiology & biotechnology*. 2011.

[142] Gang-Guk Choi et al. "Induction of axenic culture of Arthrospira (Spirulina) platensis based on antibiotic sensitivity of contaminating bacteria". In: *Biotechnology Letters* 30.1 (2008), pp. 87–92. ISSN: 1573-6776. DOI: `10.1007/s10529-007-9523-2`. URL: `https://doi.org/10.1007/s10529-007-9523-2`.

[143] Hideaki Shiraishi. "Association of heterotrophic bacteria with aggregated A. platensis exopolysaccharides: implications in the induction of axenic cultures". In: *Bioscience, Biotechnology, and Biochemistry* 79.2 (2015), pp. 331–341. URL: `https://doi.org/10.1080/09168451.2014.972333`.

[144] Martin Muhling. "Characterization of Arthrospira (Spirulina) strains". In: *Durham theses, Durham University* (2000). URL: `http://etheses.dur.ac.uk/1198/`.

[145] Magda Furmaniak et al. "Edible Cyanobacterial Genus Arthrospira: Actual State of the Art in Cultivation Methods, Genetics, and Application in Medicine". In: *Frontiers in Microbiology* 8 (Dec. 2017). DOI: `10.3389/fmicb.2017.02541`.

[146] UTEX Culture Collection of Algae. *UTEX LB 2340 Spirulina platensis*. URL: `https://utex.org/products/utex-lb-2340`.

[147] Avigad Vonshak. "3 Spirulina : Growth , Physiology and Biochemistry". In: 2002.

[148] M M Yakimov et al. "Alcalilimnicola halodurans gen. nov., sp. nov., an alkaliphilic, moderately halophilic and extremely halotolerant bacterium, isolated from sediments of soda-depositing Lake Natron, East Africa Rift Valley." In: *International Journal of Systematic and Evolutionary Microbiology* 51.6 (2001), pp. 2133–2143. URL: `https://ijs.microbiologyresearch.org/content/journal/ijsem/10.1099/00207713-51-6-2133`.

[149] World Wildlife Fund. *Eastern Africa: Northern Tanzania, on the border with Kenya*. URL: `https://www.worldwildlife.org/ecoregions/at0901`.

[150] Dawn Field et al. "The minimum information about a genome sequence (MIGS) specification". In: *Nature biotechnology* 26.5 (2008), 541—547. ISSN: 1087-0156. DOI: `10.1038/nbt1360`. URL: `http://europepmc.org/articles/PMC2409278`.

[151] M.M. Ashburner et al. "Gene Ontology: tool for the unification of biology. The Gene Ontology Consortium". In: *Nat Genet* 25 (May 2000), pp. 25–29.

98

[152] Ryan R Wick et al. "Bandage: interactive visualization of de novo genome assemblies: Fig. 1." In: *Bioinformatics (Oxford, England)* 31 (June 2015). DOI: 10.1093/bioinformatics/btv383.

[153] Andrea Tyler et al. "Evaluation of Oxford Nanopore's MinION Sequencing Device for Microbial Whole Genome Sequencing Applications". In: *Scientific Reports* 8 (Dec. 2018). DOI: 10.1038/s41598-018-29334-5.

[154] Tim Carver et al. "Artemis: an integrated platform for visualization and analysis of high-throughput sequence-based experimental data". In: *Bioinformatics* 28 (Jan. 2012), pp. 464–469.

[155] Stéphan Jacquet et al. "First description of a cyanophage infecting the cyanobacterium Arthrospira platensis (Spirulina)". In: *Journal of Applied Phycology* 25.1 (2013), pp. 195–203. ISSN: 1573-5176. DOI: 10.1007/s10811-012-9853-x. URL: https://doi.org/10.1007/s10811-012-9853-x.

[156] Graham Hatfull and Roger W Hendrix. "Bacteriophages and their Genomes". In: *Current opinion in virology* 1 (Oct. 2011), pp. 298–303. DOI: 10.1016/j.coviro.2011.06.009.

[157] Peter Peduzzi et al. "The virus's tooth: Cyanophages affect an African flamingo population in a bottom-up cascade". In: *The ISME journal* 8 (Jan. 2014). DOI: 10.1038/ismej.2013.241.

[158] Paulina Deptula et al. "BluB/CobT2 fusion enzyme activity reveals mechanisms responsible for production of active form of vitamin B_{12} by Propionibacterium freudenreichii". eng. In: *Microbial Cell Factories* 14 (Nov. 2015), p. 186. ISSN: 1475-2859. DOI: 10.1186/s12934-015-0363-9.

[159] M. T. Steen et al. "Neural-tube defects are associated with low concentrations of cobalamin (vitamin B12) in amniotic fluid". eng. In: *Prenatal Diagnosis* 18.6 (June 1998), pp. 545–555. ISSN: 0197-3851.

[160] B. Hemmer et al. "Subacute combined degeneration: clinical, electrophysiological, and magnetic resonance imaging findings". eng. In: *Journal of Neurology, Neurosurgery, and Psychiatry* 65.6 (Dec. 1998), pp. 822–827. ISSN: 0022-3050.

[161] Sally P. Stabler. "Vitamin B12 Deficiency". In: *New England Journal of Medicine* 368.2 (Jan. 2013), pp. 149–160. ISSN: 0028-4793. DOI: 10.1056/NEJMcp1113996. URL: http://dx.doi.org/10.1056/NEJMcp1113996.

[162] Carlos G Acevedo-Rocha et al. "Microbial cell factories for the sustainable manufacturing of B vitamins". In: *Current Opinion in Biotechnology* 56 (2019). Food Biotechnology • Plant Biotechnology, pp. 18 –29. ISSN: 0958-1669. DOI: https://doi.org/10.1016/j.copbio.2018.07.006. URL: http://www.sciencedirect.com/science/article/pii/S0958166918300740.

[163] C. Kay Holtman et al. "High-Throughput Functional Analysis of the Synechococcus elongatus PCC 7942 Genome". In: *DNA Research* 12.2 (2005), pp. 103–115. DOI: 10.1093/dnares/12.2.103. eprint: /oup/backfile/content_public/journal/dnaresearch/12/2/10.1093_dnares_12.2.103/3/dnares_12_2_103.pdf. URL: http://dx.doi.org/10.1093/dnares/12.2.103.

[164] Sean A. Newmister et al. "Structural Insights into the Function of the Nicotinate Mononucleotide:phenol/p-cresol Phosphoribosyltransferase (ArsAB) Enzyme from Sporomusa ovata". In: *Biochemistry* 51.43 (Oct. 2012), pp. 8571–8582. ISSN: 0006-2960. DOI: 10.1021/bi301142h. URL: http://dx.doi.org/10.1021/bi301142h.

[165] Ron Caspi et al. "The MetaCyc database of metabolic pathways and enzymes and the BioCyc collection of pathway/genome databases". In: *Nucleic Acids Research* 38.Database issue (Jan. 2010), pp. D473–D479. ISSN: 0305-1048. DOI: 10.1093/nar/gkp875. URL: http://www.ncbi.nlm.nih.gov/pmc/articles/PMC2808959/.

[166] *ssuE - FMN reductase (NADPH) - Escherichia coli (strain K12) - ssuE gene & protein*. URL: http://www.uniprot.org/uniprot/P80644 (visited on 07/28/2017).

[167] Gordon R. O. Campbell et al. "Sinorhizobium meliloti bluB is necessary for production of 5,6-dimethylbenzimidazole, the lower ligand of B12". eng. In: *Proceedings of the National Academy of Sciences of the United States of America* 103.12 (Mar. 2006), pp. 4634–4639. ISSN: 0027-8424. DOI: 10.1073/pnas.0509384103.

[168] Amrita B. Hazra et al. "Analysis of substrate specificity in CobT homologs reveals widespread preference for DMB, the lower axial ligand of vitamin B 12". In: *Chemistry & biology* 20.10 (2013), pp. 1275–1285. URL: http://www.sciencedirect.com/science/article/pii/S1074552113003074.

[169] Michael J Gray and Jorge C Escalante-Semerena. "The cobinamide amidohydrolase (cobyric acid-forming) CbiZ enzyme: a critical activity of the cobamide remodelling system of Rhodobacter sphaeroides." In: *Molecular microbiology* 74 5 (2009), pp. 1198–210.

[170] Shan Yi et al. "Versatility in Corrinoid Salvaging and Remodeling Pathways Supports Corrinoid-Dependent Metabolism in Dehalococcoides mccartyi". In: *Applied and Environmental Microbiology* 78.21 (2012), pp. 7745–7752. ISSN: 0099-2240. DOI: 10.1128/AEM.02150-12. eprint: https://aem.asm.org/content/78/21/7745.full.pdf. URL: https://aem.asm.org/content/78/21/7745.

[171] Carmen L. Zayas and Jorge C. Escalante-Semerena. "Reassessment of the Late Steps of Coenzyme B12 Synthesis in Salmonella enterica: Evidence that Dephosphorylation of Adenosylcobalamin-5'-Phosphate by the CobC Phosphatase Is the Last Step of the Pathway". In: *Journal of Bacteriology* 189.6 (2007), pp. 2210–2218. ISSN: 0021-9193. DOI: 10.1128/JB.01665-06. eprint: https://jb.asm.org/content/189/6/2210.full.pdf. URL: https://jb.asm.org/content/189/6/2210.

[172] B Cameron et al. "Genetic analysis, nucleotide sequence, and products of two Pseudomonas denitrificans cob genes encoding nicotinate-nucleotide: dimethylbenzimidazole phosphoribosyltransferase and cobalamin (5'-phosphate) synthase." In: *Journal of Bacteriology* 173.19 (1991), pp. 6066–6073. ISSN: 0021-9193. DOI: 10.1128/jb.173.19.6066-6073.1991. eprint: https://jb.asm.org/content/173/19/6066.full.pdf. URL: https://jb.asm.org/content/173/19/6066.

[173] KFriedmann HC. "Vitamin B 12 biosynthesis. Evidence for a new precursor vitamin B 12 5'-phosphate." In: *J Biol Chem* 243 (1968), pp. 2065–2075.

[174] & SK KON JE KFORD ES HOLDSWORTH. "The biosynthesis of vitamin B12-like compounds." In: *The Biochemical journal* 59 (1955), pp. 86–93.

[175] Jeffrey G. Lawrence and John R. Roth. "Evolution of Coenzyme B12 Synthesis Among Enteric Bacteria: Evidence for Loss and Reacquisition of a Multigene Complex". In: *Genetics* 142.1 (1996), pp. 11–24. ISSN: 0016-6731. eprint: https://www.genetics.org/content/142/1/11.full.pdf. URL: https://www.genetics.org/content/142/1/11.

[176] M D Lundrigan, W Köster, and R J Kadner. "Transcribed sequences of the Escherichia coli btuB gene control its expression and regulation by vitamin B12." In: *Proceedings of the National Academy of Sciences* 88.4 (1991), pp. 1479–1483. ISSN: 0027-8424. DOI: 10.1073/pnas.88.4.1479. eprint: https://www.pnas.org/content/88/4/1479.full.pdf. URL: https://www.pnas.org/content/88/4/1479.

[177] Anne M. Ruffing and Howland D.T. Jones. "Physiological Effects of Free Fatty Acid Production in Genetically Engineered Synechococcus elongatus PCC 7942". In: *Biotechnology and bioengineering* 109.9 (Sept. 2012), pp. 2190–2199. ISSN: 0006-3592. DOI: 10.1002/bit.24509. URL: http://www.ncbi.nlm.nih.gov/pmc/articles/PMC3428126/.

[178] R Biopharm AG. *VitaFast® Vitamin B12 (Cyanocobalamin) (AOAC-RI)*. URL: https://food.r-biopharm.com/products/aoac-ri-certified-vitafast-vitamin-b12-cyanocobalamin/.

[179] Anantharajappa Kumudha. "Effect of Different Extraction Methods on Vitamin B12 from Blue Green Algae, Spirulina Platensis". In: *Pharmaceutica Analytica Acta* 06 (Jan. 2015). DOI: 10.4172/2153-2435.1000337.

[180] Inc. Siji Joseph Agilent Technologies. *Analysis of water-soluble vitamins from multivitamin tablets for nutrition labeling*. URL: https://www.agilent.com/cs/library/applications/5990-7950EN.pdf.

[181] Natalia B. Ivleva et al. "LdpA: a component of the circadian clock senses redox state of the cell". eng. In: *The EMBO journal* 24.6 (Mar. 2005), pp. 1202–1210. ISSN: 0261-4189. DOI: 10.1038/sj.emboj.7600606.

[182] *DNAWorks (v3.2.4)*. URL: https://hpcwebapps.cit.nih.gov/dnaworks/.

[183] *Codon Usage Database*. URL: http://www.kazusa.or.jp/codon/.

[184] *pgam3 - phosphoglycerate mutase - Synechococcus elongatus PCC 7942*. URL: https://biocyc.org/gene?orgid=SYNEL\&id=SYNPCC7942_2078.

[185] Sagaya Selva Kumar, Raghuraj Chouhan, and Munna Thakur. "Trends in analysis of vitamin B-12". In: *Analytical biochemistry* 398 (Nov. 2009), pp. 139–49. DOI: 10.1016/j.ab.2009.06.041.

[186] Asta Juzeniene and Zivile Nizauskaite. "Photodegradation of cobalamins in aqueous solutions and in human blood". In: *Journal of Photochemistry and Photobiology B: Biology* 122 (2013), pp. 7 –14. ISSN: 1011-1344. DOI: https://doi.org/10.1016/j.jphotobiol.2013.03.001. URL: http://www.sciencedirect.com/science/article/pii/S1011134413000444.

[187] Cristiana Paul and David M. Brady. "Comparative Bioavailability and Utilization of Particular Forms of B12 Supplements With Potential to Mitigate B12-related Genetic Polymorphisms". In: *Integrative medicine (Encinitas, Calif.)* 16 (Feb. 2017), pp. 42–49.

[188] N. F. Tsinoremas et al. "Efficient gene transfer in Synechococcus sp. strains PCC 7942 and PCC 6301 by interspecies conjugation and chromosomal recombination". eng. In: *Journal of Bacteriology* 176.21 (Nov. 1994), pp. 6764–6768. ISSN: 0021-9193.

[189] Pamela A. Silver et al. Anna H. Chen 1 Bruno Afonso. "Spatial and Temporal Organization of Chromosome Duplication and Segregation in the Cyanobacterium Synechococcus elongatus PCC 7942". In: *PLoS One* (2012). URL: `https://www.ncbi.nlm.nih.gov/pubmed/23112856`.

[190] J.H. Martens et al. "Microbial production of Vitamin B". In: *Applied microbiology and biotechnology* 58 (Apr. 2002), pp. 275–85. DOI: `10.1007/s00253-001-0902-7`.

[191] Thorsten Heidorn et al. "Chapter Twenty-Four - Synthetic Biology in Cyanobacteria: Engineering and Analyzing Novel Functions". In: *Synthetic Biology, Part A*. Ed. by Chris Voigt. Vol. 497. Methods in Enzymology. Academic Press, 2011, pp. 539 –579. DOI: `https://doi.org/10.1016/B978-0-12-385075-1.00024-X`. URL: `http://www.sciencedirect.com/science/article/pii/B978012385075100024X`.

[192] Regan L. Bailey, Keith West, and Robert E Black. "The epidemiology of global micronutrient deficiencies". English (US). In: *Annals of Nutrition and Metabolism* 66 (June 2015), pp. 22–33. ISSN: 0250-6807. DOI: `10.1159/000371618`.

[193] Maddaly Ravi et al. *The beneficial effects of spirulina focusing on its immunomodulatory and antioxidant properties*. English. DOI: 10.2147/NDS.S9838. July 2010. URL: `https://www.dovepress.com/the-beneficial-effects-of-spirulina-focusing-on-its-immunomodulatory-a-peer-reviewed-article-NDS` (visited on 07/27/2017).

[194] S. A. Schug et al. "Acetaminophen as an adjunct to morphine by patient-controlled analgesia in the management of acute postoperative pain". eng. In: *Anesthesia and Analgesia* 87.2 (Aug. 1998), pp. 368–372. ISSN: 0003-2999.

[195] Market research store. "Acetaminophen (Paracetamol) Market for Pharmaceuticals, Dye Industry and Chemical Industry - Global Industry Perspective, Comprehensive Analysis, Size, Share, Growth, Segment, Trends and Forecast, 2014 - 2020". In: (Jan. 2016). URL: `https://www.marketresearchstore.com/report/acetaminophen-market-z45985`.

[196] Jagannath B. Lamture. *Aniline and Its Analogs*. Notion Press, Inc., 2018.

[197] Giuseppe Quartarone et al. "Beckmann rearrangement of acetophenone oximes to the corresponding amides organo-catalyzed by trifluoroacetic acid for sustainable NSAIDs synthesis". In: *Applied Catalysis A: General* 472 (2014), pp. 167 –177. ISSN: 0926-860X. DOI: `https://doi.org/10.1016/j.apcata.2013.12.026`. URL: `http://www.sciencedirect.com/science/article/pii/S0926860X13007709`.

[198] Jean Vanden Eynde. "How Efficient Is My (Medicinal) Chemistry?" In: *Pharmaceuticals* 9 (May 2016), p. 26. DOI: 10.3390/ph9020026.

[199] Lenuta-Maria Suta et al. "Alternative Synthesis of Paracetamol and Aspirin Under Non-conventional Conditions". In: *Revista de Chimie -Bucharest- Original Edition-* 65 (June 2014), pp. 621–623.

[200] Swapnil N. Mane, Sagar M. Gadalkar, and Virendra K. Rathod. "Intensification of paracetamol (acetaminophen) synthesis from hydroquinone using ultrasound". In: *Ultrasonics Sonochemistry* 49 (2018), pp. 106 –110. ISSN: 1350-4177. DOI: https://doi.org/10.1016/j.ultsonch.2018.07.029. URL: http://www.sciencedirect.com/science/article/pii/S1350417718304619.

[201] John Christopher Anderson et al. "Method for biosynthesis of acetaminophen". Pat. WO2016069155 A2. International Classification C12P13/02, C12N1/21; Cooperative Classification C12N9/1029, C12N9/0073, C12P13/02. May 2016. URL: http://www.google.com/patents/WO2016069155A2.

[202] CR Andersson et al. "Application of bioluminescence to the study of circadian rhythms in cyanobacteria". In: *Methods in enzymology* 305 (2000), 527—542. ISSN: 0076-6879. DOI: 10.1016/s0076-6879(00)05511-7. URL: https://doi.org/10.1016/S0076-6879(00)05511-7.

[203] James N Kinney et al. "Elucidating Essential Role of Conserved Carboxysomal Protein CcmN Reveals Common Feature of Bacterial Microcompartment Assembly". In: *The Journal of biological chemistry* 287 (Mar. 2012), pp. 17729–36. DOI: 10.1074/jbc.M112.355305.

[204] Fathima Shihana et al. "A modified low-cost colorimetric method for paracetamol (acetaminophen) measurement in plasma". In: *Clinical toxicology (Philadelphia, Pa.)* 48 (Jan. 2010), pp. 42–6. DOI: 10.3109/15563650903443137.

[205] Wook Jin Kim et al. "Development of synebrick vectors as a synthetic biology platform for gene expression in Synechococcus elongatus PCC 7942". English. In: *Frontiers in Plant Science* 8 (Mar. 2017). ISSN: 1664-462X. DOI: 10.3389/fpls.2017.00293.

[206] Agilent Technologies (Shanghai) Co. Ltd Rongjie Fu. *Modernizing the USP Monograph for Acetaminophen.* URL: https://www.agilent.com/cs/library/applications/5991-3579EN.pdf.

[207] J P Glynn and S E Kendal. "Letter: paracetamol measurement". In: *Lancet* 1 (June 1975), pp. 1147–8.

[208] W A Dechtiaruk, G F Johnson, and H M Solomon. "Gas chromatographic method for acetaminophen (N acetyl p aminophenol) based on sequential alkylation". In: *Clinical chemistry* 22 (July 1976), pp. 879–83.

[209] Robin E. Chambers and Ken Jones. "Comparison of a Gas Chromatographic and Colorimetric Method for the Determination of Plasma Paracetamol". In: *Annals of Clinical Biochemistry* 13.1-6 (1976). PMID: 952476, pp. 433–434. DOI: 10.1177/000456327601300132. eprint: https://doi.org/10.1177/000456327601300132. URL: https://doi.org/10.1177/000456327601300132.

[210] Octavian Calinescu et al. "HPLC Separation of Acetaminophen and its Impurities Using A Mixed-mode Reversed-Phase/Cation Exchange Stationary Phase". In: *Journal of Chromatographic Science* 50.4 (Apr. 2012), pp. 335–342. ISSN: 0021-9665. DOI: 10.1093/chromsci/bmr043. eprint: http://oup.prod.sis.lan/chromsci/article-pdf/50/4/335/1090615/bmr043.pdf. URL: https://doi.org/10.1093/chromsci/bmr043.